2015

Release, Stability and Functionality of Nanodelivered Hydrophobic (Lutein and Beta-Carotene) and Hydrophilic (Folic Acid) Antioxidants Using Zein Nanoparticles

Thanida Chuacharoen
Louisiana State University and Agricultural and Mechanical College

RELEASE, STABILITY AND FUNCTIONALITY OF NANODELIVERED HYDROPHOBIC (LUTEIN AND BETA-CAROTENE) AND HYDROPHILIC (FOLIC ACID) ANTIOXIDANTS USING ZEIN NANOPARTICLES

A Dissertation

Submitted to the Graduate Faculty of the
Louisiana State University and
Agricultural and Mechanical College
in partial fulfillment of the
requirements for the degree of
Doctor of Philosophy

in

The Interdepartmental Program in Engineering Science

by
Thanida Chuacharoen
B.S., Chulalongkorn University, 2003
M.S., Kasetsart University, 2006
December 2015

Dedicated to my parents, Mr. Hyu and Mrs. Ladda Chuacharoen, especially my beloved aunt, Miss Sirirat Sae-Chua and to my siblings, Miss Rattiya Chuacharoen and Mr. Supakij Chuacharoen for their unconditional love, support and encouragement through all these years in the US.

ACKNOWLEDGEMENTS

I would like to express my special appreciation and thanks to my advisor Professor Dr. Cristina M. Sabliov for her warmth, support and encouragement through all the difficulties of graduate school. I am grateful to her for giving me the opportunity to be a part of this emerging, challenging and exciting research. She has been my tremendous mentor in the truest sense and her guidance has been instrumental in shaping both dissertation research as well as my overall development as a professional. Without her immense patience and encouragement throughout my PhD, this journey would have been much more grueling.

I would especially like to thank Dr. Zhimin Xu, Dr. Francisco R.Hung, Dr. Rhett W. Stout and professor Dr. T. Gregory Guzik for serving as my committee members. Their timely and valuable inputs, and willingness to evaluate this work are greatly appreciated.

I am really thankful to my co-advisor, Dr. Carlos Astete for his great insights, encouragement, and willingness to help at all times for all laboratory issues. I would also like to thank everyone in my laboratory, Toni Borel, Lacey Simon, Caleb Darensbourg, Kurt Ristroph, McKenzei Windham, Sumit Libi, and especially Sara Navarro for all their warmth and help. I would also like to thank Dr. Rafael Cueto for training me with the DLS, Dr. George G. Stanley from the Chemistry Department for training and letting me use his FTIR equipment, Mrs. Ying Xiao for her assistance with the TEM and SEM, and Mrs. Karen McDonough for her help with cell studies. Again, I am grateful to Dr. Carlos Astete for his assistance with the NMR. I really thank them all for supporting and making the laborious lab work experience a pleasant endeavor through all these years.

I would also like to thank everyone in the Biological and Agricultural Engineering Department, especially Dr. Subramaniam Sathivel, Dr. Steven Hall, Dr. Marybeth Lima, Dr. Daniel Hayes, Dr. W. Todd Monroe, Dr. Chandra Theegala, and Dr. Dorin Boldor for their valuable input, support and smiles, and the administrative staff, Mrs. Angela Singleton, Mrs. Donna Elisar, and Mr. Thomas D. McClure for their kind assistance in so many ways.

I would like to thank all my friends in Baton Rouge in particular Beatrice Terigar, Tammy Brown, Juan Li, Yuhsin Hsueh, all my Thai friends, and special thank to Chanachok Chokwitthaya for being great friends, patient listeners and a great source of inspiration as always.

A special thank goes to the Royal Thai Government for providing the PhD scholarship, and all staff at the office of Educational affairs for their support and taking care of me through all these years in the US.

This work would not be possible without the love, affection, support and faith of my family. I am thankful to my beloved parents and my siblings for providing me with the best education, support, and encouragement necessary to make me the person I am today. Without them I would never have been able to achieve my goals. Lastly, million thanks go to my beloved aunt who raised me as my second mom. I did not have a chance to say goodbye to you, but your memory will be with me always, *R.I.P*.

TABLE OF CONTENTS

LIST OF TABLES

LIST OF FIGURES

ABSTRACT

Nanodelivery systems enable innovations that can benefit foods and human health on a large scale in the coming years. The instabilities of antioxidants during food processing and during digestion are drawbacks that can be successfully addressed by nanoentrapment. This research provided technical strategies to synthesize zein nanoparticles loaded with hydrophobic/hydrophilic antioxidants, and to study the release profiles and physical stability of nanocarriers and chemical stability of entrapped bioactives under on-shelf and GI conditions. The results supported the potential of zein nanoparticles stabilized by surfactants to improve chemical stability of entrapped lutein, and to slowly release lutein under PBS conditions. Same particles enhanced functionality by means of protecting antioxidant activity of entrapped β-carotene in the presence of milk as food matrix under simulated gastrointestinal environments. Lastly, folic acid modified zein nanoparticles sustained the release of folic acid, showed a good biocompatibility, and diminished the toxic effect of folic acid on cells. The increased uptake, particularly by the over-expressing folate-receptor cells indicated that zein nanoparticles can be developed into versatile targeted delivery systems. These findings strongly support the ability of zein nanoparticles to act as effective antioxidant nanodelivery systems for innovative applications in the food and pharmaceutical industries.

CHAPTER 1
LITERATURE REVIEW

Nanotechnology has led to several innovative solutions for delivery of bioactives, including antioxidants. Antioxidants such as lutein, β-carotene, folic acid etc. have been loaded into engineered nanocarriers designed to optimize the potential of nanodelivered compounds, with the purpose of delivering them to the site of action with minimized loss ensured by physical-chemical stability of particles and carefully controlled release mechanisms for improved functionality of the bioactive as an antioxidant.

1. 1. Nanodelivered Antioxidants

β-Carotene and other carotenoids such as zeaxanthin and lutein exert antioxidant properties by scavenging singlet oxygen or free radicals in lipid phases (Sies et al., 1992). Folic acid, also known as folate, is a hydrophilic antioxidant. It is widely used as a recognizing folate receptor (FR) agent, which is over-expressed on the surface of several cancer cells (Ai et al., 2012). Hence, folic acid is used as a targeting agent in addition to being used as an antioxidant. Bioactives of interest to the present research, lutein, β-carotene, and folic acid are discussed in more detail below.

1.1.1. Lutein

Lutein is a derivative of the xanthophyll family, synthesized only by plants. The nutritional benefit of lutein lies in its ability to reduce the risk of developing age-related macular degradation (AMD), which is a deterioration of the macula, resulting in a multifactorial disease leads to blindness (Bian et al., 2012; Kruger et al., 2002). Lutein can protect retinal pigment epithelial cells (RPE) from photo-oxidative damage due to its

ability to filter blue light at a wavelength 445 nm (maximum absorption peak) and to modulate inflammation-related genes so much that it can partially break the vicious cycle between oxidative stress and inflammatory response in RPE (Bian et al., 2012; Domingos et al., 2014). As a powerful antioxidant, lutein works by quenching singlet oxygen or neutralizing photosensitizers (Anonymous, 2005) and also plays an important role in the prevention of cardiovascular disease, stroke, lung cancer, and breast cancer (Duvvuri 2005). The stereoisomer of lutein [(3R, 3'R, 6'R)-beta, epsilon-carotene-3,3'-diol] is shown in Figure 1.1. Lutein, a lipophilic molecule, is water-insoluble because of the presence of a long chromophore of conjugated double bonds (polyene chain). It can be easily oxidized and degraded, translating into a high sensitivity of lutein to light and heat (Mitri et al., 2011).

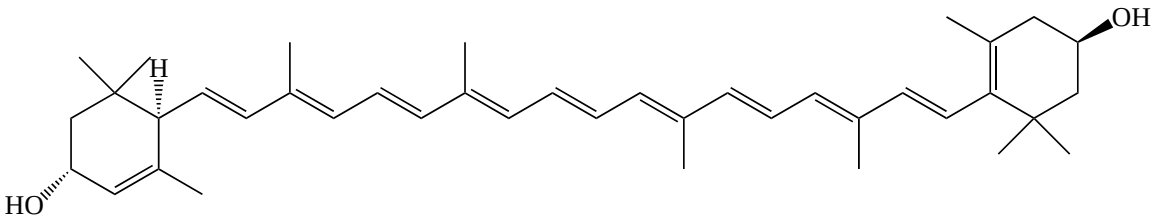

Figure 1.1. Structure of lutein

1.1.2. β-Carotene

β-Carotene is a major component of provitamin A carotenoids with numerous benefits such as reducing the incidence of cancers, preventing chronic and cardiovascular diseases, improving eye health, protecting cells from oxidative damages, and protecting skin from ultraviolet-A induced photoaging (Shi et al., 2004; Terao et al., 2011; Boon et al., 2010; Paiva and Russell 1999). In comparison with α-tocopherol (αT), β-carotene has a lower reactivity toward radicals and a weaker antioxidant property in solution. However, it is more lipophilic than αT, which enables it to scavenge radicals within the

lipophilic compartment, resulting in more efficient antioxidant properties, compared to αT (Niki et al., 1995). The C_{40} polyene structure of β-carotene, which contains a significant number of double bonds (Figure 1.2), makes β-carotene very sensitive to degradation by oxidation, particularly to enzymatic oxidation by oxygenases under human digestive system (Pénicaud et al., 2011; Mueller and Boehm 2011).

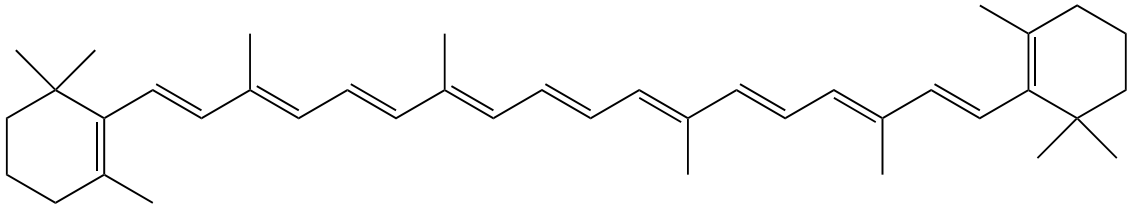

Figure 1.2. Structure of β-carotene

1.1.3. Folic Acid

Folic acid (pteroyl-L-glutamic acid, vitamin B_9), a water-soluble vitamin, is critical in aiding rapid cell division and growth, essential in the cell production and maintenance of new cells, especially during infancy and pregnancy (Yoo and Park 2004). Children and adults need folic acid to synthesize and repair DNA and RNA, and to produce healthy red blood cells (Lamers et al., 2006). It is important for pregnant women to have enough folic acid to prevent major birth defects (Antony 1992). Folic acid, a collective term of pteroylglutamic acid and oligoglutamic acid conjugated as shown in Figure 1.3, is a hydrophilic antioxidant that protects bioconstituents from free radical damage, which can lead to oxidative stress and can inhibit lipid peroxidation (Joshi et al., 2001). Another advantage of folic acid is that it can be covalently linked with the carboxyl group of other chemicals to make cancer drug nanocarriers without losing its folate receptor (FR) binding ability for cancer targeting (Kim et al., 2007).

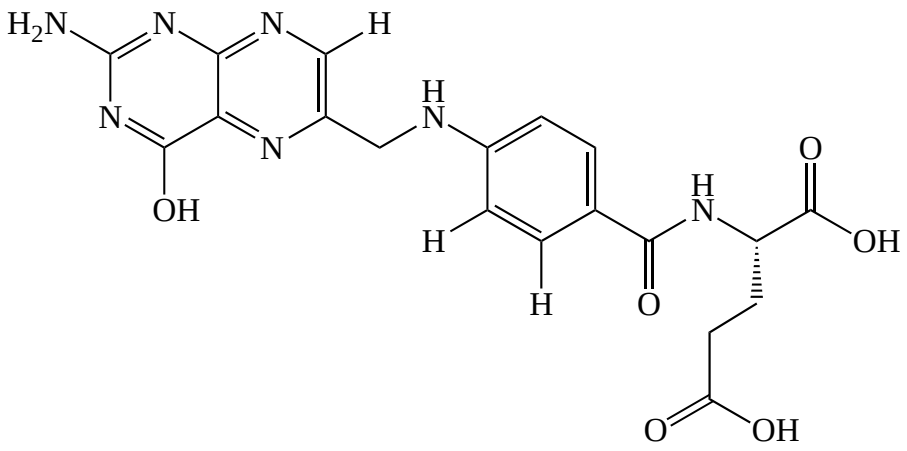

Figure 1.3. Structure of folic acid

The major drawbacks of antioxidants such as those described is that they are low very sensitive to light and heat during processing and storage, leading to decreased effectiveness and increased costs. Nanodelivery systems have been proposed as a valid option to preserve the functional properties of antioxidants during undesirable conditions and to enhance their physiological potency.

1.2. Nanodelivery System

The purpose of the nanodelivery system is to protect the entrapped compounds from chemical and biological degradation during on-shelf or during GI transit for improved bioactive functionality. Because of its biodegradation profile, and low toxicity of the end-products of degradation, zein has recently gained a reputation as a preferred nanocarrier for entrapment, controlled release applications, and stabilization of fat-soluble compounds in nanodelivery systems (Shukla and Cheryan 2001). Zein nanoparticles have the ability to also physically entrap hydrophilic bioactives or to chemically link bioactives, Due to its versatility as a carrier for hydrophobic and hydrophilic bioactives, zein was selected as the nanocarrier of choice in this research.

1.2.1. Zein nanoparticles: Synthesis, Properties, and Applications

Zein, a three-quarter hydrophobic maize protein, consists of at least 12 amino acid signal peptides such as glutamic acid (21–26%), leucine (20%), proline (10%) and alanine (10%) (Figure 1.4, Appendix A.1) (Shukla and Cheryan 2001; Phillips and McClure 1985). α-Zein, one of the four main types of zein, has an average molecular weight of approximately 21-24 kDa (Momany et al., 2006) and possesses high hydrophobic properties.

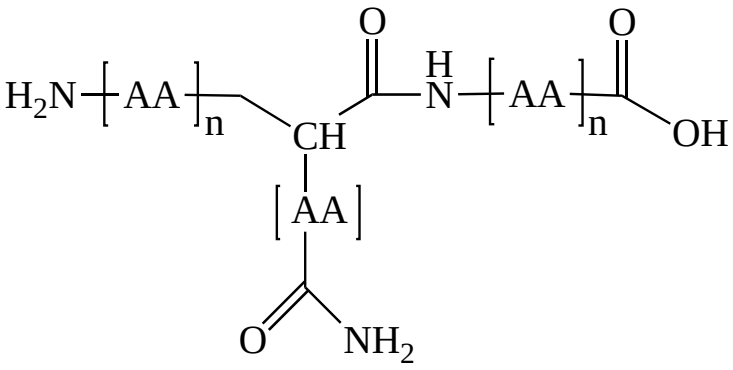

Figure 1.4. Structure of zein (AA represents amino acid group)

Recently, several attempts have been made to synthesize zein nanoparticles, with the goal of protecting bioactives from degradation, improving their functionality, and sustaining their release kinetic profiles. Entrapment of drugs and bioactive compounds such as 5-fluorouracil, essential oils, thymol, DNA, curcumin, coumarin, vitamin D_3, and lutein in zein nanoparticles of 115 to 900 nm was achieved by processes such as phase separation, anti-solvent precipitation (desolvation), coacervation technique, electrohydrodynamic atomization, supercritical fluid (SEDS), modified liquid-liquid dispersion, and nanoprecipitation (Table 1.1) (Lai and Guo 2011; Zou et al., 2012; Zhong and Jin 2009; Gomez-Estaca et al., 2012; Podaralla and Perumal 2012; Hu et al., 2012). Podaralla and Perumal, 2012 demonstrated a new method to prepare zein nanoparticles

using pH controlled nanoprecipitation to entrap 6,7-dihydroxycoumarin as a hydrophobic model. Lecithin and pluronic F68 in 2:1 (w/w) ratio were used as surfactants to stabilize the nanoparticles. Average particle size and the entrapment efficiency of coumarin-loaded zein nanoparticles were 365 nm and 62% respectively. The release study in PBS (pH 7.4) showed that zein nanoparticles with a combination of surfactants can sustain the release of the entrapped coumarin compounds up to 9 days (Podaralla and Perumal 2010).

The study of lutein-loaded zein nanoparticles by Hu et al., 2012 successfully used supercritical fluids (SEDS) to synthesize nanoparticles with the average particle size 205 nm and the entrapment efficiency 60%. As generally recognized as safe (GRAS) by FDA approved for oral use in food applications, a novel method of preparing stable zein nanoparticles, stabilized by gum arabic for encapsulation of peppermint oil, was proposed. The purpose of this research was to replace ethanol with nonflammable propylene glycol, which is good for the food application (Chen and Zhong 2015).

Zein nanoparticles could enhance curcumin dispersion as food-coloring incorporated in aqueous foods (Gomez-Estaca et al., 2012). Lutein and vitamin D_3 were used as entrapped bioactives in zein nanoparticles, and their release profiles and chemical stability results showed that zein nanodelivery system played an important role as a promising bioactive nanocarrier (Hu et al., 2012; Luo et al., 2011). Additionally, the abilities of the zein system to improve solubility and maximize the antioxidant and antimicrobial properties of essential oils such as thymol, oregano, cassia, and red thyme have been successfully demonstrated (Zhang et al., 2014; Parris et al., 2005; Wu et al., 2012; Li et al., 2013). For example, thymol antimicrobial agents showed better activities against *S. aureus* when loaded in zein nanoparticles, compared with its unloaded form

(Zhang et al., 2014). In pharmaceutical application, drug delivery has gained benefits from zein nanoparticles as well, their potential can overcome the limitations of metallic nanoparticles. The study of Lai et al., 2011 stated that drug-loaded zein nanoparticles were an efficient system to target 5-fluorouracil at the liver through intravenous delivery. Another work of drug-loaded zein nanoparticles modified as fluorescent nanocarriers was studied in L929 and MCF-7 cell lines. The fluorescent particles were compatible for cells and were less toxic with 80% cell viability reported. Zein nanoparticles have also been developed as a skin therapy carrier for entrapped terpinen-4-ol to prevent allergies when apply directly to skin (Marini et al., 2013).

1.3. Loading Mechanism

A variety of possible drug loading mechanisms, including electrostatic attractions, hydrophobic interactions, and covalent bonding, have been employed for delivery of various drugs with nanoparticles. Compatibility between the drug and the polymeric matrix in which entrapped dictates the entrapment efficiency and release of the drug. Zein nanoparticles are suitable for hydrophobic entrapment due to the hydrophobic nature of zein. It can potentially co-precipitate with hydrophobic lutein or β-carotene via liquid-liquid dispersion method with strong hydrophobic interactions and hydrogen bonds. For instance, lutein was physically entrapped and delivered with zein nanoparticles to approach lutein release profile (Hu et al., 2012). Zein can form drug-protein complexes with a strong affinity, as examined by the NMR technique. The results concluded that the main factors responsible for the kinetic release of the entrapped drugs are the molecular affinity and the hydrophobic characteristic of the drugs (Sousa et al., 2012).

Table 1.1. Synthesis, analysis, and purpose of zein nanoparticle studied for delivery of bioactive compounds

Nanodelivery system	Synthesis	Analysis	Purpose	Reference
6,7-dihydroxycoumarin (DHC)-loaded zein nanoparticles	pH controlled precipitation stabilized by pluronic F68 and lecithin	Characterization (size, PDI, zeta potential, entrapment efficiency, drug loading, and morphology)	Study the influence of pH of the aqueous phase, buffer type, ionic strength, surfactant, and zein concentration	(Podaralla and Perumal 2012)
Lutein-loaded zein nanoparticles	Supercritical Fluid (SEDS)	Characterization (size, PDI, zeta potential, entrapment efficiency, drug loading, and morphology) and release profile	Examine the effect of temperature, pressure, ratio of lutein:zein, and flow rate on nanoparticle properties	(Hu et al., 2012)
Curcumin-loaded zein nanoparticles	Electrohydrodynamic atomization	Formation, characterization (size, solid state, entrapment efficiency, drug loading, and morphology and stability	Improve coloring capacity and dispersion	(Gomez-Estaca et al., 2012)
Vitamin D_3-loaded zein nanoparticles	Phase separation coated with carboxymethyl chitosan	Characterization (size, PDI, zeta potential, entrapment efficiency, drug loading, and morphology), chemical stability, and controlled release property	Provide better release and chemical stability of entrapped vitamin D_3	(Luo et al., 2011)
Tea tree oil (TTO)-loaded zein nanoparticles	Anti-solvent precipitation (desolvation)	Characterization (size, PDI, zeta potential, entrapment efficiency and morphology)	Develop a topical application	(Marini et al., 2013)
Peppermint oil-loaded zein nanoparticles	Precipitation stabilized by gum arabic	Characterization (size, PDI, zeta potential, entrapment efficiency, drug loading, and morphology) and release profile	Replace ethanol with nonflammable propylene glycol	(Chen and Zhong 2015)
Essential oil-loaded zein nanoparticles	Liquid-liquid dispersion	Morphology, structure, antioxidant and antimicrobial activities under three different pH conditions	Improve solubility and preserve antioxidant and antimicrobial activities of essential oils	(Wu et al., 2012)

(Table 1.1. continued)

Nanodelivery system	Synthesis	Analysis	Purpose	Reference
Essential oil-loaded zein nanoparticles	Phase separation	Characterization (size, PDI, zeta potential, entrapment efficiency, drug loading, and morphology), *in vitro* digestion by pepsin and microbial enzymes	Maximize the antimicrobial properties of oils	(Parris et al., 2005)
Thymol-loaded zein nanoparticles	Liquid-liquid dispersion stabilized by sodium caseinate and chitosan	Fabrication, characterization (size, PDI, zeta potential, entrapment efficiency, drug loading, and morphology) and antimicrobial activities	Compare the antimicrobial activity of nanoentrapped thymol with unentrapped form	(Zhang et al., 2014)
Thymol-loaded zein nanoparticles	Modified antisolvent process stabilized by sodium caseinate	Fabrication, characterization (size, PDI, zeta potential, entrapment efficiency, drug loading, and morphology), release profile, antioxidant and antimicrobial properties	Modify the antisolvent procedure and investigate antioxidant and antimicrobial activities of entrapped thymol	(Li et al., 2013)
5-fluorouracil (5-FU)-loaded zein nanoparticles	Phase separation	Characterizaton (size, PDI, zeta potential, entrapment efficiency, drug loading, and morphology), *in vitro* release, and stability	Target liver through intravenous delivery in a mouse model	(Lai and Guo 2011)
Fluorescent 5-fluorouracil (5-FU)-loaded zein nanoparticles	Liquid-liquid dispersion conjugated with quantum dots	Characterization (size, PDI, zeta potential, entrapment efficiency, drug loading, and morphology), release profile, biocompatibility, and cytotoxicity	Develop cellular imaging and drug delivery application	(Aswathy et al., 2012)
DNA-loaded zein nanoparticles	Coacervation technique	Characterization (size, PDI, zeta potential, entrapment efficiency, drug loading, and morphology), sustain release, cell cytotoxicity, and cellular internalization	Develop DNA vehicle for gene delivery	(Regier et al., 2012)

On the other hand, hydrophilic bioactives such as ascorbic acid can be effectively delivered when entrapped in hydrophilic polymers such as chitosan (Alishahi et al., 2011; Ji et al., 2012). Covalent attachment of the drug is pursued when the drug, natively hydrophilic is to be delivered by a polymer hydrophobic in nature. A good example is the development of polymer-bioactive conjugates, such as folic acid-conjugated PLGA nanoparticles, with applications ranging from tissue engineering to biosensors (Elvira et al., 2005), and cell targeting. The type of mechanism employed in the entrapment of the bioactive dictates not only its successful entrapment and delivery, but also its release mechanism, which in return controls the bioavailability of the drug and bioaccessibility over time at the desired site of action, for optimum functionality of the delivered bioactive.

1.4. Release Mechanism

Nanomaterial composition, nanoparticle morphology, polymer degradation profile, the presence of chemical agents such as surfactants, cross-linking agents, and the interaction forces between the nanoparticle carriers and its entrapped compound versus interaction between the bioactive and the environment to which applied have an impact on the release mechanism of the drug. There are three possible mechanisms that describe the release of bioactives from nanoparticle matrix (Figure 1.5). *(I)* Diffusion and desorption of bioactives: normally nanoparticles swell by hydration, so bioactive compounds must be dissolved in water before being released. *(II)* Cleavage of the covalently link between the polymer and the bioactives: the covalent link between the compounds and the polymer is cleaved, and the bioactives are desorbed or released from the swollen nanoparticles, and *(III)* Degradation of the nanoparticle matrix: enzymatic

activity can lead to matrix degradation, resulting in the release of the entrapped compounds. Overall, bioactive diffusion and nanoparticle degradation are the main mechanisms which govern the release of the entrapped compounds.

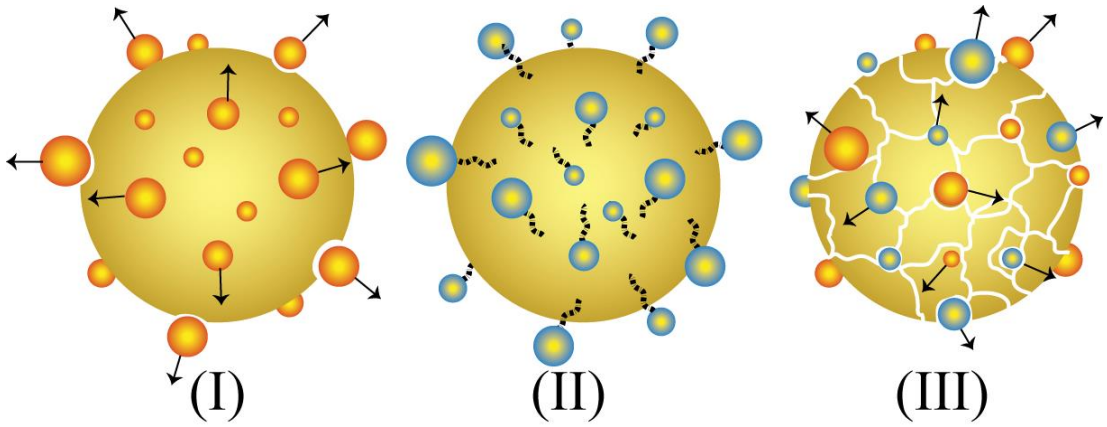

Figure 1.5. Three possible release mechanisms of the entrapped compounds: *(I)* Diffusion and desorption, *(II)* Cleavage of the covalently-link between the compounds and the nanoparticle matrix, and *(III)* Diffusion of compounds combined with degradation of the nanoparticle matrix

1.4.1. Release Profile Characteristic

Zero-order release is the most desired profile in drug delivery system; however, bi-phasic and tri-phasic profiles were reported in the literature for various bioactives delivered with nanoparticles, depending on the characteristics of nanodevices such as size and composition of nanoparticles (Figure 1.6). The release of the non-entrapped compounds available on the surface of the particles at the beginning stage of the release is referred to as the initial burst release (phase I). Rapid release observed after the burst release is usually correlated with massive swelling, along with the erosion and deformation of nanoparticles (Figure 1.6 (a)). However, slow and minimal release following zero-order kinetics can happen after the burst release because of slow diffusion, which may be attributed to binding of the drug to the polymer (Figure 1.6 (b)).

In the tri-phasic profile (Figure 1.6 (c)), phase I is described as a burst release. Phase II often shows a slow release phase or lag-phase, due to drug slowly diffusing through degraded polymer matrix. Phase III is usually a period of faster release, often attributed to the onset of erosion, which is also called the second burst. However it is possible to have the rapid release in phase II and slower release at the end, depending on type of nanodevice (Fredenberg et al., 2011).

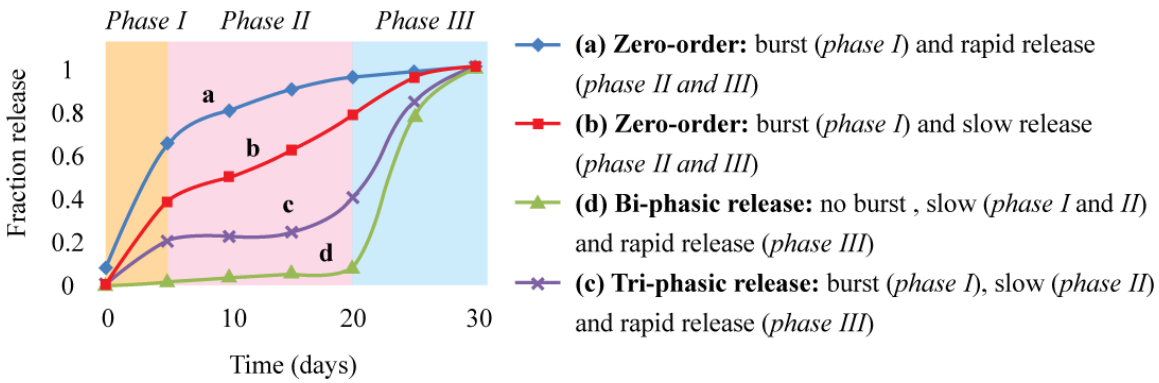

Figure 1.6. Release profile characteristics

For example, the release profile of folic acid-loaded PLGA nanoparticles studied by Stevanovic et al. 2008, indicated that folic acid released over a period of time followed a tri-phasic profile. The first phase was a burst effect resulting from the release of the drug that was adsorbed to the outer particle surface. Seventeen percent of the entrapped folic acid was released in the first day of degradation. The second phase was slow and lasted from the first day until the twelfth day because of the diffusion of the drug out of the matrix. The third phase occurred due to polymer degradation increasing permeability of the drug in the polymer matrix. In total, 82% of the entrapped folic acid was released at the end of the experimental time (30 days) (Stevanovi et al., 2008). Alishahi et al., 2011 studied shelf life and delivery enhancement of vitamin C from

chitosan nanoparticles. The release of vitamin C was pH-dependent, and was found to be faster in saline buffer solution (PBS, pH 7.4) than in 0.1 M HCl (pH 1.2). The entrapped vitamin C release showed a bi-phasic release profile. At the first stage, diffusion mostly controlled the release process, and then the ion exchange between polymer and release medium caused the erosion of the nanoparticles, which enhanced the release rate (Alishahi et al., 2011). Different release profiles and kinetics can be achieved by selectively choosing the materials for the nanoparticle synthesis. As another example, the study of lutein released from 205 nm zein nanoparticles reported by Hu et al., 2012 suggested an initial burst effect of lutein (15%) in the first 40 min, and the release profile displayed a near zero-order kinetic, which was accomplished by the swelling/erosion of zein matrix, and was deemed desirable for controlled delivery applications. The lutein entrapped deeper in the zein matrix were released within 120 min by diffusion mechanism. Another example of the kinetic release was obtained from the modified folic acid conjugated with terminated amine groups of chitosan nanoparticles in PBS at 37°C, which was found to be sustained until 24 days (Table 1.2) (Zu et al., 2011).

The barrier properties of the encapsulating wall can be tailored to protect the stability and functionality of the entrapped compound from undesirable environments (e.g. temperature, pH, oxygen, enzymes), and to alter the release profile of the compounds after ingestion during GI transit. These mechanisms are still not clearly understood, but they are topics of importance for the successful use of nanodelivery systems in functional foods.

1.5. Physicochemical Stability

Some of the issues associated with nanoparticle stability, which would negatively impact their use in foods, are sedimentation, agglomeration, crystal growth, and the change of crystallinity state (Wu et al., 2011). High pressure or temperature exposure during manufacturing, storage and distribution, can cause physical and chemical nanoparticle instability (Wu et al., 2011). Several studies have been published addressing nanoparticles and bioactive stability under various storage and delivery conditions. Lai and Guo, 2011 tested physical stability of zein nanoparticles with entrapped 5-fluorouracil after 6 months under different temperature conditions (4°C, 25°C, and 40°C) to find that zein nanoparticles stored at 4°C were more stable; this result was determined by measuring drug loading, which decreased only 1% after 6 months (Lai and Guo 2011). Normally, the best storage temperature recommended for a protein like zein is less than 4°C. Higher temperatures can cause protein degradation (Lai and Guo 2011). The stability of zein nanoparticles under digestion conditions with pepsin at pH 3.5 indicated that zein nanoparticles formed aggregates and completely dissolved after 52 hours (Parris et al., 2005). Morris et al., 2011 also studied the stability by measuring particle size of tripolyphosphate (TPP)–chitosan nanoparticles. After 12 months under different temperature conditions (4°C, 25°C, and 40°C), the data showed that the size of nanoparticles stored under 40°C decreased after 6 months due to chitosan fracture as a result of hydrolysis (Morris et al., 2011). Entrapped lutein in the lipid bilayer of liposome resulted in the unchanged structure of nanoliposome, and enhanced stability of the entrapped bioactive during processing and storage. Lutein nanocrystals have been

developed to maintain chemical stability of the bioactive under lyophilized conditions (Mitri et al., 2011).

1.6. Functionality (Antioxidant Activity)

The use of nanoentrapment techniques has been proposed as viable means to preserve the scavenging properties of antioxidants during manufacturing, storage and distribution, and to enhance their physiological potency. For example, Wu et al., 2012 studied the effect of zein nanoparticles on the antioxidant properties of essential oils using 2,2-diphenyl-1-picrylhydrazyl radical (DPPH) and ferric ion spectrophotometric assays. They concluded that entrapping essential oils in zein nanoparticles could increase their solubility without affecting their antioxidant ability, thus supporting the use of nanodelivery systems in foods (Wu et al., 2012). The effect of entrapment on antioxidant activity was reported by the study of α-tocopherol and tocotrienol-rich fraction entrapped in poly(lactide-co-glycolide) nanoparticles, observed by measuring the percent inhibition of cholesterol oxidation. The result showed that the activity of the nanodelivered antioxidant was higher compared to the corresponding emulsion system at 48 hours (Alqahtani et al., 2015).

1.7. Cellular Targeting and Cytotoxicity

The general pathway for nanoparticle cellular uptake is the receptor-mediated endocytosis process (Zhang et al., 2012). There have been several attempts to surface modify nanodelivery systems to create targeting nanocarriers, using folic acid as a ligand for targeting, detecting or delivering chemotherapeutic agents to cancer cell (Table 1.2). The ability of surface-modified particles to be endocytosed by cells expressing folate-receptors was enhanced, resulting in high drug levels and improved chemotherapeutic

efficacy with fewer side effects of the chemotherapeutic drug (Zhang et al., 2012). Cellular studies have been employed to investigate the targeting ability of folic acid when conjugated with nanoparticles, and the toxicity of these folic acid-conjugated nanoparticles to healthy cells. High-level positive folate receptor expression such as human cervical carcinoma cells (HeLa) (Zhang et al., 2012; Zhang et al., 2010; Ai et al., 2012), human colon adenocarcinoma cell line (Caco-2) (Teng et al., 2013), HepG2 cell line (Zhou et al., 2010), and human ovarian cancer cells (SKOV3 cells) (Boddu et al., 2012) were commonly used for cellular uptake and cytotoxicity studies involving folic acid, compared with negative-folate receptor expression, for example human lung adenocarcinoma epithelial cells (A549) (Zhang et al., 2012) and human acute lymphoblastic leukemia (CERF-CEM) (Ai et al., 2012). The cytotoxicity of zein nanoparticles with loaded 5-fluorouracil (5-FU) revealed that the empty zein nanoparticles were compatible with L929 and MCF-7 cancer cell lines. The survival rate was decreased with the increased concentration of the loaded drugs and in the presence of conjugated quantum dots to zein nanoparticles (Aswathy et al., 2012). The imaging results revealed that modified folate nanoparticles were uptaken into high level-folate receptor cells at a greater amount than cells with less folate-receptors.

1.8. Nanoparticle-Food Matrix Interaction

There are several requirements needed for incorporating nanodelivered compounds as food bioactive ingredients into food products. Most importantly, the food must be safe for consumption; sensorial properties of the foods appearance, flavor, and color have to meet consumer expectations, and the use of the nanodelivery systems in foods must be justified (e.g. an additional health benefit of the nano-enable food). The

Table 1.2. Modification, functionality, and analysis method of folic acid modified nanoparticles as targeting nanocarriers

Nanodelivery system	Modification	Analysis	Functionality	Reference
FA-conjugated Au nanoparticles	Reaction between carboxyl group of glutathione attached on the surface of gold (Au) nanoparticles and amino group of folic acid (FA)	*Cellular studies:* human cervical carcinoma cells (HeLa) and human lung adenocarcinoma epithelial cells (A549), which have different amounts of folate receptors on their surface, evaluated by cytotoxicity, cellular uptake (imaging), and cancer cell assay (quantification)	Targeting and detecting cancer cells	(Zhang et al., 2010)
FITC-FA-conjugated Au nanoparticles	Conjugation of the folic acid (FA)-gold nanoparticles (Au) with fluorescein isothiocyanate (FITC)	*Cellular studies:* human cervical carcinoma cells (HeLa) and human acute lymphoblastic leukemia (CERF-CEM) by intracellular uptake and cytotoxicity (MTT assay)	Targeting to tumors by imaging	(Ai et al., 2012)
FA modified PLGA nanoparticles	Condensation between carboxylic groups of poly(lactide-*co*-glycolide) (PLGA) and amine groups from poly(ethylene glycol) (PEG) or folate decorated PEG (PEG-FA)	*Cellular studies:* HepG2 cell line, evaluated by cellular uptake using confocal laser scanning microscopy and protein adsorption	Enhancing SPI-folic acid nanoparticles uptake in cancer cells	(Zhou et al., 2010)
PEG-FA-conjugated PLGA nanoparticles	Coupling di-block copolymer (PLGA-PEG-NH_2) with folic acid (FA)	*Cellular studies:* FA-receptor-positive human ovarian cancer cells (SKOV3 cells), evaluated by qualitative and quantitative cellular uptake and cytotoxicity	Targeting chemotherapeutic agents to tumor cells	(Boddu et al., 2012)

(Table 1.2. continued)

Nanodelivery system	Modification	Analysis	Functionality	Reference
FA non-covalent conjugated carbon nanotubes	Folic acid (FA) coated on nanoparticle surface using a simple, rapid 'one pot' synthesis method (without chemical functionalization)	*Cellular studies:* THP-1 cells, evaluated by the internalization using Giemsa staining with light microscopy, and cytotoxicity using the MTT assay	Interacting with cell over-expressing FA receptor in the diagnosis of cancer	(Castillo et al., 2013)
PEG-FA-conjugated β-CD nanoparticles	Click reaction of bisazide-terminated poly(ethylene glycol) (PEG) as linker with alkyne terminated folate (FA) and alkyne-terminated β-cyclodextrins (β-CD)	*Cellular studies:* human cervical carcinoma cells (HeLa) and human lung adenocarcinoma epithelial cells (A549), evaluated by cytotoxicity and cellular uptake imaging	Enhancing site-specific intracellular delivery against the folate receptor	(Zhang et al., 2012)
FA-conjugated nanoparticles coated with PEG	Reaction between the activated folic acid (FA) and terminated amino groups of poly(ethylene glycol) (PEG)	*Interaction study:* conjugation between folate-nanoparticles and the folate-binding protein, evaluated by surface plasmon resonance	Targeting to the folate-binding protein	(Stella et al., 2000)
Oil-loaded FA-conjugated CS nanoparticles	Reaction between the activated folic acid (FA) and terminated amino groups of chitosan (CS)	*Release study: in vitro* release kinetic properties in PBS at 37°C, which showed sustained release characteristics of oil for 576 hours	Developing a tumor-targeted drug delivery system	(Zu et al., 2011)
SPI-FA-conjugated nanoparticles	Reaction between the activated folic acid (FA) and soy protein isolate (SPI) using carbo-diimide catalyzing method	*Cellular studies:* human colon adenocarcinoma cell line (Caco-2), evaluated by cellular uptake study	Enhancing SPI-FA nanoparticles uptake in cancer cells	(Teng et al., 2013)

literature is very scarce when it comes to nanoparticle-food interaction, maybe due to a lack of methodologies able to detect organic nanoparticles in a complex organic food matrix. For example, one study focused on the entrapment of vitamin D_2 within β-lactoglobulin based nanoparticles. The lipophilic nanocarrier was incorporated into non-fat beverages as a means to reduce fat for a healthy diet. The nanoparticle system was transparent, so it did not detrimentally affect the appearance of the food product, and it provided a good protection of the entrapment vitamin D_2 in β-lactoglobulin-pectin nanoparticles, which was deemed successful as a means of fortification of non-fat foods or beverages with a hydrophopic nutraceutical (Ron et al., 2010). Another example is the use of Ca^{2+} cross-linked alginic acid nanoparticles to successfully entrap and disperse a hydrophobic natural colorant, β-carotene in water (Astete et al., 2009). Zein nanoparticles also provided a way to achieve a better solubility and coloring capacity of hydrophobic compounds incorporated into water-based foods. For example, Gomez-Estaca et al., 2012 prepared zein nanoparticles by electrohydrodynamic atomization with entrapped hydrophobic curcumin as a food-coloring. The nanoparticles dispersed better and the entrapped curcumin presented good coloring capacity when incorporated into semi-skimmed milk as aqueous food products compared to commercial curcumin (Gomez-Estaca et al., 2012).

1.9. Gastrointestinal (GI) Tract

Nanoparticle physical-chemical characteristics (e.g. particle size, polydispersity, surface charge, hydrophobicity, and morphology), stability and functionality of the nanocarriers are obviously changed, depending on the types of matrices of entrapment, under the conditions encountered during transit through the gastrointestinal (GI) tract,

with a significant impact on the delivery of the bioactive. For example, nanoemulsions improved solubility and enhanced bioaccessibility of the entrapped fish oil (Talegaonkar et al., 2010). Zein nanoparticles with entrapped essential oils subjected to digestion with digestive pepsin at a concentration ratio of 10:1 were completely digested after 52 hours in pH 3.5 at 37°C (Parris et al., 2005). The potential of nanoentrapment to prevent phenolic phytochemicals from the oxidative degradation in the GI tract was confirmed by entrapping the phytochemicals in nanoparticles as reviewed by Li et al., 2015 (Li et al., 2015).

1.10. Objective

Nanoparticle physical properties, entrapment efficiency, release mechanism, stability and functionality of the nanodelivered bioactive are all important factors to be considered in designing or choosing an appropriate delivery system for a specific use. Various environments, including processing, storage conditions (e.g. heat, light, and time), food matrix, and GI conditions will impact physical stability of the nanoparticles, the release mechanism, the chemical stability and functionality of the entrapped antioxidants. This impact will be different depending on the type of the entrapped antioxidants, the type of nanoparticles, the loading mechanism, and surface modification of the nanoparticles.

The goal of this research was to assess the effect of nanoentrapment (physical and covalent) of antioxidants (lutein, β-carotene, and folic acid) on their functionality (stability, release, antioxidant activity, targeting) under on-shelf and GI conditions (temperature, UV, pH). First, hydrophobic antioxidant lutein was physically entrapped in zein nanoparticles. The physical stability of zein nanoparticles, the release mechanism,

along with chemical stability and the degradation of the entrapped lutein, were studied under storage and on-shelf conditions (Chapter 2). Second, the effect of food matrix interaction and simulated GI tract were hypothesized to have an impact on the stability and functionality of entrapped antioxidants; this was studied using β-carotene entrapped in zein nanoparticles (Chapter 3). As a novel system, zein nanoparticles with entrapped and covalently linked folic acid were developed and tested under PBS conditions in terms of controlled release, cytotoxicity and cellular uptake to support the hypothesis that surface modified zein nanoparticles can be potentially used as delivery systems for hydrophilic drugs and/or targeting nanodelivery systems to folate-receptor expressing cells (Chapter 4). The results of this research are critical in the development of nanoparticles able to achieve an efficient controlled release, enhanced stability, and improved functionality of nanodelivered hydrophobic and hydrophilic antioxidants in food and pharmaceutical applications.

1.11. References

Ai, J., Y. Xu, D. Li, Z. Liu, and E. Wang (2012). "Folic acid as delivery vehicles: targeting folate conjugated fluorescent nanoparticles to tumors imaging". *Talanta,* 101 32-37.

Alishahi, A., A. Mirvaghefi, M. R. Tehrani, H. Farahmand, S. Koshio, F. A. Dorkoosh, and M. Z. Elsabee (2011). "Chitosan nanoparticle to carry vitamin C through the gastrointestinal tract and induce the non-specific immunity system of rainbow trout (Oncorhynchus mykiss)". *Carbohydrate Polymers,* 86 (1), 142-146.

Alqahtani, S., L. Simon, C. E. Astete, A. Alayoubi, P. W. Sylvester, S. Nazzal, Y. Shen, Z. Xu, A. Kaddoumi, and C. M. Sabliov (2015). "Cellular uptake, antioxidant and antiproliferative activity of entrapped α-tocopherol and γ-tocotrienol in poly (lactic-co-glycolic) acid (PLGA) and chitosan covered PLGA nanoparticles (PLGA-Chi)". *Journal of colloid and interface science,* 445 243-251.

Anonymous, (2005). "Lutein and zeaxanthin. Monograph". *Altern Med Rev,* 10 (2), 128-35.

Antony, A. C. (1992). "The biological chemistry of folate receptors". *Blood,* 79 (11), 2807-20.

Astete, C. E., C. M. Sabliov, F. Watanabe, and A. Biris (2009). "Ca2+ Cross-Linked Alginic Acid Nanoparticles for Solubilization of Lipophilic Natural Colorants". *Journal of Agricultural and Food Chemistry,* 57 (16), 7505-7512.

Aswathy, R. G., B. Sivakumar, D. Brahatheeswaran, T. Fukuda, Y. Yoshida, T. Maekawa, and D. S. Kumar (2012). "Biocompatible fluorescent zein nanoparticles for simultaneous bioimaging and drug delivery application". *Advances in Natural Sciences: Nanoscience and Nanotechnology,* 3 (2), 025006.

Bian, Q., S. Gao, J. Zhou, J. Qin, A. Taylor, E. J. Johnson, G. Tang, J. R. Sparrow, D. Gierhart, and F. Shang (2012). "Lutein and zeaxanthin supplementation reduces photooxidative damage and modulates the expression of inflammation-related genes in retinal pigment epithelial cells". *Free Radic Biol Med,* 53 (6), 1298-307.

Boddu, S. H., R. Vaishya, J. Jwala, A. Vadlapudi, D. Pal, and A. Mitra (2012). "Preparation and characterization of folate conjugated nanoparticles of doxorubicin using PLGA-PEG-FOL polymer". *Med chem,* 2 (Suppl 4), 68-75.

Boon, C. S., D. J. McClements, J. Weiss, and E. A. Decker (2010). "Factors influencing the chemical stability of carotenoids in foods". *Crit Rev Food Sci Nutr,* 50 (6), 515-32.

Castillo, J. J., T. Rindzevicius, L. V. Novoa, W. E. Svendsen, N. Rozlosnik, A. Boisen, P. Escobar, F. Martínez, and J. Castillo-León (2013). "Non-covalent conjugates of single-walled carbon nanotubes and folic acid for interaction with cells over-expressing folate receptors". *Journal of Materials Chemistry B,* 1 (10), 1475-1481.

Chen, H. and Q. Zhong (2015). "A novel method of preparing stable zein nanoparticle dispersions for encapsulation of peppermint oil". *Food Hydrocolloids,* 43 593-602.

Domingos, L. D., A. A. Xavier, A. Z. Mercadante, A. J. Petenate, R. A. Jorge, and W. H. Viotto (2014). "Oxidative stability of yogurt with added lutein dye". *J Dairy Sci,* 97 (2), 616-23.

Duvvuri, S. J., Kumar G.; Pal, Dhananjay; Mitra, Ashim K. (2005). "Lutein and zeaxanthin. Monograph". *Altern Med Rev,* 10 (2), 128-35.

Elvira, C., A. Gallardo, J. Roman, and A. Cifuentes (2005). "Covalent Polymer-Drug Conjugates". *Molecules,* 10 (1), 114-125.

Fredenberg, S., M. Wahlgren, M. Reslow, and A. Axelsson (2011). "The mechanisms of drug release in poly(lactic-co-glycolic acid)-based drug delivery systems—A review". *International Journal of Pharmaceutics,* 415 (1–2), 34-52.

Gomez-Estaca, J., M. P. Balaguer, R. Gavara, and P. Hernandez-Munoz (2012). "Formation of zein nanoparticles by electrohydrodynamic atomization: Effect of the main processing variables and suitability for encapsulating the food coloring and active ingredient curcumin". *Food Hydrocolloids,* 28 (1), 82-91.

Hu, D., C. Lin, L. Liu, S. Li, and Y. Zhao (2012). "Preparation, characterization, and in vitro release investigation of lutein/zein nanoparticles via solution enhanced dispersion by supercritical fluids". *Journal of Food Engineering,* 109 (3), 545-552.

Ji, J., D. Wu, L. Liu, J. Chen, and Y. Xu (2012). "Preparation, characterization, and in vitro release of folic acid-conjugated chitosan nanoparticles loaded with methotrexate for targeted delivery". *Polymer Bulletin,* 68 (6), 1707-1720.

Joshi, R., S. Adhikari, B. S. Patro, S. Chattopadhyay, and T. Mukherjee (2001). "Free radical scavenging behavior of folic acid: evidence for possible antioxidant activity". *Free Radic Biol Med,* 30 (12), 1390-9.

Kim, S.-L., H.-J. Jeong, E.-M. Kim, C.-M. Lee, T.-H. Kwon, and M.-H. Sohn (2007). "Folate receptor targeted imaging using poly (ethylene glycol)-folate: in vitro and in vivo studies". *Journal of Korean medical science,* 22 (3), 405-411.

Kruger, C. L., M. Murphy, Z. DeFreitas, F. Pfannkuch, and J. Heimbach (2002). "An innovative approach to the determination of safety for a dietary ingredient derived from a new source: case study using a crystalline lutein product". *Food Chem Toxicol,* 40 (11), 1535-49.

Lai, L. and H. Guo (2011). "Preparation of new 5-fluorouracil-loaded zein nanoparticles for liver targeting". *Int J Pharm,* 404 317 - 323.

Lai, L. F. and H. X. Guo (2011). "Preparation of new 5-fluorouracil-loaded zein nanoparticles for liver targeting". *Int J Pharm,* 404 (1-2), 317-23.

Lamers, Y., R. Prinz-Langenohl, S. Brämswig, and K. Pietrzik (2006). "Red blood cell folate concentrations increase more after supplementation with [6S]-5-methyltetrahydrofolate than with folic acid in women of childbearing age". *The American Journal of Clinical Nutrition,* 84 (1), 156-161.

Li, J., Y. Li, T.-C. Lee, and Q. Huang (2013). "Structure and Physical Properties of Zein/Pluronic F127 Composite Films". *Journal of Agricultural and Food Chemistry,* 61 (6), 1309-1318.

Li, Z., H. Jiang, C. Xu, and L. Gu (2015). "A review: Using nanoparticles to enhance absorption and bioavailability of phenolic phytochemicals". *Food Hydrocolloids,* 43 153-164.

Luo, Y., B. Zhang, M. Whent, L. Yu, and Q. Wang (2011). "Preparation and characterization of zein/chitosan complex for encapsulation of α-tocopherol, and its in vitro controlled release study". *Colloids and Surfaces B: Biointerfaces,* 85 (2), 145-152.

Marini, V. G., S. Martelli, C. Zornio, T. Caon, and V. Soldi (2013). "Zein nanoparticles as a carrier system for terpinen-4-ol". *Internet]. Cited on,* 10 (11).

Mitri, K., R. Shegokar, S. Gohla, C. Anselmi, and R. H. Muller (2011). "Lipid nanocarriers for dermal delivery of lutein: preparation, characterization, stability and performance". *Int J Pharm,* 414 (1-2), 267-75.

Mitri, K., R. Shegokar, S. Gohla, C. Anselmi, and R. H. Muller (2011). "Lutein nanocrystals as antioxidant formulation for oral and dermal delivery". *Int J Pharm,* 420 (1), 141-6.

Momany, F. A., D. J. Sessa, J. W. Lawton, G. W. Selling, S. A. Hamaker, and J. L. Willett (2006). "Structural characterization of alpha-zein". *J Agric Food Chem,* 54 (2), 543-7.

Morris, G. A., J. Castile, A. Smith, G. G. Adams, and S. E. Harding (2011). "The effect of prolonged storage at different temperatures on the particle size distribution of tripolyphosphate (TPP) – chitosan nanoparticles". *Carbohydrate Polymers,* 84 (4), 1430-1434.

Mueller, L. and V. Boehm (2011). "Antioxidant activity of beta-carotene compounds in different in vitro assays". *Molecules,* 16 (2), 1055-69.

Niki, E., N. Noguchi, H. Tsuchihashi, and N. Gotoh (1995). "Interaction among vitamin C, vitamin E, and beta-carotene". *The American Journal of Clinical Nutrition,* 62 (6), 1322S-1326S.

Paiva, S. A. and R. M. Russell (1999). "Beta-carotene and other carotenoids as antioxidants". *J Am Coll Nutr,* 18 (5), 426-33.

Parris, N., P. Cooke, and K. Hicks (2005). "Encapsulation of essential oils in zein nanospherical particles". *J Agric Food Chem,* 53 4788 - 4792.

Parris, N., P. H. Cooke, and K. B. Hicks (2005). "Encapsulation of essential oils in zein nanospherical particles". *J Agric Food Chem,* 53 (12), 4788-92.

Pénicaud, C., N. Achir, C. Dhuique-Mayer, M. Dornier, and P. Bohuon (2011). "Degradation of β-carotene during fruit and vegetable processing or storage: reaction mechanisms and kinetic aspects: a review". *Fruits,* 66 (06), 417-440.

Phillips, R. and B. McClure (1985). "Elevated protein-bound methionine in seeds of a maize line resistant to lysine plus threonine". *Cereal chemistry (USA).*

Podaralla, S. and O. Perumal (2010). "Preparation of Zein Nanoparticles by pH Controlled Nanoprecipitation". *J Biomed Nanotechnol,* 6 312 - 317.

Podaralla, S. and O. Perumal (2012). "Influence of formulation factors on the preparation of zein nanoparticles". *AAPS PharmSciTech,* 13 (3), 919-27.

Regier, M. C., J. D. Taylor, T. Borcyk, Y. Yang, and A. K. Pannier (2012). "Fabrication and characterization of DNA-loaded zein nanospheres". *Journal of nanobiotechnology,* 10 (1), 1-13.

Ron, N., P. Zimet, J. Bargarum, and Y. D. Livney (2010). "Beta-lactoglobulin–polysaccharide complexes as nanovehicles for hydrophobic nutraceuticals in non-fat foods and clear beverages". *International Dairy Journal,* 20 (10), 686-693.

Shi, J., Q. Qu, Y. Kakuda, D. Yeung, and Y. Jiang (2004). "Stability and synergistic effect of antioxidative properties of lycopene and other active components". *Crit Rev Food Sci Nutr,* 44 (7-8), 559-73.

Shukla, R. and M. Cheryan (2001). "Zein: the industrial protein from corn". *Industrial Crops and Products,* 13 (3), 171-192.

Sies, H., W. Stahl, and A. R. Sundquist (1992). "Antioxidant functions of vitamins. Vitamins E and C, beta-carotene, and other carotenoids". *Ann N Y Acad Sci,* 669 7-20.

Sousa, F. F., A. Luzardo-Alvarez, J. Blanco-Mendez, and M. Martin-Pastor (2012). "NMR techniques in drug delivery: application to zein protein complexes". *Int J Pharm,* 439 (1-2), 41-8.

Stella, B., S. Arpicco, M. T. Peracchia, D. Desmaële, J. Hoebeke, M. Renoir, J. D'Angelo, L. Cattel, and P. Couvreur (2000). "Design of folic acid- conjugated nanoparticles for drug targeting". *Journal of pharmaceutical sciences,* 89 (11), 1452-1464.

Stevanovi, Magdalena, Radulovi, Aleksandra, Jordovi, Branka, Uskokovi, and Dragan (2008). "Poly(DL-lactide-co-glycolide) Nanospheres for the Sustained Release of Folic Acid". *Journal of Biomedical Nanotechnology,* 4 (3), 349-358.

Talegaonkar, S., G. Mustafa, S. Akhter, and Z. Iqbal (2010). "Design and development of oral oil-in-water nanoemulsion formulation bearing atorvastatin: in vitro assessment". *Journal of Dispersion Science and Technology,* 31 (5), 690-701.

Teng, Z., Y. Luo, T. Wang, B. Zhang, and Q. Wang (2013). "Development and application of nanoparticles synthesized with folic acid conjugated soy protein". *Journal of agricultural and food chemistry,* 61 (10), 2556-2564.

Terao, J., Y. Minami, and N. Bando (2011). "Singlet molecular oxygen-quenching activity of carotenoids: relevance to protection of the skin from photoaging". *Journal of clinical biochemistry and nutrition,* 48 (1), 57.

Wu, L., J. Zhang, and W. Watanabe (2011). "Physical and chemical stability of drug nanoparticles". *Advanced Drug Delivery Reviews,* 63 (6), 456-469.

Wu, L., J. Zhang, and W. Watanabe (2011). "Physical and chemical stability of drug nanoparticles". *Adv Drug Deliv Rev,* 63 (6), 456-69.

Wu, Y., Y. Luo, and Q. Wang (2012). "Antioxidant and antimicrobial properties of essential oils encapsulated in zein nanoparticles prepared by liquid–liquid dispersion method". *LWT - Food Science and Technology,* 48 (2), 283-290.

Yoo, H. S. and T. G. Park (2004). "Folate receptor targeted biodegradable polymeric doxorubicin micelles". *J Control Release,* 96 (2), 273-83.

Zhang, H., Z. Cai, Y. Sun, F. Yu, Y. Chen, and B. Sun (2012). "Folate- conjugated β-cyclodextrin from click chemistry strategy and for tumor- targeted drug delivery". *Journal of Biomedical Materials Research Part A,* 100 (9), 2441-2449.

Zhang, Q., J. K. Cundiff, S. D. Maria, R. J. McMahon, M. S. Wickham, R. M. Faulks, and E. A. van Tol (2014). "Differential digestion of human milk proteins in a simulated stomach model". *J Proteome Res,* 13 (2), 1055-64.

Zhang, Y., Y. Niu, Y. Luo, M. Ge, T. Yang, L. Yu, and Q. Wang (2014). "Fabrication, characterization and antimicrobial activities of thymol-loaded zein nanoparticles stabilized by sodium caseinate–chitosan hydrochloride double layers". *Food Chemistry,* 142 (0), 269-275.

Zhang, Z., J. Jia, Y. Lai, Y. Ma, J. Weng, and L. Sun (2010). "Conjugating folic acid to gold nanoparticles through glutathione for targeting and detecting cancer cells". *Bioorganic & medicinal chemistry,* 18 (15), 5528-5534.

Zhong, Q. and M. Jin (2009). "Zein nanoparticles produced by liquid–liquid dispersion". *Food Hydrocolloids,* 23 (8), 2380-2387.

Zhou, J., G. Romero, E. Rojas, S. Moya, L. Ma, and C. Gao (2010). "Folic Acid Modified Poly (lactide- co- glycolide) Nanoparticles, Layer- by- Layer Surface Engineered for Targeted Delivery". *Macromolecular Chemistry and Physics,* 211 (4), 404-411.

Zou, T., Z. Li, S. S. Percival, S. Bonard, and L. Gu (2012). "Fabrication, characterization, and cytotoxicity evaluation of cranberry procyanidins-zein nanoparticles". *Food Hydrocolloids*, 27 (2), 293-300.

Zu, Y., Q. Zhao, X. Zhao, S. Zu, and L. Meng (2011). "Process optimization for the preparation of oligomycin-loaded folate-conjugated chitosan nanoparticles as a tumor-targeted drug delivery system using a two-level factorial design method". *International journal of nanomedicine*, 6 3429.

CHAPTER 2
STABILITY AND CONTROLLED RELEASE OF LUTEIN LOADED IN ZEIN NANOPARTICLES WITH AND WITHOUT LECITHIN AND PLURONIC F127 SURFACTANTS

2.1. Introduction

Lutein, a naturally occurring carotenoid, has numerous benefits on human health such as reducing age-related macular degradation (AMD) (Bian et al., 2012), protecting RPE cells from photo-oxidative (Domingos et al., 2014), providing antioxidant activity, and preventing several diseases (Li et al., 2010). Due to its chemical structure, lutein can be easily oxidized and degraded due to light and heat (Mitri et al., 2011) and also has low water solubility, poor absorption, and low bioavailability (Kotake-Nara and Nagao 2011). To take full advantage of its potential as an antioxidant, novel delivery systems have been developed to enhance its ability to be dispersed in water, as well as its physicochemical stability during processing and storage conditions. Delivery systems developed for antioxidant delivery include solid lipid nanoparticles, nanocrystals, and nanoliposomes (Mitri et al., 2011; Mitri et al., 2011; Tan et al., 2013). All these forms were associated with an increase in the stability of the incorporated drug against physical-chemical degradation. Specially, it has been shown that loss of lutein was faster when entrapped in single-layer (SL) emulsion, compared to layer-by-layer (LBL) emulsion, stabilized by gum Arabic (Lim et al., 2014).

The addition of stabilizing surfactants to the delivery systems is hypothesized as one of the simplest and most effective strategies to sustain the release profiles, to improve the physical stability of the nanodelivery system and chemical stability of entrapped fat-soluble drugs (Podaralla and Perumal 2012). An effective example in this regard is development of a core/shell nanoparticle made with lecithin as the core and pluronic

F127 as a shell layer, for delivery of positively charged proteins engineered to provide protection, sustained release, and enhanced stability and functionality of entrapped bioactives (Oh et al., 2006; Choi et al., 2010).

A number of recently published studies provided advancing evidence that protein-based polymeric nanoparticles synthesized from gliadin, soy proteins, lectins, and zein can be successfully made specifically for food applications (Elzoghby et al., 2012). Among these natural potential nanocarriers, zein is particularly interesting as a naturally occurring polymer for synthesis of nanodelivery systems. It is a hydrophobic compound classified as generally recognized as safe (GRAS) as a direct human food ingredient by the Food and Drug Administration (FDA) (Elzoghby et al., 2012). Even though data is available on characteristics of zein nanoparticles loaded with various antioxidants, little is known about stability of lutein entrapped in zein nanoparticles when exposed to various processing and storage conditions, and on the effect of surfactants on the release and stability of lutein under these conditions.

The objective of this chapter was to assess lutein thermal and photo-stability, and lutein release from zein nanoparticles in the presence and absence of lecithin and pluronic F127 co-surfactants. Lutein-loaded zein nanoparticles, made with and without surfactants, were synthesized using a solvent-free liquid-liquid dispersion method. A combination of phospholipid soybean lecithin and tri-block copolymer pluronic F127 was used in the formulation as surfactants to promote physicochemical stability of the nanoparticles and entrapped bioactives. Lutein emulsions were prepared in parallel to be used as a control. Dynamic light scattering (DLS) and transmission electron microscopy (TEM) were used to characterize particle physical stability. Lutein release from

nanoparticles suspended in PBS was quantified in the absence and presence of surfactants; the degradation of released lutein was determined under the same release conditions. In addition, thermal and photo-oxidation of lutein were measured as indicators of lutein chemical stability. The hypothesis was that lutein entrapped in zein nanoparticles was more stable under various storage conditions and that the electrostatic affinity between the zein nanoparticles and surfactants will result in a more sustained release of lutein and improved chemical stability of the entrapped bioactive.

2.2. Materials and Methods

2.2.1. Materials and Reagents

Zein (Z3625), pluronic F127, chloroform, and ethanol were purchased from Sigma Aldrich (St. Louis, MO, USA). Soybean lecithin, hydrochloric acid, and sodium hydroxide were purchased from Fisher Chemical (Fisher Scientific International, Fairlawn, NJ). Lutein was provided by Kemin Foods,L.C. (Iowa, USA). Nanopure water obtained using Nanopure Diamond from Barnstead international (IA, USA) was used for all solution preparation. 100kDA Spectra/POR cellulose ester Biotech membrane tubing and closures was purchased from Spectrum Laboratories Inc. (CA, USA). All other reagents and components used in this study were of analytical grade.

2.2.2. Synthesis of Zein Nanoparticles with Entrapped Lutein

Nanoparticles were synthesized by a liquid-liquid dispersion method, as follows. Briefly, 10 mg of zein was dissolved in 1 mL ethanol-aqueous solution (70:30% (v/v)). A lutein solution was prepared at 0.75 mg/mL with 100% ethanol and was added dropwise to the zein solution at a ratio of 1:1 under mild stirring conditions. The mixture was injected into 7.5 mL of an aqueous phase containing a combination of lecithin and

pluronic F127 0.045:0.09% (w/v) as surfactants. The sample was then processed in a microfluidizer at 30,000 PSI for 3 cycles (M-110P, Microfluidics, MA, USA). Subsequently, the sample underwent evaporation to remove ethanol under vacuum (at approximately 500-600 mmHg) and nitrogen injection (80 mmHg) in a rotovapor (Buchi R-124, Buchi Analytical Inc., DE, USA). The lutein-loaded zein nanoparticles produced after complete evaporation of ethanol were washed by dialysis using a 100kDa Spectra/POR CE membrane (Spectrum Rancho, CA, USA). The nanoparticle suspension was placed in the membrane and suspended in 1.5 L nanopure water for 48 hours; the dialysis medium was changed every 8 hours to remove free surfactants. The suspension was collected and kept at room temperature for further analysis. Zein nanoparticles without surfactants were prepared in parallel using the same method, with the exception that surfactants were not added to the aqueous phase. The lutein emulsion made with surfactants followed the same protocol was served as a control.

2.2.3. Particle Size, Polydispersity Index (PDI), and Zeta Potential Analyses

Freshly-made zein nanoparticle samples were characterized by measuring average diameter size, PDI, and zeta potential by dynamic light scattering (DLS), using a Malvern Zetasizer Nano ZS (Malvern Instruments Ltd., Worcestershire, U.K.). Before the measurements were taken, samples were prepared at a final concentration of 0.1-0.3 mg/mL, optimum for the instrument. All measurements were performed in triplicate.

2.2.4. Morphology Analysis

Morphology of freshly-made zein nanoparticle was observed by transmission electron microscopy (TEM). One droplet of the sample was placed on a copper grid of

400 mesh with a carbon film, and the excess sample was removed with a filter paper. Uranyl acetate was used as a negative stain to improve the contrast of the sample.

2.2.5. Entrapment Efficiency (EE) Measurement

One milliliter of the freshly-made lutein-loaded zein nanoparticle sample was centrifuged at 64,000 g for 1 hour, from which 95% of particles were recovered (data not shown). The supernatant and the nanoparticle pellet were collected. Both samples were broken by ethanol and then lutein was extracted with chloroform (1:1 ratio). The relative solubility of lutein in chloroform (6000 mg/L) is 20 times higher than that in ethanol (300 mg/L) (Craft and Soares 1992). The concentration of lutein was measured using a UV/Vis spectrophotometer (GENESYS 6:Thermo Spectronic) with glass cells of 1 cm path length recorded at 445 nm. The absorbance value was converted to lutein concentration based on the standard curve for lutein in 1:1 ethanol and chloroform. Entrapment efficiency (%) was estimated as the ratio of lutein amount in pellet to theoretical lutein entrapped as described by $\frac{\text{Lutein amount in pellet}}{\text{Theoretical amount of available lutein}} \text{ x } 100 =$ % EE. All measurements were performed in triplicate.

2.2.6. Lutein Release from Zein Nanoparticles in Phosphate-Buffered Saline (PBS)

The release of the entrapped lutein from zein nanoparticles was studied in 0.01 M phosphate-buffered saline (PBS) solution (pH 7.4) at 37°C; 0.5% of Tween 20 was added to PBS to improve the solubility of lutein released. Briefly, 10 mL of freshly-prepared nanoparticles were added to 20 mL of Tween 20 enhanced PBS and mixed thoroughly. The mixture was divided and placed into 1.5 mL centrifuge tubes, placed into a shaking incubator (C25KC incubator shaker, New Brunswick Scientific, NJ, USA) at 37°C and 100 rpm. At pre-defined time intervals, a centrifuge tube was sampled and

centrifuged at 64,000 g (Allegra 64R centrifuge, Beckman coulter, Inc., CA, USA) for 1 hour. The supernatant was removed and extracted with ethanol and chloroform (1:1 ratio) and then vortexed for 10 minutes. The extracted lutein was determined in the supernatant by measuring the absorbance at 445 nm using a UV/Vis spectrophotometer as described under entrapment efficiency section. The wavelength was selected to avoid interference from degraded products of lutein, consisting of low-molecular-weight and short-chain aldehydes and ketones, with a maximum absorbance ranging from 270 to 345 nm (Landrum 2009). All measurements were performed in triplicate.

2.2.7. Degradation of Lutein Entrapped in Zein Nanoparticles

The degradation of lutein entrapped in zein nanoparticles (with and without surfactants) and lutein entrapped in surfactant-stabilized emulsion was determined by measuring and adding the amount of lutein detected in both pellet and supernatant under the same release condition.

2.2.8. Physical-Chemical Stability of Zein Nanoparticles with Entrapped Lutein

Freshly-made samples were stored in darkness at three different temperatures: 4°C in a refrigerator, 25°C at room temperature and 40°C in an incubator over one month. Samples were monitored for changes in average particle size, surface characteristic, and entrapment efficiency at the sampling time points of 7, 15, and 30 days of storage. All experiments were performed in triplicate.

2.2.9. Photo-Chemical Stability of Lutein Entrapped in Zein Nanoparticles

Nanoparticle and emulsion samples were placed in transparent glass vials and stored in a lightproof cabinet where they were exposed to 365 nm UV lamps (100 W: Blak-Ray model B 100AP) for up to 10 hours. At exposure time intervals (0.5, 1, 2, 3, 5,

7, and 10 hours), 1 mL was withdrawn from each sample and then extracted and analyzed by measuring lutein concentration using UV-Vis spectrophotometer (GENESYS 6: Thermo Spectronic) at 445 nm. The experiment was performed in triplicate.

2.2.10. Degradation Reaction Kinetics

A general reaction rate for the lutein degradation and release kinetics can be described by $-\frac{d[C]}{dt} = k[C]^n$: where *C* is the lutein amount (μg), *k* is the reaction rate constant, and *n* is the order of the reaction. The correlation coefficient (R^2) was used as an indicator of the best fitting of the kinetic models for lutein release and degradation studies. The degradation of lutein against UV exposure, followed first-order kinetic as described by $\ln(\frac{[C]}{[C_0]}) = -kt$, similar to the results found in other studies (Lim et al., 2014; Dhuique-Mayer et al., 2007; Aparicio-Ruiz et al., 2011; Abdel-Aal el et al., 2010). Lutein degradations under PBS conditions and storage as a function of time and temperatures followed second-order kinetics as described by $\frac{1}{[C]} = \frac{1}{[C_0]} + kt$: where *C* is the lutein amount (μg) at time *t*, C_0 is the initial amount of lutein (μg), *t* is the time (hours or days) and *k* is the reaction rate derived from the slope of linear regressions.

2.2.11. Data Statistical Analysis

All experiments were performed in triplicate and the results were reported as the mean ± standard error. Statistical analysis was performed in SAS (version 9.4, SAS Institute Inc., NC, USA). The analysis of variance (ANOVA) was used to determine significant differences between the systems. The significance level (*P*) was set at 0.05.

2.3. Results and Discussion

2.3.1. Physicochemical Characterizations

A liquid-liquid dispersion method was successfully used to synthesize lutein-loaded zein nanoparticles in the presence and absence of surfactants. The combination of lecithin and pluronic F127 was used to stabilize the nanoparticles. Pluronic F127 is a hydrophilic non-ionic surfactant copolymer consisting of a hydrophobic block of polypropylene located between two hydrophilic blocks of polyethylene glycol. Gel formation at higher temperatures efficiently overcomes the natural brittleness of zein, supporting its delivery system application (Li et al., 2013). Lecithin, a phospholipid food emulsifier or stabilizer, has a hydrophilic head, phosphatidylcholine (PC) and two hydrophobic tails, phosphatidylethanolamine (PE) and phosphotidylinositol (PI) (Wang and Wang 2008).

Because of its partly mixed structure, lecithin can be used as an effective and stable emulsifier to interact simultaneously with both hydrophilic and hydrophobic substances (Choi et al., 2010). One or more layers of lecithin cover the surface of the hydrophobic zein nanoparticles, with lutein entrapped inside the zein matrix by electrostatic interaction. The hydrophilic head of lecithin connects with hydrophilic polyethylene glycol of pluronic F127 and the hydrophobic polypropylene possibly connects with zein matrix resulting in a hydrophilic zein nanoparticle loaded with hydrophobic lutein, which is useful to disperse this bioactive to the aqueous environment while protecting it from degradation (Figure 2.1).

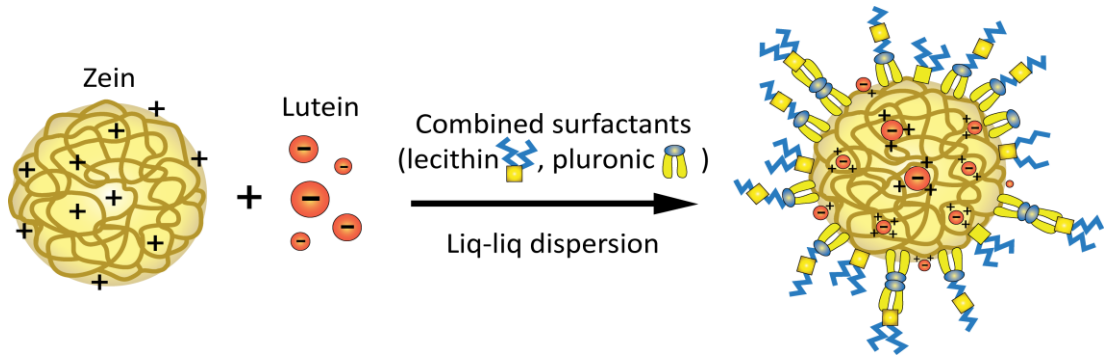

Figure 2.1. Schematic formation of lutein-loaded zein nanoparticle stabilized by lecithin and pluronic F127 surfactants

Lutein-loaded zein nanoparticles and unloaded nanoparticles, with and without surfactants, were characterized immediately after purification (Table 2.1). Average particle size, PDI, and zeta potential of freshly-made samples were measured after 24 hours dialysis in buffer (pH 7.4) (Podaralla and Perumal 2012). The statistical results of size, PDI, and zeta potential showed no significant difference between zein nanoparticles made with and without surfactants. The average particle size of lutein loaded in zein nanoparticles with and without surfactants was 216.5±29 nm and 156.1±18 nm, respectively. While zein nanoparticles formed in the presence of surfactants had a relatively small polydispersity (less than 0.3), a higher PDI range of 0.33-0.48 was observed for nanoparticles made without combined surfactants.

Table 2.1. Characteristics of unloaded and lutein-loaded zein nanoparticles made with surfactants (SF) or without surfactants (NSF)

Sample [a]	**Size (nm)**	**PDI (a.u)**	**Zeta Potential (mV)**	**EE (%)**
ZN SF	208.8±8.0	0.19±0.04	-47.6±1.6	-
LTZN SF	216.5±29	0.26±0.09	-30.9±3.3	83.0±5.8*
ZN NSF	149.2±5.5	0.48±0.07	-31.9±4.3	-
LTZN NSF	156.1±18	0.33±0.06	-21.0±8.6	69.1±11.4

Note: Values are expressed as mean ± standard error (n=3). [a] ZN and LTZN represent formulations of zein nanoparticles and lutein-loaded zein nanoparticles, SF and NSF represent formulations with and with no surfactants respectively. Mass ratio of zein:lutein was 1:0.075 (%, w/w) and mass ratio of lecithin:pluronic F127 was 0.045:0.09 (%, w/v). * shows statistically significant difference.

The size results were confirmed by TEM (Figure 2.2). Particles with surfactants showed a spherical shape with a rough surface, with some particles connected in a surfactant mesh (Figure 2.2 A and B). Nanoparticles without surfactants showed smaller size, with more spherical morphology, but were less uniform in size and more likely to agglomerate (Figure 2.2 C and D) resulting in higher PDI values as measured by DLS. Similar zein nanoparticle images were reported in other studies (Zhang et al., 2014; Parris et al., 2005).

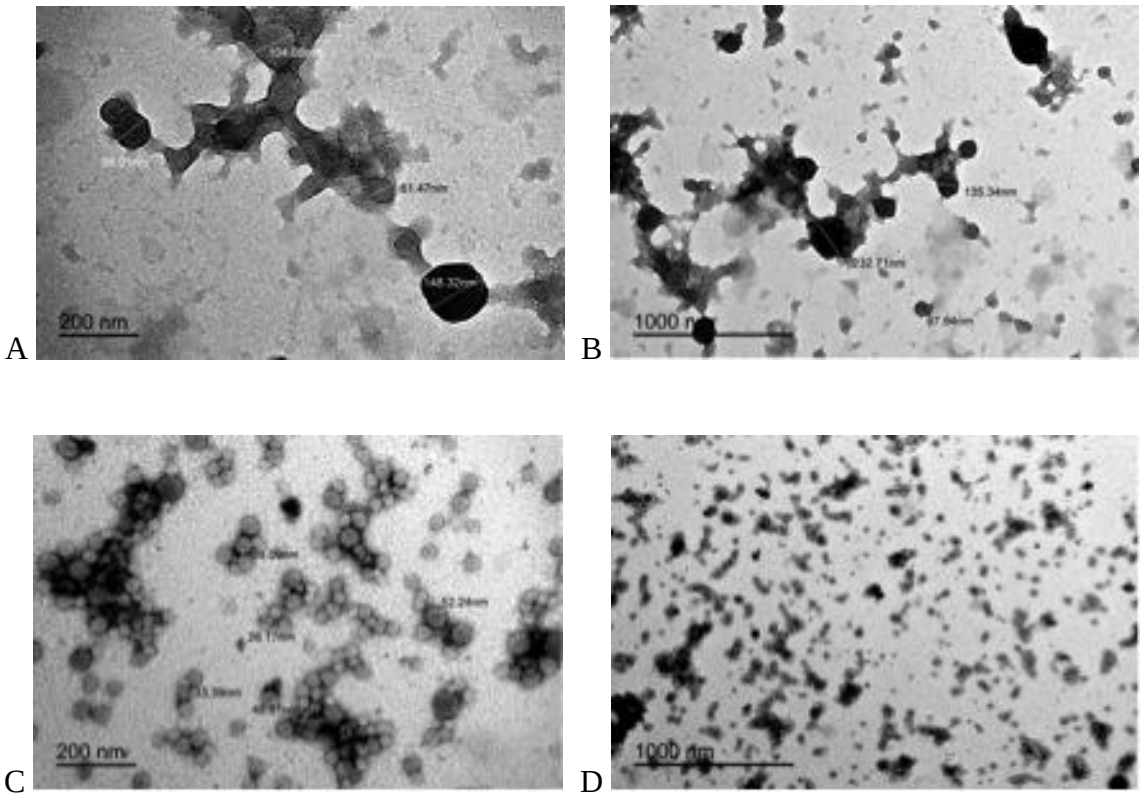

Figure 2.2. Transmission Electron Microscope (TEM) images of zein nanoparticles with surfactants (A and B) and without surfactants (C and D)

Zeta potential has long been accepted as a good measure for assessing stability of a nanoparticles system. A high degree of stability of the nanodelivery system is expected at zeta potential values higher than +30 mV or lower than -30 mV on the basis

of charge repulsion between the nanoparticles (Murdock et al., 2008). Particles covered by surfactants were found to be more negatively charged (-47.6±1.6 mV) than particles without surfactants (-31.9±4.3 mV), indicating a good stability of the surfactant stabilized particles. Entrapment of lutein resulted in a change in zeta potential from -30.9±3.3 mV to a less negative value of -21.0±8.6 mV for particles made without surfactants. The hydrophobic interaction between lutein and zein nanoparticles as nonpolar molecules contributed to the rearrangement in the zein structure to accommodate the entrapped bioactive, resulting in the observed zeta potential change.

The presence of surfactants not only affected average particle size, PDI, and zeta potential, but also lutein entrapment inside the zein matrix. Without surfactants, entrapment efficiency was around 69.1±11.4%; with the addition of surfactants to the system, which resulted in a thicker and denser zein matrix, the entrapment efficiency increased to 83±5.8%, revealing a statistically significant difference between the two systems. This result was expected; Xu and Hanna (Xu and Hanna 2006), suggested that addition of surfactants to the system can stabilize particles and therefore increase entrapment efficiency.

Both lecithin, an anionic phospholipid (Wang and Wang 2008) which forms an ionic complex with positively charged protein, and the added pluronic F127, which were used simultaneously to stabilize the nanoparticles, were found to confer a negative charge to the particles suitable for inducing the electrostatic interactions that allowed for good nanoparticle stability while increasing lipophilic drug loading (Oh et al., 2006).

2.3.2. Lutein Release from Zein Nanoparticles in PBS

Phosphate buffered saline (PBS) is a water-based salt buffer solution commonly used in biological research, particularly for testing drug release. The release kinetic of lutein from zein nanoparticles made with and without surfactants in an aqueous buffer PBS was evaluated (Figure 2.3). The release profile of zein nanoparticles can be described as a two-phase pattern, with an initial-burst release within 24 hours followed by zero-order release profile (Table 2.3). For particles made without surfactants (LTZN NSF), lutein released in the initial-burst phase amounted for 43.26%, whereas zein nanoparticles made with surfactants (LTZN SF) only released 19.83% lutein (Figure 2.3). The results are not surprising as surface-associated lutein was expected to be released quickly from the surface of the particles when surfactants were not present to inhibit lutein release. Release of lutein after 24 hours followed zero-order kinetics (Table 2.3) with 51.51% lutein released at 168 hours from nanoparticles without surfactants versus only 42.67% in the presence of surfactants (Figure 2.3). Hydrophobic interaction between lecithin, lutein, and the polypropylene chains of pluronic F127 inhibited the hydrolytic degradation of zein and slowed the release of lutein. In the absence of surfactants rapid protein swelling resulted in a faster release of the entrapped bioactive by diffusion through aqueous channels formed in the hydrated swelled zein matrix (Choi et al., 2010). The results supported the hypothesis that the electrostatic affinity between the zein nanoparticles and surfactants; the combined lecithin and pluronic F127, were responsible for a more sustained release of lutein. Statistical results supported that release of lutein from zein nanoparticles with surfactant was significantly different than release of lutein from zein nanoparticles without surfactant.

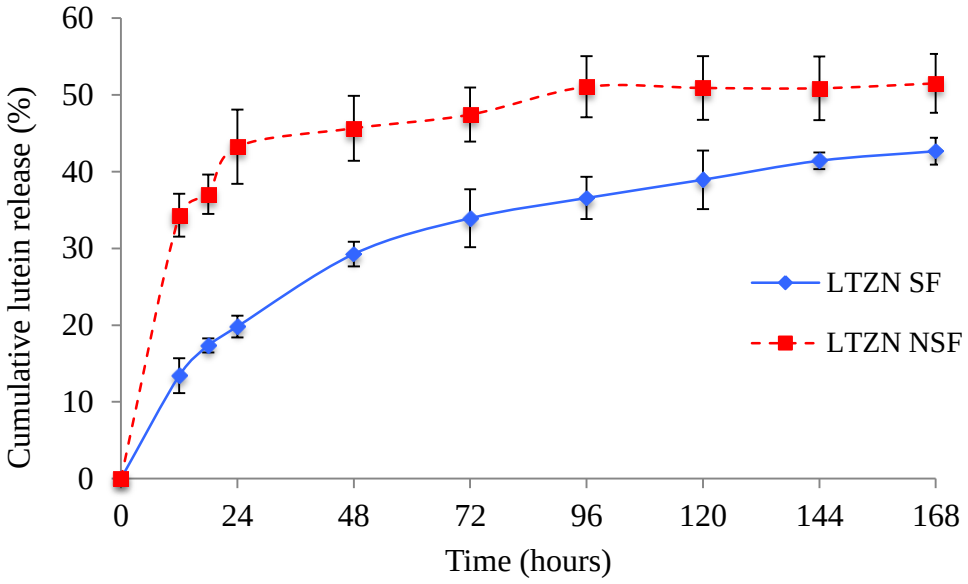

Figure 2.3. Two-pattern release profiles consisting of an initial burst release within 24 hours and the following zero-order release of lutein from zein nanoparticles made with (LTZN SF) and without surfactants (LTZN NSF) in PBS solution (pH 7.4) at 37°C and 100 rpm for 7 days

2.3.3. Entrapped Lutein Degradation in PBS

Lutein is more susceptible to degradation than common carotenes due to conjugated double bonds and the two hydroxyl groups, considered more heat sensitive (Dhuique-Mayer et al., 2007). The degradation of lutein was assessed for lutein entrapped in zein nanoparticles with (LTZN SF) and without surfactants (LTZN NSF) and the result was compared to that of lutein in emulsified form with the same surfactants (LTEM SF) (Figure 2.4). Lutein degradation profiles followed second-order kinetics with no significant different values (0.00003-0.00004) of the degradation rate constant (k) among all systems studied (Table 2.3). Emulsified lutein degraded rapidly to approximately 40% under PBS condition after 168 hours, in accordance with findings reported by Shi and Chen (Shi and Chen 1997), who found that 25-30% pure lutein in distilled water degraded at the same time.

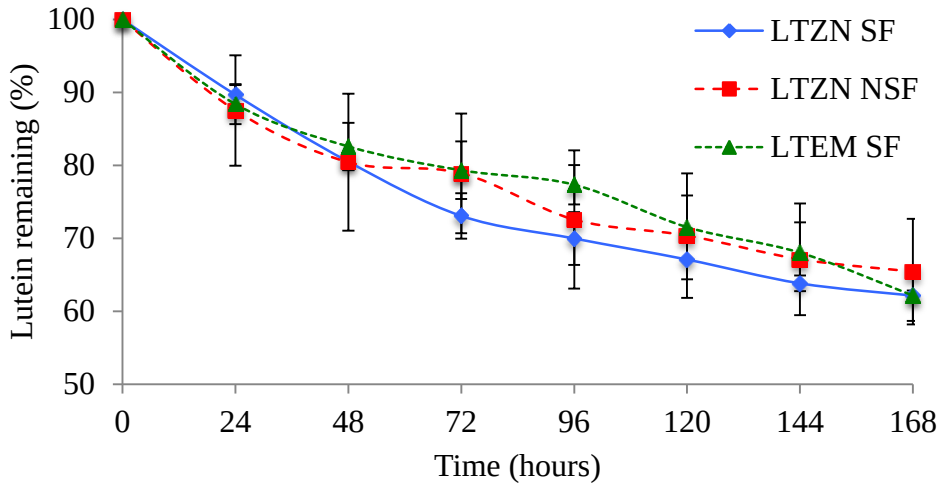

Figure 2.4. Degradation profiles following second-order reaction of lutein loaded in zein nanoparticles with (LTZN SF) and without (LTZN NSF) surfactants and lutein emulsion made with surfactants (LTEM SF) in PBS solution (pH 7.4) at 37°C and 100 rpm for 7 days

2.3.4. Physical-Chemical Stability as a Function of Time and Temperature

Physical stability of zein nanoparticles was investigated at 4°C, 25°C, and 40°C over 30 days by measuring size, PDI, and zeta potential. Chemical stability of entrapped lutein was assessed in parallel, by measuring the absorbance using a UV/Vis spectrophotometer at 445 nm (Table 2.2). Zein nanoparticles with and without surfactants were stable at low temperature, measuring between 156.1±18 to 216.5±29 nm when stored at 4°C for 30 days. Nanoparticles increased in size over time when stored at higher temperature, especially in the absence of surfactants. For example, while size of nanoparticles with surfactants-increased to 380.5±51 nm over 30 days of storage at 25°C, particles without surfactants measured up to 3103±332 nm at the same temperature. At 40°C, sizes bigger than 1 μm were detected after 7 days of storage for the nanoparticles made without surfactants. The PDI generally increased with temperature and storage time

(from 0.27 to 0.80). Zeta potential ranged from -18 mV to -25 mV for nanoparticles without surfactants, and between -15.2 mV to -38 mV for particles made with surfactants.

Table 2.2. Characteristics of lutein-loaded in zein nanoparticles at different storage temperatures over 30 days

Sample	Temperature	Time (days)	Size (nm)	PDI (a.u)	Zeta Potential (mV)
LTZN SF	4°C	0	216.5±50	0.27±0.05	-30.9±3.3
		7	195.7±19	0.29±0.05	-31.1±10.8
		15	183.0±26	0.27±0.06	-32.2±10.7
		30	168.6±2	0.27±0.04	-33.0±10.8
	25°C	0	216.5±50	0.27±0.05	-30.9±3.3
		7	170.8±65	0.38±0.05	-23.3±2.4
		15	221.0±74	0.35±0.06	-21.8±9.5
		30	380.8±51	0.36±0.07	-15.2±0.3
	40°C	0	216.5±50	0.27±0.05	-30.9±3.3
		7	134.5±40	0.54±0.07	-38.0±1.9
		15	203.1±49	0.24±0.06	-31.8±7.4
		30	229.5±27	0.29±0.03	-29.5±2.9
LTZN NSF	4°C	0	156.1±18	0.26±0.06	-21.0±8.6
		7	142.4±32	0.32±0.11	-23.8±1.0
		15	189.2±55	0.26±0.07	-24.6±1.7
		30	198.9±47	0.39±0.13	-25.0±2.6
	25°C	0	156.1±18	0.26±0.06	-21.0±8.6
		7	567.7±203	0.56±0.07	-24.6±1.7
		15	1406.1±279	0.47±0.13	-23.7±1.5
		30	3103±332	0.58±0.15	-23.6±1.4
	40°C	0	156.1±18	0.26±0.06	-21.0±8.6
		7	1096.1±253	0.58±0.05	-18.0±2.7
		15	2434.5±535	0.73±0.19	-21.0±0.6
		30	3599.5±94	0.80±0.10	-22.7±4.2

Note: Values are expressed as mean ± standard error (n=3).

The surfactants not only provided long-term storage stability over 30 days for the nanosuspension, but they also delayed the degradation of lutein (Figure 2.5). Only 26% of entrapped lutein was degraded after 30 days at 25°C when entrapped in LTZN SF, compared to 54% which degraded at the same time when entrapped in LTZN NSF.

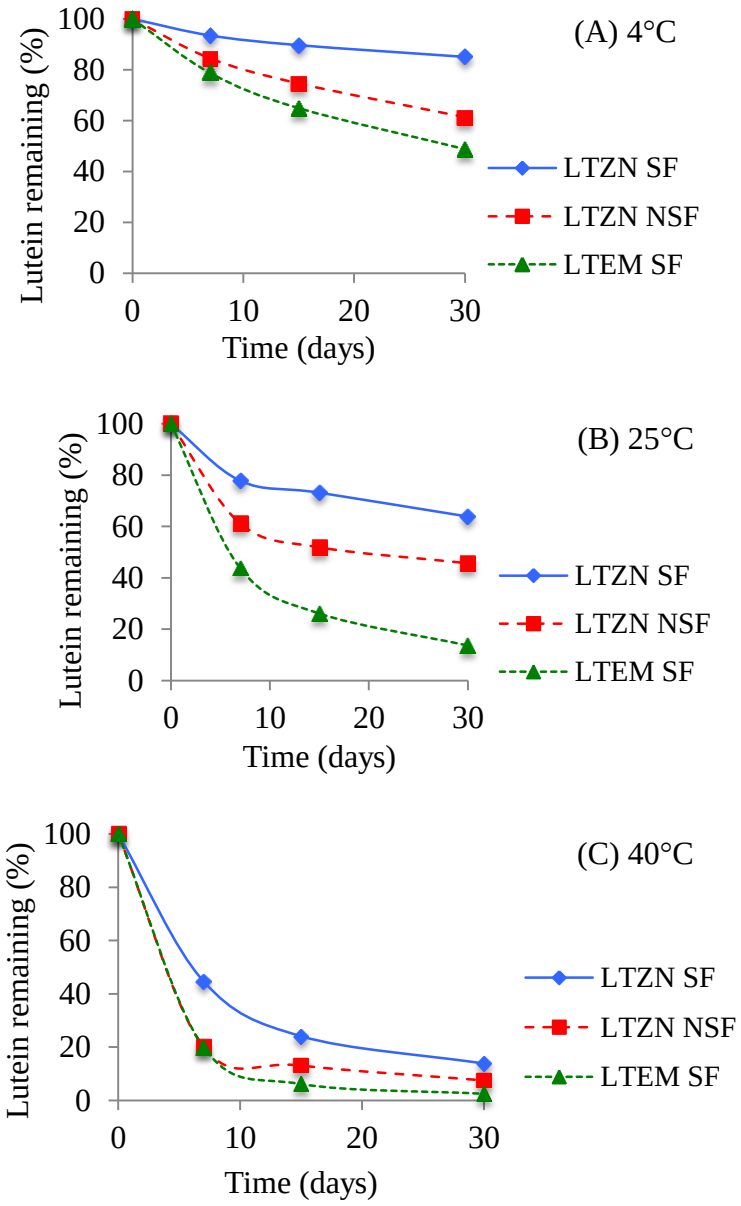

Figure 2.5. Degradation profiles following second-order reaction of lutein entrapped in zein nanoparticles at different storage temperatures (A: 4°C, B: 25°C, and C: 40°C) over 30 days

Similar trends were found at 40°C in both particles; 13.8% and 7.5% of retained lutein remained in the lutein-zein nanoparticles with and without surfactants, respectively. Emulsified lutein degraded faster than lutein entrapped in zein nanoparticles at all temperatures. Lutein degradation under various temperatures for 30 days followed

second-order kinetics, similarly to degradation of lutein in particles suspended in PBS for 7 days (Table 2.3). The lowest degradation rate (*k*) values of nanoentrapped lutein were also found in the presence of zein nanoparticles in the presence of surfactants at all storage temperatures. Increased temperature resulted in increasing the degradation for all systems. Thus, it is concluded that while the preferred storage condition of lutein in 4°C (Lai and Guo 2011), stability of lutein can be improved by loading it in surfactant covered zein nanoparticles even at higher temperatures.

2.3.5. Photo-Chemical Stability against UV Exposure

Photochemical stability against UV light of lutein loaded in zein nanoparticles with surfactant and without surfactant was compared to lutein emulsified form made with the same surfactants. There was statistical significance in the surfactants and time as main effects. Emulsified lutein underwent photochemical degradation very quickly (Figure 2.6). After 10 hours, only 1.42% entrapped lutein remained in the lutein emulsions whereas 15.91% lutein was protected by entrapment in zein nanoparticles without surfactants (Figure 2.6). The zein nanoparticles combined with surfactants were able to provide the greatest protection against UV light-induced lutein degradation, with 46.53% of lutein remaining inside the zein nanoparticles after UV light exposure for 10 hours.

The lowest degradation rate constant was found for lutein loaded in zein nanoparticles combined with surfactants (0.0753) whereas zein nanoparticles without surfactants was higher (0.1869) indicating that the rate of lutein degradation in the presence of zein nanoparticles plus the effect of surfactants was noticeably retarded compared with lutein delivered in emulsified form (0.4093) (Table 2.3).

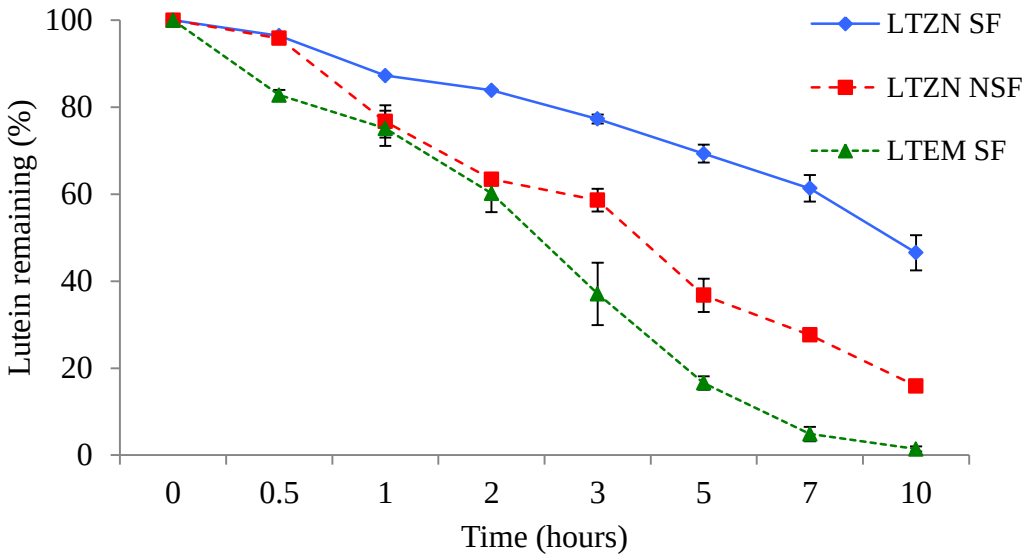

Figure 2.6. Photo-chemical stability profiles following first-order reaction of lutein loaded in zein nanoparticles with (LTZN SF) and without surfactants (LTZN NSF) and emulsified lutein with surfactants (LTEM SF) exposed to UV light for 10 hours

The improved photo-chemical stability of lutein against UV light when entrapped in zein nanoparticles was mainly based on the competitive absorption of UV photons by zein. Zein has been proven to absorb UV due to aromatic amino acids such as phenylalanine in its sequence (Stoscheck 1990). Moreover, the effect of surfactants surrounding zein nanoparticles was another contributor for improved stability of lutein. Lecithin was successfully used as UV protectant previously (Sundaram and Curry 1996). The possible mechanism for the ability of lecithin to protect lutein from degradation was due to energy transfer from the excited lutein species to lecithin. Thus, photo-stability against UV light of the entrapped lutein was significantly improved by the UV absorption of zein nanoparticles with the support of the combined lecithin and pluronic F127 as surfactants.

Table 2.3. Fitting model for release and degradation of lutein-loaded zein nanoparticles

Experiment	**Sample**	**Time**	**Kinetic model**	**K**	**R^2**
Release	LTZN SF	0-24 hours	Zero-order (Initial burst)	0.90930	0.95203
	LTZN NSF			2.02800	0.88626
	LTZN SF	24-168 hours	Zero-order	0.00120	0.83448
	LTZN NSF			0.01270	0.92693
Degradation	LTZN SF	168 hours	2^{nd} order	0.00004	0.96389
	LTZN NSF			0.00003	0.91575
	LTEM SF			0.00003	0.97666
Physical stability	LTZN SF 4°C LTZN SF 25°C LTZN SF 40°C	30 days	2^{nd} order	0.00006	0.92430
				0.00020	0.84325
				0.00210	0.99788
	LTZN NSF 4°C LTZN NSF 25°C LTZN NSF 40°C	30 days	2^{nd} order	0.00020	0.99243
				0.00050	0.75685
				0.00420	0.98458
	LTEM SF 4°C LTEM SF 25°C LTEM SF 40°C	30 days	2^{nd} order	0.00040	0.99878
				0.00210	0.99502
				0.01210	0.96126
Photo-chemical stability	LTZN SF	10 hours	1^{st} order	0.07530	0.98454
	LTZN NSF			0.18690	0.99256
	LTEM SF			0.40930	0.98301

Note: LTZN and LTEM represent formulations of lutein-loaded zein nanoparticles and emulsified lutein, SF and NSF represent formulations with and with no surfactants respectively. K and R^2 represent the degradation rate constant and correlation coefficient, respectively.

2.4. Conclusion

Zein nanoparticles loaded with 7.5% lutein stabilized by the combined lecithin and pluronic F127 surfactants were successfully synthesized using a solvent-free liquid-liquid dispersion method. The addition of surfactants increased particle size and improved polydispersity index. Zeta potential slightly changed, and entrapment efficiency increased significantly. In the presence of the surfactants, the burst release decreased and the release kinetic was subsequently sustained. Zein nanoparticles showed a great ability to protect lutein from degradation under various storage conditions as

compared to the emulsified lutein. The preferred storage condition of lutein-loaded zein nanoparticles with surfactants was 4°C for 30 days. In addition, this complex formulation provided a good protection against UV light for 10 hours. Based on characteristics, release, and stability data, it was suggested that with the addition of surfactants to improve entrapment efficiency of hydrophobic bioactives and to protect lutein against chemical degradation, zein nanoparticles could provide better protection against bioactive losses during thermal and neutral conditions than other delivery systems such as emulsions.

2.5. References

Abdel-Aal el, S. M., J. C. Young, H. Akhtar, and I. Rabalski (2010). "Stability of lutein in wholegrain bakery products naturally high in lutein or fortified with free lutein". *J Agric Food Chem,* 58 (18), 10109-17.

Aparicio-Ruiz, R., M. I. Mínguez-Mosquera, and B. Gandul-Rojas (2011). "Thermal degradation kinetics of lutein, β-carotene and β-cryptoxanthin in virgin olive oils". *Journal of Food Composition and Analysis,* 24 (6), 811-820.

Bian, Q., S. Gao, J. Zhou, J. Qin, A. Taylor, E. J. Johnson, G. Tang, J. R. Sparrow, D. Gierhart, and F. Shang (2012). "Lutein and zeaxanthin supplementation reduces photooxidative damage and modulates the expression of inflammation-related genes in retinal pigment epithelial cells". *Free Radic Biol Med,* 53 (6), 1298-307.

Choi, W. I., K. C. Yoon, S. K. Im, Y. H. Kim, S. H. Yuk, and G. Tae (2010). "Remarkably enhanced stability and function of core/shell nanoparticles composed of a lecithin core and a pluronic shell layer by photo-crosslinking the shell layer: In vitro and in vivo study". *Acta Biomaterialia,* 6 (7), 2666-2673.

Craft, N. E. and J. H. Soares (1992). "Relative solubility, stability, and absorptivity of lutein and .beta.-carotene in organic solvents". *Journal of Agricultural and Food Chemistry,* 40 (3), 431-434.

Dhuique-Mayer, C., M. Tbatou, M. Carail, C. Caris-Veyrat, M. Dornier, and M. J. Amiot (2007). "Thermal degradation of antioxidant micronutrients in citrus juice: kinetics and newly formed compounds". *J Agric Food Chem,* 55 (10), 4209-16.

Domingos, L. D., A. A. Xavier, A. Z. Mercadante, A. J. Petenate, R. A. Jorge, and W. H. Viotto (2014). "Oxidative stability of yogurt with added lutein dye". *J Dairy Sci,* 97 (2), 616-23.

Elzoghby, A. O., W. M. Samy, and N. A. Elgindy (2012). "Protein-based nanocarriers as promising drug and gene delivery systems". *Journal of Controlled Release,* 161 (1), 38-49.

Kotake-Nara, E. and A. Nagao (2011). "Absorption and metabolism of xanthophylls". *Marine drugs,* 9 (6), 1024-1037.

Lai, L. F. and H. X. Guo (2011). "Preparation of new 5-fluorouracil-loaded zein nanoparticles for liver targeting". *Int J Pharm,* 404 (1-2), 317-23.

Landrum, J. T. 2009. *Carotenoids: physical, chemical, and biological functions and properties*: CRC Press.

Li, B., F. Ahmed, and P. S. Bernstein (2010). "Studies on the singlet oxygen scavenging mechanism of human macular pigment". *Arch Biochem Biophys,* 504 (1), 56-60.

Li, J., Y. Li, T. C. Lee, and Q. Huang (2013). "Structure and physical properties of zein/pluronic f127 composite films". *J Agric Food Chem,* 61 (6), 1309-18.

Lim, A. S. L., C. Griffin, and Y. H. Roos (2014). "Stability and loss kinetics of lutein and β-carotene encapsulated in freeze-dried emulsions with layered interface and trehalose as glass former". *Food Research International,* 62 (0), 403-409.

Mitri, K., R. Shegokar, S. Gohla, C. Anselmi, and R. H. Muller (2011). "Lipid nanocarriers for dermal delivery of lutein: preparation, characterization, stability and performance". *Int J Pharm,* 414 (1-2), 267-75.

Mitri, K., R. Shegokar, S. Gohla, C. Anselmi, and R. H. Muller (2011). "Lutein nanocrystals as antioxidant formulation for oral and dermal delivery". *Int J Pharm,* 420 (1), 141-6.

Murdock, R. C., L. Braydich-Stolle, A. M. Schrand, J. J. Schlager, and S. M. Hussain (2008). "Characterization of nanomaterial dispersion in solution prior to in vitro exposure using dynamic light scattering technique". *Toxicological Sciences,* 101 (2), 239-253.

Oh, K. S., S. K. Han, H. S. Lee, H. M. Koo, R. S. Kim, K. E. Lee, S. S. Han, S. H. Cho, and S. H. Yuk (2006). "Core/Shell nanoparticles with lecithin lipid cores for protein delivery". *Biomacromolecules,* 7 (8), 2362-7.

Oh, K. S., S. K. Han, H. S. Lee, H. M. Koo, R. S. Kim, K. E. Lee, S. S. Han, S. H. Cho, and S. H. Yuk (2006). "Core/Shell Nanoparticles with Lecithin Lipid Cores for Protein Delivery". *Biomacromolecules,* 7 (8), 2362-2367.

Parris, N., P. H. Cooke, and K. B. Hicks (2005). "Encapsulation of essential oils in zein nanospherical particles". *J Agric Food Chem,* 53 (12), 4788-92.

Podaralla, S. and O. Perumal (2012). "Influence of Formulation Factors on the Preparation of Zein Nanoparticles". *AAPS PharmSciTech,* 13 (3), 919-927.

Shi, X. M. and F. Chen (1997). "Stability of lutein under various storage conditions". *Food / Nahrung,* 41 (1), 38-41.

Stoscheck, C. M. (1990). "Quantitation of protein". *Methods Enzymol,* 182 50-68.

Sundaram, K. M. S. and J. Curry (1996). "Photostabilization of the botanical insecticide azadirachtin in the presence of lecithin as UV protectant". *Journal of Environmental Science and Health, Part B,* 31 (5), 1041-1060.

Tan, C., S. Xia, J. Xue, J. Xie, B. Feng, and X. Zhang (2013). "Liposomes as vehicles for lutein: preparation, stability, liposomal membrane dynamics, and structure". *Journal of agricultural and food chemistry,* 61 (34), 8175-8184.

Wang, G. and T. Wang (2008). "Oxidative stability of egg and soy lecithin as affected by transition metal ions and pH in emulsion". *J Agric Food Chem,* 56 (23), 11424-31.

Xu, Y. and M. A. Hanna (2006). "Electrospray encapsulation of water-soluble protein with polylactide. Effects of formulations on morphology, encapsulation efficiency and release profile of particles". *Int J Pharm,* 320 (1-2), 30-6.

Zhang, Y., Y. Niu, Y. Luo, M. Ge, T. Yang, L. Yu, and Q. Wang (2014). "Fabrication, characterization and antimicrobial activities of thymol-loaded zein nanoparticles stabilized by sodium caseinate–chitosan hydrochloride double layers". *Food Chemistry,* 142 (0), 269-275.

CHAPTER 3
THE POTENTIAL OF ZEIN NANOPARTICLES TO PROTECT ENTRAPPED BETA-CAROTENE IN THE PRESENCE OF MILK UNDER SIMULATED GASTROINTESTINAL (GI) CONDITIONS

3.1. Introduction

Zein, a three-quarter hydrophobic maize protein, consists of at least 12 amino acid signal peptides, especially leucine and proline, which are related to the antioxidant activity specific to peptide hydrolysates (Peña‐Ramos et al., 2004; Sodek and Wilson 1971; Geraghty et al., 1981). Because of its outstanding characteristics of interest to the food industry, zein has been used in formation of coatings and films. Many synthesis methods have been developed to form zein nanoparticles. A liquid-liquid dispersion method was used by Zhong and Jin, 2009 as a simple and scalable process to produce zein nanoparticles with a diameter of 100-200 nm (Zhong and Jin 2009). Additionally, Oh et al., 2006 and Choi et al., 2010 succeeded in making emulsified lecithin core/pluronic F127 shell nanoparticles as an effective sustained-release system for positively-charged proteins to protect the entrapped compounds and enhance their stability and functionality (Oh et al., 2006; Choi et al., 2010).

To study the stability of compounds entrapped in zein nanoparticles under physiological conditions, essential oils were incorporated into zein nanoparticles. The particles were subjected to digestion with pepsin at a concentration ratio of 10:1 and completely digested after 52 hours in phosphate-citrate buffer pH 3.5 at 37°C (Parris et al., 2005). Wu et al., 2012 studied the effect of nanoparticles on antioxidant properties of essential oils. They concluded that entrapping essential oils in zein nanoparticles could

increase their solubility without affecting their antioxidant ability, thus furthering the use of nanodelivery systems in foods (Wu et al., 2012).

β-carotene is a major component of provitamin A carotenoids with numerous benefits (Shi et al., 2004; Terao et al., 2011; Boon et al., 2010; Regier et al., 2012; Paiva and Russell 1999). It is for these antioxidant health benefits that there is an increasing interest in fortifying food or pharmaceutical products with β-carotene. Due to its ability to scavenge active free radicals, β-carotene can safely protect cellular tissues from lethal events such as peroxidation of unsaturated lipids (Pénicaud et al., 2011). β-Carotene can be cleaved by oxygenase enzymes into central cleavage retinal and eccentric cleavage products called apo-carotenoids in digestive system (Mueller and Boehm 2011). The review published by Alminger et al., 2014, stated that β-carotene is considered relatively labile in the gastric and duodenal compartments; however, after which it is partly degraded in the jejunal and ileal compartments, where its absorption takes place (Alminger et al., 2014).

Besides enzymes and pH conditions, the impact of food matrices influence β-carotene bioavailability as it has been discussed in many studies (Biehler et al., 2011; Hedren et al., 2002; Van Loo-Bouwman et al., 2014). The release of β-carotene from the delivering matrix determines the amount of bioavailable β-carotene in digestive systems. A lipid diet was associated with a higher amount of bioaccessible β-carotene compared to that of the low-lipid diet under simulated *in vitro* intestinal conditions, which was consistent with the results from an *in vivo* study (Van Loo-Bouwman et al., 2014). Biehler et al., 2011 additionally clarified the effect of digestive enzymes on dietary fats; pancreatin can cleave triglycerides into smaller units, which enhance the rate of

carotenoid micellarization, whereas pepsin did not (Biehler et al., 2011). Therefore, the *in vitro* digestion with digestive pepsin and subsequently pancreatin has been widely utilized for screening to predict the degradation pathway, bioaccessibility, and functionality of β-carotene under closed physiological conditions (Alminger et al., 2014; Hur et al., 2011).

As mentioned earlier, the direct use of β-carotene in foods is limited due in its poor water-solubility, low bioavailability, chemical instability and sensitivity to oxidation, its degradation during GI transit, and the food matrix effect. These factors reduce the effectiveness of β-carotene, which is not delivered in sufficient amount to the specific sites where its antioxidant action is needed. Several systems including nanoemulsion, multi-layer nanoemulsion, colloidosome, solid lipid nanoparticles, and lipid nanocapsules have been applied to improve the ability to use of β-carotene in foods, but most studies have been limited to flavor, solubility, dispersibility, and instability assessment of nanodelivered β-carotene (Boon et al., 2010).

The aim of this chapter was to assess the potential of zein nanoparticles to improve the physicochemical stability and the antioxidant functionality of entrapped β-carotene incorporated into milk under simulated gastrointestinal environments. β-Carotene-loaded zein nanoparticles (BZ) and nanoemulsified β-carotene (BE), both stabilized by lecithin and pluronic F127, were synthesized and added to liquid milk. Physicochemical stability under *in vitro* enzymatic digestion, with pepsin for 2 hours followed by pancreatin for 24 hours, was analyzed by measuring the change in nanoparticle size, polydispersity index (PDI), zeta potential, and morphology. Chemical stability was investigated by measuring the degradation of β-carotene by

spectrophotometric method, and antioxidant activity was measured using 2,2'-azinobis-(3-ethyl benzthiazoline-6-sulphonic acid) (ABTS) and thiobarbituric acid reactive substance (TBARS) assays. This study is critically needed to develop nanostructure delivery systems capable to stabilize and preserve the antioxidant properties of entrapped bioactives, in order to enhance its physiological potency in the gastrointestinal tract.

3.2. Materials and Methods

3.2.1. Materials and Reagents

Zein, pluronic F127, chloroform, ethanol, β-carotene, AAPH (2,2'-azobis (2-methylpropionamidine) dihydrochloride), pepsin from porcine gastric mucosa (812 units/mg protein), and pancreatin from porcine pancreas (4xUSP specifications) were purchased from Sigma-Aldrich (Sigma Chemical Co. Ltd., St. Louis, MO). Soybean lecithin, hydrochloric acid, and sodium hydroxide were purchased from Fisher Chemical (Fisher Scientific International, Fairlawn, NJ). Nanopure water was obtained using Nanopure Diamond (Barnstead international, IA, USA). 100kDA cellulose ester Biotech membrane tubing and closures were purchased from Spectrum Laboratories Inc. (CA, USA). Whole milk powder (26.3% w/w fat content) was purchased from a local market, and reconstituted, using nanopure water, according to manufacturer instruction (10% w/v). All other reagents and components used in this study were analytical grade.

3.2.2. Synthesis

The synthesis of zein nanoparticles by a liquid-liquid dispersion method was detailed as follows. Briefly, 1% of zein solution was prepared by dissolving zein powder in 70:30% (v/v) ethanol-aqueous solution. A β-carotene solution was prepared at 0.1% in ethyl acetate and was added dropwise to the zein solution at a ratio of 1:1 under mild

stirring conditions. The mixture was injected into an aqueous phase containing a combination of lecithin and pluronic F127 0.045:0.090% (w/v) as surfactants at a ratio of 1:7.5. The sample was then processed in a microfluidizer at 30,000 PSI for 3 cycles (M-110P, Microfluidics, MA, USA). Subsequently, the sample underwent evaporation under vacuum (at approximately 500-600 mmHg) to remove solvent and nitrogen injection (80 mmHg) in a rotovapor (Buchi R-124, Buchi Analytical Inc., DE, USA). After the evaporation was completed, the free ethyl acetate suspension was dialyzed using a 100kDa Spectra/POR CE membrane (Spectrum Rancho, CA, USA) for 48 hours with 8 hours changing dialysis medium (nanopure water) to remove free surfactants. The β-carotene loaded in zein nanoparticles (BZ) was collected and kept at 4°C for further analysis. The β-carotene emulsion (BE) stabilized with surfactants was made in parallel to serve as control.

3.2.3. Particle size, Polydispersity Index (PDI), and Zeta potential Analyses

Freshly-made BZ sample were investigated using a Zetasizer Nano ZS (Malvern Instruments Ltd., Worcestershire, U.K.). Briefly, the samples were diluted to a final concentration of 0.2-0.32 mg/mL, using a buffer at pH 7.4 (0.1 M), which prevented particle aggregation. All measurements were performed in triplicate.

3.2.4. Morphology Analysis

Morphology of zein nanoparticles was also monitored by transmission electron microscopy (TEM) over 26 hours. Briefly, each sample was dropped on a 400 mesh copper grid with a carbon film, and the excess sample was removed with a filter paper. The sample was dried at room temperature and stained using uranyl acetate as a negative stain to improve the contrast of the sample.

3.2.5. Milk Sample Preparation

The degradation and antioxidant property of β-carotene loaded in zein nanoparticles and nanoemulsion form incorporated into a food matrix under simulated gastrointestinal conditions were investigated by measuring β-carotene amount and evaluating their antioxidant activity using ABTS and TBARS assays, respectively. Whole milk powder, which has a complex matrix structure and consists of plenty sources of nutrition was chosen as the matrix. Nanoentrapped and emulsified forms were formulated in different diluting ratio to reach an appropriate final β-carotene concentration of 25 μg/mL before used for comparative purposes.

3.2.6. Simulated Gastrointestinal System

Simulated gastric fluid (SGF) and simulated intestinal fluid (SIF) with digestive enzymes were prepared according to the United States Pharmacopoeia (US. Pharmacopeia. XXIV, 2006). SGF consists of 3.2 mg/mL pepsin in 0.03 M of NaCl at pH 1.2 adjusted by HCl to denature protein and activate pepsin. SIF consists of 10 mg/mL of pancreatin in 0.05 M of KH_2PO_4 at pH 7.5 adjusted by NaOH.

3.2.7. Physical-Chemical Stabilities

3.2.7.1. Physical Stability Analysis of Zein Nanoparticles (Size, PDI, Zeta Potential, and Morphology)

A freshly-made sample kept in a dialysis membrane tube (20kDA RC cellulose) was stored in SGF for 2 hours and subsequently moved to SIF for 6 and 24 hours at 37°C in a shaking incubator. The sample was monitored for changes in size, surface characteristic, and morphology at 0, 2, 8, and 26 hours of the total exposure time. All experiments were performed in triplicate.

3.2.7.2. Chemical Stability Analysis of Entrapped β-Carotene (Degradation)

In parallel with physical study, the concentration of β-carotene remaining in each sample at each time point during digestion was determined by spectrophotometric analysis after saponification and extraction. Briefly, after enzymatic reaction stopped using HCl, 2 mL of each sample was cooled down and then was saponified with 1 mL of 50% (w/v) KOH. The same volume of ethanol was consequently added to the mixture to precipitate fat, and incubated the mixture at room temperature for 30 min. Four milliliters of chloroform were added to extract β-carotene. The mixture was gently shaken and centrifuged at 7,000 g (Allegra 64r centrifuge, Beckman Coulter, Inc., CA) for 5 min to facilitate separation of aqueous and organic phases. The latter layer was collected and the remaining aqueous phase β-carotene was extracted twice. Absorbance of final combined organic extracts was measured using a UV/Vis spectrophotometer (GENESYS 6:Thermo Spectronic, Thermo Scientific, Inc., MA) with glass cells of 1 cm path length recorded at 460 nm. The absorbance value was converted by standard curve and the result was reported as the concentration of β-carotene (μg) per 1 mL of sample. All experiments were performed in triplicate.

3.2.8. Antioxidant Activity

The samples were prepared under SGIF conditions for ABTS and TBAR studies. AAPH used as a free radical generator (Shi et al., 2004), was added to the samples before GI incubation. For TBARS assay, 10-fold decreased concentration of β-carotene was used to avoid prooxidant effect and protein precipitation was employed to overcome the effect of bioactive peptides hydrolyzed from milk which interfered with the antioxidant activity of nanodeliverd β-carotene during measurement.

Each sample was mixed well with SGF at a ratio of 1:1 and divided into centrifuged tubes and incubated at 37°C under 100 rpm shaking for 2 hours. Subsequently, the pH in the sample was adjusted to 1.2 using a high concentration of HCl to stop enzymatic reaction. The same amount of SIF with SGF was added to each tube, and the tubes were continuously incubated at 37°C under 100 rpm shaking for 24 hours. At 6 and 24 hours, a sample tube was randomly taken and heated at 95°C for 5 min to stop enzymatic reaction. Then, the mixture was ready for analysis.

3.2.8.1. ABTS (2,2'-azinobis-(3-ethyl benzthiazoline-6-sulphonic acid))

The free radical scavenging activity of entrapped β-carotene loaded zein nanoparticles (BZ) and emulsified forms (BE) and their mixtures with milk (MBZ and MBC) were investigated according to the method described by Jrad et al., 2014 (Jrad et al., 2014) with a slight modification. Briefly, the $ABTS^{+}\bullet$ radical cation was prepared by dissolving 7 mM of $ABTS^{+}$ with 2.45 mM potassium persulfate and the mixture was kept in the darkness for 15 hours at room temperature before use. The $ABTS^{+}\bullet$ solution was then diluted with 5 mM sodium phosphate buffer, pH 7.4 to reach an absorbance of 0.70±0.02 using a UV/Vis spectrophotometer read at 734 nm. Then, 50 µl of each sample was well mixed with 150 µl of the $ABTS^{+}\bullet$ solution, and incubated for 10 min at 25°C. The radical scavenging activity of the samples, expressed as an inhibition percentage (%), was calculated with the equation by $Activity\ (\%) = \left[1 - \frac{A_r - A_b}{A_i - A_b}\right] x100$. Where A_i is the absorbance of the initial $ABTS^{+}\bullet$ radical solution, A_r is the absorbance of the remaining radical sample, and A_b is the absorbance of the blank (blanks were water added to simulated digestion medium). All experiments were performed in triplicate.

3.2.8.2. TBARS (Thiobarbituric Acid Reactive Substance)

The second assay was used to study lipid peroxidation for all samples in the presence of milk (M, MBZ, and MBE) using a modified version of the TBARS assay described by King et al., 1962 and Spanier and Trayler, 1991 (King 1962; Spanier and Traylor 1991). This assay defined the TBARS value as mg of MDA per liter sample based on the conversion of 1 mole of TMP is treated as equivalent to 2 moles of reacting equivalents of MDA by multiplying the number of μM of TMP standard concentration per liter of sample by 72.07 (a molecular weight of MDA) (Spanier and Traylor 1991). Briefly, 500 μl of a supernatant from each sample after precipitation with 10% trichloroacetic acid, followed by centrifugation was added to 2 mL of TBAR solution. The mixture was heated at 95°C for 60 min, cooled on ice, and was subsequently centrifuged at 7,000 g for 10 min. The sample was then determined by reading the absorbance using a UV/Vis spectrophotometer at 532 nm. Calibration was done with a malonaldehyde (MDA) standard prepared from tetramethoxypropane (TMP). The TBARS value of sample (mg/L) was calculated by multiplying the slope of the TMP standard curve and the absorbance of the sample with the equation by $TBARS\ (mg/L) = slope * A_i * D$. The result must be multiplied by the dilution factor. Where A_i is the absorbance of the sample read at 532 nm and *D* is dilution factor (3 for this procedure). All experiments were performed in triplicate.

3.2.9. Statistical Analysis

All experiments were performed in triplicate, and results reported as the mean value ± standard error. The statistical analysis was performed using SAS (SAS version 9.4, SAS Institute Inc., NC, USA). The analysis of variance (ANOVA) was used to

determine significant differences between the systems and exposure times with P value < 0.05 was used for statistical evaluation.

3.3. Results and Discussion

3.3.1. Particle size, PDI, and Zeta potential

Particle size, PDI, and zeta potential of freshly prepared samples were measured after 48 hours of dialysis (Table 3.1). Statistically significant differences were found for size, zeta potential and entrapment properties between the nanoparticles and nanoemulsions. The size of β-carotene loaded zein nanoparticles layered by surfactants was 168.17±22.36 nm, while its emulsified form without zein core was 32.44±0.87 nm. Nonionic amphiphilic pluronic F127 can efficiently help to overcome the natural brittleness of zein matrix (Li et al., 2013). The incorporation of pluronic F127 with lecithin results in an effective and stable emulsifier as indicated by the small size of the emulsion and nanoparticles. The PDI values were within 0.29-0.33 and zeta potential used to indicate the stability of a nanoparticle system was -42.83±1.52 and -14.67±2.65 mV for BZ and BE, respectively (Table 3.1).

Table 3.1. Characteristics of β-carotene-loaded zein nanoparticles (BZ) and nano-emulsified β-carotene (BE) stabilized by lecithin and pluronic F127

Sample	Size (nm)	PDI (a.u.)	Zeta Potential (mV)	Initial concentration (μg/mL)
BZ	168.17±22.36[a]	0.29±0.01 [a]	-42.83±1.52 [a]	39.91±2.58 [a]
BE	32.44±0.87[b]	0.33±0.03 [a]	-14.67±2.65 [b]	25.95±2.10 [b]

Note: Values are expressed as mean ± standard error of mean (n=3). Superscripts with a and b show statistically significant difference between nanoentrapped β-carotene and nanoemulsified forms.

Previously published data showed that unloaded zein nanoparticles showed a positive surface charge. When they were stabilized by surfactants such as lecithin or

pluronic, the surface charge shifted from positive to negative, and showed a further decrease in the negatively charge when loaded with the bioactive compound (Li et al., 2013). The zein core increasing hydrophobic property contributed to a higher initial amount of β-carotene loaded in the particles (39.91±2.58 μg/mL) compared to that entrapped in the nanoemulsified form (25.95±2.10 μg/mL).

3.3.2. Physicochemical Stabilities under Simulated GI Conditions

3.3.2.1. Physical Stability of Zein Nanoparticles (Particle size, PDI, Zeta potential and Morphology)

Statistical analysis for nanoparticle size, PDI, and zeta potential after GI exposure over 26 hours revealed that there were significant differences between nanoparticles and nanoemulsified form at all times. At a 2 hours exposure to SGF, particle size was significantly changed, while PDI and zeta potential increased in the presence of pepsin (Table 3.2).

Table 3.2. Characteristics of β-carotene loaded zein nanoparticles (BZ) and nano-emulsified β-carotene (BE) under simulated GI conditions

Sample	Condition	Time	Size (nm)	PDI (a.u)	Zeta Potential (mV)
BZ	SGF	0 h	171.80 ± 6.60^{ax}	0.28 ± 0.01^{ax}	-43.93 ± 2.29^{ax}
		2 h	155.10 ± 4.11^{ay}	0.38 ± 0.05^{ay}	-25.50 ± 0.40^{ay}
	SIF	8 h	71.95 ± 2.79^{az}	0.70 ± 0.09^{az}	-12.53 ± 1.41^{az}
		26 h	518.80 ± 18.68^{aw}	0.63 ± 0.03^{aw}	-3.03 ± 0.46^{aw}
BE	SGF	0 h	34.90 ± 1.29^{bx}	0.38 ± 0.03^{bx}	-15.13 ± 2.07^{bx}
		2 h	36.29 ± 0.48^{by}	0.78 ± 0.03^{by}	-13.47 ± 1.28^{by}
	SIF	8 h	68.26 ± 7.35^{bz}	0.67 ± 0.06^{bz}	-20.67 ± 0.70^{bz}
		26 h	1446.21 ± 37.56^{bw}	0.99 ± 0.01^{bw}	-3.20 ± 0.81^{bw}

Note: Values are expressed as mean ± standard error of mean (n=3). SGF and SIF represent simulated gastric fluid and simulated intestinal fluid at different exposure times (hours). Superscripts with a-b and x-w show statistically significant difference due to nanodelivered β-carotene forms and exposure times, respectively.

The exposure was continued under SIF with pancreatin for 24 hours. Under these conditions, the size of the particles decreased dramatically from 171.80±6.60 nm under gastric (2 hours) to 71.95±2.79 nm under intestinal media (8 hours). With longer exposure to the simulated GI media however size and PDI increased significantly, while zeta potential reached near-zero mV, indicating low stability of the particles. The DLS data was confirmed by TEM images, showing that particles were stable under SGF, but not under SIF conditions (Figure 3.1).

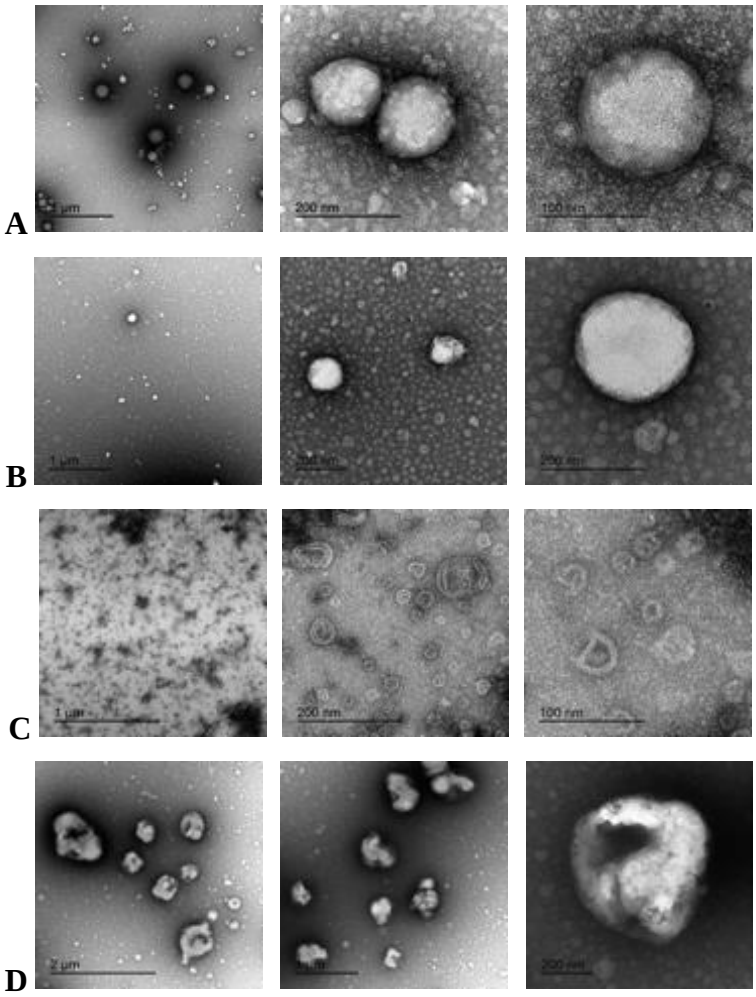

Figure 3.1. TEM images of β-carotene loaded in zein nanoparticles (BZ) stabilized by lecithin and pluronic F127 (A), BZ after 2 hours under SGF condition (B), BZ after 8 hours under SIF condition (C), and BZ after 26 hours under SIF condition (D) at various magnifications

TEM images indicated that particles slightly changed in size after 2 hours under SGF exposure, but with subsequent exposure to intestinal conditions, the particles were distorted in shape and agglomerated after 6 hours under SIF condition. Zein digestion by protease led to the distorted shape, while the agglomeration was most likely triggered when the pH approached the isoelectric point (pI=6.8) (Shukla and Cheryan 2001).

These phenomena may be descripted by the degradation of zein under simulated gastrointestinal fluid (Hurtado-Lopez and Murdan 2006), which indicated that pepsin digests α-zein but not its degraded products such as dimers and tetramers, while pancreatin can digest both α-zein and its dimers, resulting in the dramatically dropped size to 71.95±2.79 nm of BZ nanoparticles when moved to SIF at 8 hours.

3.3.2.2. Chemical Stability of Entrapped β-Carotene (Degradation)

The chemical degradation of β-carotene can be spectrophotometrically measured by its color fading over time which may be due to the digestive enzymes (Patras et al., 2009). Digestive pepsin and pancreatin proteases, which are capable of digesting protein in the stomach, were used to hydrolyze zein nanoparticles resulting in the release of β-carotene compounds. In the presence of milk, milk fat components are mainly digested in the gastric condition (Gallier et al., 2012), and the presence of lipids in food matrix enhance more bioavailability of β-carotene relative to that of β-carotene from natural sources (Boon et al., 2010).

The initial amount of β-carotene was reduced to 60.51±1.99% and 57.31±5.04% during exposure to SGF in the particles and emulsions, respectively. After a 26 hours total exposure time (2 hours to SGF and 24 hours to SIF), 18.30±1.29% and 4.41±2.51% was found in nanoentrapped and emulsified forms, respectively (Table 3.3). The

improved retention of the β-carotene in the particles was due to hydrophobic interaction between entrapped β-carotene and zein matrix responsible for an enhanced resistance against enzymatic hydrolysis. Emulsions, by contrast of smaller sizes than particles and hence higher surface area/volume were more susceptible to digestion and higher degradation of entrapped β-carotene. Nanoemulsified β-carotene degradation under lipid digestion was also studied by Troncoso et al., 2012 (Troncoso et al., 2012), who concluded that the digestion rate was strongly dependent on the size of nanoemulsion, the smaller droplet diameter, the higher the rate of digestion. When incorporated in milk, rich in fat-soluble components, the presence of lipids in the food matrix was proven to enhance the bioavailability of β-carotene relative to bioavailability of β-carotene in its natural form and stability β-carotene compounds. The protective role of the milk matrix on β-carotene is limited by pepsinolysis under gastric conditions and lipolysis by pancreatic lipase at the end of the digestive process (Gallier et al., 2012). In the presence of milk, 59.29±2.28% of β-carotene remained in nanoparticle form, compared to 49.52±2.73% in emulsified form after 2 hours exposure to SGF and 24 hours exposure to SIF. Statistically significant main effects were found as a function of delivery system for β-carotene and time (Table 3.3).

Zein nanoparticles showed a high potential to protect β-carotene from degradation for longer compared to nanoemulsified form under digestive system. The degradation of zein under GI environments, resulting in release of entrapped β-carotene, was described by Parris et al., 2005 (Parris et al., 2005) who found that less than half of the initial amount of zein nanoparticles were digested after 4 hours of exposure under

simulated gastric condition with the presence of pepsin, and was completely digested after 52 hours, supporting our data.

Table 3.3. Concentration (μg/mL) of entrapped β-carotene in zein nanoparticles (BZ) and nanoemulsion (BE) remaining under simulated GI conditions in the absence and presence of milk

Condition	β-Carotene remaining (%)			
	Without Milk		With Milk	
	BZ	BE	MBZ	MBE
SGF0h	100.00 ± 0.00^{ax}	100.00 ± 0.00^{bx}	100.00 ± 0.00^{cx}	100.00 ± 0.00^{dx}
SGF2h	60.51 ± 1.99^{ay}	57.31 ± 5.04^{by}	97.34 ± 0.02^{cy}	76.26 ± 1.52^{dy}
SIF8h	32.37 ± 0.97^{az}	17.01 ± 1.85^{bz}	69.01 ± 1.05^{cz}	50.53 ± 2.18^{dz}
SIF26h	18.30 ± 1.29^{aw}	4.41 ± 2.51^{bw}	59.29 ± 2.28^{cw}	49.52 ± 2.73^{dw}

Note: Values are expressed as mean ± standard error of mean (n=3). SGF and SIF represent simulated gastric fluid and simulated intestinal fluid at different exposure times (hours). M represents formulation with milk. Superscripts with a-d, and x-w show statistically significant difference due to nanodelivered β-carotene forms and exposure times, respectively.

Several previous *in vitro* studies concluded that the degradation of β-carotene under gastrointestinal tract conditions depends on its structure, isomerization, the food matrix in which incorporated, and the digestive conditions to which exposed. Our results showed the entrapped β-carotene in both forms were highly degraded (~82%-96%) after 26 hours of total digestive time, relative to β-carotene from natural sources such as carrot, red tomato, and spinach (50%-85% degradation under *in vitro* gastrointestinal system) (Blanquet-Diot et al., 2009).

The difference is attributed to the fact that β-carotene incorporated within the natural complex food matrix is not fully released during digestion (Williams et al., 1998). Thus, the degradation rate of the β-carotene in nanoemulsified form was highest, followed by β-carotene entrapped in zein nanoparticles, and β-carotene in natural form in

natural food matrices. In the presence of milk, the degradation rate was highly diminished, indicating that dietary fat has the ability to improve stability β-carotene during storage and delivery in the gastrointestinal tract.

3.3.3. Antioxidant Activity

Multiple mechanistic assays must be employed to evaluate the antioxidant property of bioactive compounds in foods. Several screening studies rely on ABTS assay to measure free radical scavenging activity of β-carotene in dairy products including human milk and infant formula (Hernández-Ledesma et al., 2007; Martysiak-Zurowska and Wenta 2012), while TBARS is commonly used to determine the secondary product formed from lipid peroxidation, particularly in milk system (King 1962; Spanier and Traylor 1991).

3.3.3.1. ABTS

The antioxidant activity of β-carotene was monitored by its ability to scavenge the $ABTS^{+}$ radical cation, which was measured based on the loss of green color of $ABTS^{+}$ radical in the presence of antioxidants. The ability of natural milk components to have antioxidant properties should be considered in this assay. When casein and whey proteins are hydrolyzed with gastric and pancreatic enzymes, respectively, the bioactive peptides are released resulting in the biological effect on the total antioxidant capacity of milk (Hernández-Ledesma et al., 2007).

Antioxidant activity levels of β-carotene in the particle form showed higher scavenging activity (% ABTS inhibition) in both digestive conditions. The nano-entrapped β-carotene had an antioxidant activity 10.38% (15.18±0.47% to 4.80±0.05%) and 4.85% (62.67±0.78% to 57.81±0.14%) higher than that of the emulsified form in

SGF at 2 hours and SIF at 26 hours, respectively (Table 3.4). With the addition of milk, both systems showed higher efficiency in scavenging the free radical. The % ABTS inhibition was higher in the antioxidant-spiked milk than the regular milk (70.09±0.36% of milk in SGF). After being hydrolyzed in SIF, the difference between the antioxidant activity of nano-entrapped β-carotene and nanoemulsified β-carotene was smaller. The antioxidant activity was constant across delivery systems and times under GIF exposure, measuring ~96-97%. It was apparent that the impact on antioxidant activity of the hydrolyzed peptides derived from milk proteins shielded the subtle effect of the delivery system on antioxidant activity. The progression from lower to higher % ABTS inhibition over time is related to the natural progression of the digestion process, and the increased amount of β-carotene gradually released over time.

The antioxidant activity of milk is mostly attributed to casein and its derivative peptides (Zulueta et al., 2009; Tsopmo et al., 2011). The investigation of Mauron et al., 2005 (Anonymous, 2005) indicated the biological availability of amino acids, particularly tryptophan in milk powder was not diminished under production process and *in vitro* digestion with pepsin and pancreatin. The results of Tsopmo et al., 2011 (Tsopmo et al., 2011) supported the antioxidant activity of tryptophan derived from enzymatically-digested milk, able to scavenge peroxyl radical and inhibit lipid hydroperoxide formation. Additionally, the enzymatically-hydrolyzed zein was also shown to possess an antioxidant activity by acting as a hydrogen donor or radical stabilizer (Kong and Xiong 2006).

Table 3.4. Antioxidant activity (% ABTS Inhibition) of entrapped β-carotene in zein nanoparticles (BZ) and nanoemulsion (BE) under simulated GI conditions in the absence and presence of milk

Condition	% ABTS inhibition			
	Without Milk		With Milk	
	BZ	BE	MBZ	MBE
SGF0h	10.36 ± 0.51^{ax}	5.36 ± 0.01^{bx}	73.56 ± 0.87^{cx}	72.03 ± 0.20^{dx}
SGF2h	15.18 ± 0.47^{ay}	4.80 ± 0.05^{by}	84.56 ± 0.37^{cy}	83.72 ± 0.48^{dy}
SIF8h	67.83 ± 1.38^{az}	57.82 ± 0.27^{bz}	97.10 ± 0.29^{cz}	96.63 ± 0.19^{dz}
SIF26h	62.67 ± 0.78^{aw}	57.81 ± 0.14^{bw}	96.53 ± 0.05^{cw}	96.00 ± 0.09^{dw}

Note: Values are expressed as mean ± standard error of mean (n=3). SGF and SIF represent simulated gastric fluid and simulated intestinal fluid at different exposure times (hours). M represents formulation with milk. Superscripts with a-d and x-w show statistically significant difference due to nanodelivered β-carotene forms and exposure times, respectively.

3.3.3.2. TBARS

TBARS is a widely used assay for detecting the formation of MDA (malondialdehyde), a secondary metabolite of oxidation formed as a result of the polyunsaturated fatty acid degradation, from lipid oxidative deterioration of fat-containing foods. The MDA is reacted with two molecules of thiobarbituric acid (TBA) to form a pink complex (TBARS) detected by spectrophotometric quantitation at 532 nm for maximum absorption. The TBARS value is defined as mg of MDA per liter of milk.

The mechanism began with milk substrates, which were oxidized with added AAPH. The oxidation is inhibited by the presence of β-carotene as an antioxidant, and it can be detected by adding TBA to form TBARS which is diminished depending on the ability of β-carotene. The interference of excessive milk substances during measurement is minimized by protein precipitation and centrifugation (King 1962).

The total antioxidant capacity of milk was initially 0.94 mg/L and decreased to 0.72 mg/L after 2 hours of digestion by pepsin. After 26 hours in SIF condition, the value was increased to 0.86 mg/L (Figure 3.2). The initial TBARS value closed to the range of 1.02 to 1.31 mg/L of MDA concentration measured from 4 commercial milk powders reported by Fenaille et al., 2001 (Fenaille et al., 2001).

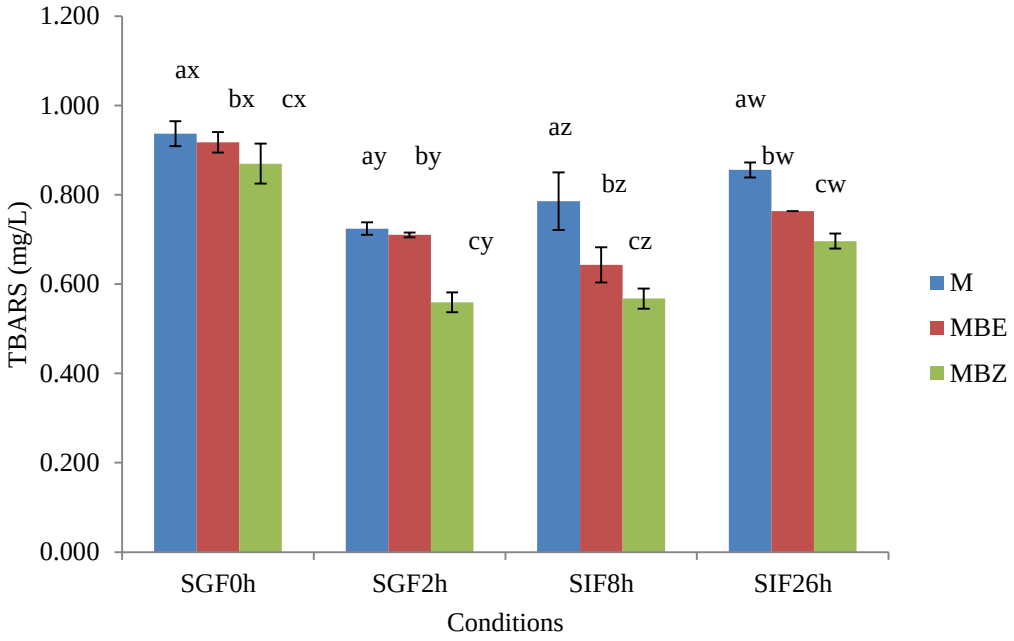

Figure 3.2. TBARS values (µg MDA/L) of milk (M), milk spiked with β-carotene loaded zein nanoparticles (MBZ) and β-carotene in emulsified form (MBE) under simulated gastrointestinal conditions in the presence of milk. Bars represent mean ± standard error of mean (n=3). SGF and SIF represent simulated gastric fluid and simulated intestinal fluid at different exposure times (hours). Values marked with a-c and x-w show statistically significant difference due to nanodelivered β-carotene forms and exposure times, respectively.

When milk was added with nanoentrapped and nanoemulsified β-carotene forms and measured the antioxidant activity at designed times, the trends did not differ from pure milk (Figure 3.2), but the particle system produced the lowest TBARS compared to emulsified form and liquid milk. It indicated that the most effective antioxidant to inhibit MDA formation was the β-carotene entrapped in zein nanoparticles which was

statistically significant main effect to protect the functionality of its entrapped compounds against enzymatic digestive degradation.

Not only the effect of milk against TBARS values, but zein itself discussed by Kong and Xiong, 2006 (Kong and Xiong 2006) showed its hydrolysates have the peroxidation inhibition through TBARS formation, which may reinforce the antioxidative effect in particle system. As mentioned above, the hydrolyzed products, especially casein proteins after being digested by pepsin and pancreatin, were the factors that contributed to the total antioxidant capacity of whole milk (Tsopmo et al., 2011). At the initial time point, both entrapped β-carotene forms showed the lower TBARS values than milk. After 2 hours of enzymatic digestion, milk, including stabilized surfactants, zein nanoparticle core, and partly released β-carotene were digested, whereas the effect of the rest of released β-carotene and milk peptides inhibited lipid peroxidation and contributed to decreasing TBARS values. Thereafter, digested in SIF condition for 6 hours, both of β-carotene forms still showed antioxidant effect towards MDA formation, except milk, which had less the antioxidant property towards the formation of MDA, after 2 hours in SGF until 24 hours in SIF (Figure 3.2).

3.4. Conclusion

The potential of zein nanoparticles to protect and enhance antioxidant activity β-carotene was studied in comparison with nanoemulsified form under simulated GI conditions in the absence and presence of milk. Zein nanoparticles proved to protect entrapped β-carotene from degradation. ABTS assay indicated that nano-entrapped β-carotene in zein nanoparticles had an improved antioxidant activity statistically different from its nanoemulsified form. The difference was lessened in the presence of milk, due to

the intrinsic antioxidant activity of milk components. In the presence of dietary lipid components of milk, but after precipitation and removed protein, TBARS assay confirmed that antioxidant activity against MDA formation was significantly improved for β-carotene when delivered with zein nanoparticles. It was concluded that the potential of nanoentrapment of bioactives in zein nanoparticles contributed to improved stability and enhanced antioxidant activity of β-carotene versus emulsions under simulated gastrointestinal environments.

3.5. References

Alminger, M., A. M. Aura, T. Bohn, C. Dufour, S. N. El, A. Gomes, S. Karakaya, M. C. Martínez-Cuesta, G. J. McDougall, T. Requena, and C. N. Santos (2014). "In Vitro Models for Studying Secondary Plant Metabolite Digestion and Bioaccessibility". *Comprehensive Reviews in Food Science and Food Safety,* 13 (4), 413-436.

Anonymous, (2005). "Lutein and zeaxanthin. Monograph". *Altern Med Rev,* 10 (2), 128-35.

Biehler, E., A. Kaulmann, L. Hoffmann, E. Krause, and T. Bohn (2011). "Dietary and host-related factors influencing carotenoid bioaccessibility from spinach (Spinacia oleracea)". *Food Chemistry,* 125 (4), 1328-1334.

Blanquet-Diot, S., M. Soufi, M. Rambeau, E. Rock, and M. Alric (2009). "Digestive stability of xanthophylls exceeds that of carotenes as studied in a dynamic in vitro gastrointestinal system". *J Nutr,* 139 (5), 876-83.

Boon, C. S., D. J. McClements, J. Weiss, and E. A. Decker (2010). "Factors influencing the chemical stability of carotenoids in foods". *Crit Rev Food Sci Nutr,* 50 (6), 515-32.

Choi, W. I., K. C. Yoon, S. K. Im, Y. H. Kim, S. H. Yuk, and G. Tae (2010). "Remarkably enhanced stability and function of core/shell nanoparticles composed of a lecithin core and a pluronic shell layer by photo-crosslinking the shell layer: In vitro and in vivo study". *Acta Biomaterialia,* 6 (7), 2666-2673.

Fenaille, F., P. Mottier, R. J. Turesky, S. Ali, and P. A. Guy (2001). "Comparison of analytical techniques to quantify malondialdehyde in milk powders". *Journal of Chromatography A,* 921 (2), 237-245.

Gallier, S., A. Ye, and H. Singh (2012). "Structural changes of bovine milk fat globules during in vitro digestion". *J Dairy Sci,* 95 (7), 3579-92.

Geraghty, D., M. A. Peifer, I. Rubenstein, and J. Messing (1981). "The primary structure of a plant storage protein: zein". *Nucleic Acids Res,* 9 (19), 5163-74.

Hedren, E., V. Diaz, and U. Svanberg (2002). "Estimation of carotenoid accessibility from carrots determined by an in vitro digestion method". *Eur J Clin Nutr,* 56 (5), 425-30.

Hernández-Ledesma, B., A. Quirós, L. Amigo, and I. Recio (2007). "Identification of bioactive peptides after digestion of human milk and infant formula with pepsin and pancreatin". *International Dairy Journal,* 17 (1), 42-49.

Hur, S. J., B. O. Lim, E. A. Decker, and D. J. McClements (2011). "In vitro human digestion models for food applications". *Food Chemistry,* 125 (1), 1-12.

Hurtado-Lopez, P. and S. Murdan (2006). "Zein microspheres as drug/antigen carriers: a study of their degradation and erosion, in the presence and absence of enzymes". *J Microencapsul,* 23 (3), 303-14.

Jrad, Z., J.-M. Girardet, I. Adt, N. Oulahal, P. Degraeve, T. Khorchani, and H. El Hatmi (2014). "Antioxidant activity of camel milk casein before and after in vitro simulated enzymatic digestion". *Mljekarstvo,* 64 (4), 287-294.

King, R. L. (1962). "Oxidation of Milk Fat Globule Membrane Material. I. Thiobarbituric Acid Reaction as a Measure of Oxidized Flavor in Milk and Model Systems1". *Journal of Dairy Science,* 45 (10), 1165-1171.

Kong, B. and Y. L. Xiong (2006). "Antioxidant activity of zein hydrolysates in a liposome system and the possible mode of action". *J Agric Food Chem,* 54 (16), 6059-68.

Li, J., Y. Li, T. C. Lee, and Q. Huang (2013). "Structure and physical properties of zein/pluronic f127 composite films". *J Agric Food Chem,* 61 (6), 1309-18.

Li, K.-K., S.-W. Yin, Y.-C. Yin, C.-H. Tang, X.-Q. Yang, and S.-H. Wen (2013). "Preparation of water-soluble antimicrobial zein nanoparticles by a modified antisolvent approach and their characterization". *Journal of Food Engineering,* 119 (2), 343-352.

Martysiak-Zurowska, D. and W. Wenta (2012). "A comparison of ABTS and DPPH methods for assessing the total antioxidant capacity of human milk". *Acta Sci Pol Technol Aliment,* 11 (1), 83-9.

Mueller, L. and V. Boehm (2011). "Antioxidant activity of beta-carotene compounds in different in vitro assays". *Molecules,* 16 (2), 1055-69.

Oh, K. S., S. K. Han, H. S. Lee, H. M. Koo, R. S. Kim, K. E. Lee, S. S. Han, S. H. Cho, and S. H. Yuk (2006). "Core/Shell Nanoparticles with Lecithin Lipid Cores for Protein Delivery". *Biomacromolecules,* 7 (8), 2362-2367.

Paiva, S. A. and R. M. Russell (1999). "Beta-carotene and other carotenoids as antioxidants". *J Am Coll Nutr,* 18 (5), 426-33.

Parris, N., P. H. Cooke, and K. B. Hicks (2005). "Encapsulation of essential oils in zein nanospherical particles". *J Agric Food Chem,* 53 (12), 4788-92.

Patras, A., N. Brunton, S. Da Pieve, F. Butler, and G. Downey (2009). "Effect of thermal and high pressure processing on antioxidant activity and instrumental colour of tomato and carrot purées". *Innovative Food Science & Emerging Technologies,* 10 (1), 16-22.

Peña- Ramos, E. A., Y. L. Xiong, and G. E. Arteaga (2004). "Fractionation and characterisation for antioxidant activity of hydrolysed whey protein". *Journal of the Science of Food and Agriculture,* 84 (14), 1908-1918.

Pénicaud, C., N. Achir, C. Dhuique-Mayer, M. Dornier, and P. Bohuon (2011). "Degradation of β-carotene during fruit and vegetable processing or storage: reaction mechanisms and kinetic aspects: a review". *Fruits,* 66 (06), 417-440.

Regier, M. C., J. D. Taylor, T. Borcyk, Y. Yang, and A. K. Pannier (2012). "Fabrication and characterization of DNA-loaded zein nanospheres". *Journal of nanobiotechnology,* 10 (1), 1-13.

Shi, J., Q. Qu, Y. Kakuda, D. Yeung, and Y. Jiang (2004). "Stability and synergistic effect of antioxidative properties of lycopene and other active components". *Crit Rev Food Sci Nutr,* 44 (7-8), 559-73.

Shukla, R. and M. Cheryan (2001). "Zein: the industrial protein from corn". *Industrial Crops and Products,* 13 (3), 171-192.

Sodek, L. and C. M. Wilson (1971). "Amino acid compositions of proteins isolated from normal, opaque-2, and floury-2 corn endosperms by a modified Osborne procedure". *Journal of Agricultural and Food Chemistry,* 19 (6), 1144-1150.

Spanier, A. M. and R. D. Traylor (1991). "A RAPID, DIRECT CHEMICAL ASSAY FOR THE QUANTITATIVE DETERMINATION OF THIOBARBITURIC ACID REACTIVE SUBSTANCES IN RAW, COOKED, AND COOKED/STORED MUSCLE FOODS". *Journal of Muscle Foods,* 2 (3), 165-176.

Terao, J., Y. Minami, and N. Bando (2011). "Singlet molecular oxygen-quenching activity of carotenoids: relevance to protection of the skin from photoaging". *Journal of clinical biochemistry and nutrition,* 48 (1), 57.

Troncoso, E., J. M. Aguilera, and D. J. McClements (2012). "Fabrication, characterization and lipase digestibility of food-grade nanoemulsions". *Food Hydrocolloids,* 27 (2), 355-363.

Tsopmo, A., A. Romanowski, L. Banda, J. C. Lavoie, H. Jenssen, and J. K. Friel (2011). "Novel anti-oxidative peptides from enzymatic digestion of human milk". *Food Chemistry,* 126 (3), 1138-1143.

Van Loo-Bouwman, C. A., T. H. Naber, M. Minekus, R. B. van Breemen, P. J. Hulshof, and G. Schaafsma (2014). "Food matrix effects on bioaccessibility of beta-carotene can be measured in an in vitro gastrointestinal model". *J Agric Food Chem,* 62 (4), 950-5.

Williams, A. W., T. W. Boileau, and J. W. Erdman, Jr. (1998). "Factors influencing the uptake and absorption of carotenoids". *Proc Soc Exp Biol Med,* 218 (2), 106-8.

Wu, Y., Y. Luo, and Q. Wang (2012). "Antioxidant and antimicrobial properties of essential oils encapsulated in zein nanoparticles prepared by liquid–liquid dispersion method". *LWT - Food Science and Technology,* 48 (2), 283-290.

Zhong, Q. and M. Jin (2009). "Zein nanoparticles produced by liquid–liquid dispersion". *Food Hydrocolloids,* 23 (8), 2380-2387.

Zulueta, A., A. Maurizi, A. Frígola, M. J. Esteve, R. Coli, and G. Burini (2009). "Antioxidant capacity of cow milk, whey and deproteinized milk". *International Dairy Journal,* 19 (6–7), 380-385.

CHAPTER 4
DEVELOPMENT OF ZEIN NANOPARTICLES WITH COVALENTLY LINKED AND PHYSICALLY ENTRAPPED FOLIC ACID – A FOCUS ON ENTRAPMENT, CONTROLLED RELEASE, CYTOTOXICITY AND CELLULAR UPTAKE

4.1. Introduction

Folic acid (pteroyl-L-glutamic acid, vitamin B_9), a water-soluble vitamin, is an essential supplement for the production and maintenance of new cells during rapid cell division and growth, particularly in periods of pregnancy and infancy, vital in preventing the neural tube defects that cause malformation in infants (Jagerstad 2012). Both adults and children need folic acid to make normal red blood cells and prevent anemia; folic acid, or natural folates are critical in the synthesis of DNA and have the ability to replicate and prevent changes of DNA (Taylor et al., 2015). In addition to its health benefits, folic acid is used as a small targeting ligand for cancer diagnosis and therapy because folate-receptors are frequently over-expressed in a range of cancer cells (Zhao et al., 2008). Folic acid has been conjugated with a wide variety of molecules, such as chemotherapeutic agents, oligonucleotides, proteins, liposomes, as well as with imaging agents to develop folate receptor-targeted delivery systems. Recently, several folate nanotargeting systems have been proposed based on several modifications of nanoparticles (Table 1.2). For example, folic acid was physically entrapped in biodegradable polymeric nanoparticles by means of homogenization with phase separation method to maintain a sustained release of the drug, and controlled delivery of folic acid in the body (Stevanović et al., 2008). When targeting is desired, most studies report covalent attachment of folic acid rather than physical entrapment to develop targeting nanovehicles. Folate nanocarriers modified for targeting and delivery of

chemotherapeutic drugs have mostly been made from synthetic polymers such as PLGA (Boddu et al., 2012; Zhou et al., 2010), but gold nanoparticles (Zhang et al., 2010; Ai et al., 2012), and carbon nanotubes (Castillo et al., 2013) have also been surface-functionalized with folic acid, mostly for imaging purpose. While nanoparticles made of synthetic polymers have been shown to be able to control release of the entrapped drug, to increase circulation time of the drug in the blood, and to enhance cellular uptake, natural-made polymeric nanoparticles have been studied less in terms of their potential to achieve targeting and controlled release without causing adverse side effects to healthy cells when accumulated in high-level doses. Only a few studies have reported on folate-conjugated nanocarriers made with natural materials such as chitosan (Zu et al., 2011), β-cyclodextrin (Zhang et al., 2012), and soy protein (Teng et al., 2013) for delivery of hydrophobic/hydrophilic bioactives (Wang et al., 2009). The amino acid side chains of zein, specifically can be covalently attached to the activated carboxylic group of folic acid, the chemically modified zein can then be used to form targeted nanoparticles for potential cancer treatment.

The hypothesis was that zein nanoparticles (ZN NPs) covalently linked to folic acid (FA) sustained the release of the drug in addition to helping with targeting the nanoparticles to folate-binding receptors, over-expressed on the surface of cancer cells, whereas zein nanoparticles with entrapped folic acid will only be able to control the release of the bioactive without showing improved targeting of cancer cells.

The two types of particles, folic acid-covalently linked zein nanoparticles (ZN-FA NPs) and zein nanoparticles with entrapped folic acid (ZN(FA) NPs) were synthesized and characterized in parallel. The release studies of the folic acid from the

zein nanoparticles were performed in PBS at 37°C for 7 days. The cytotoxicity of the zein nanoparticles with entrapped and covalently linked folic acid was investigated using a methyl thiazolyl tetrazolium (MTT) assay, and the targeting ability of the particles was comparatively evaluated by a simple spectroscopic measurement in two different cell lines, HeLa (an over-expressing folate receptor cell type) and A549 (a deficient folate receptor cell type).

4.2 Materials and Methods

4.2.1. Materials and Reagents

Zein (Z 3625), lecithin, pluronic F127, dimethyl sulfoxide (DMSO, purity 99.5%), N-hydroxysuccinimide (NHS, purity 99.0%), 1,3-dicyclohexyl-carbodiimide (DCC, purity 95.0%), triethylamine (TEA, purity 99.5%), and 3-(4,5-Dimethylthiazol-2-yl)-2,5-diphenyltetrazolium bromide (MTT), were purchased for Sigma-Aldrich (MO, USA). Folic acid (96-102%) was purchased from Acros Organics (NJ, USA). All other materials used were of analytical grade.

4.2.2. Preparation of Folic Acid-Covalently Linked Zein Nanoparticles (ZN-FA NPs)

4.2.2.1. Preparation of Zein-Folic Acid (ZN-FA)

The N-hydroxysuccinimide ester of folic acid (NHS-FA) was first synthesized following the method of Singh et al., 2008 with slight modification (Singh et al., 2008). To avoid the degradation of folic acid, all steps were carried out in the dark. Briefly, 1 g of folic acid was dissolved in 20 mL DMSO in a round bottom flask, and 0.5 mL of triethylamine was added under stirring. Then, 520 mg of NHS and 940 mg of DCC, molar excess, were added and the solution was stirred overnight at room temperature. Afterward, the by-product, dicyclohexylurea, was removed by filtration. Then, the yellow

NHS-FA was precipitated by cold anhydrous ether containing 30% acetone, and then washed 3 times with the same solution. The product was then dried in a vacuum oven over night at room temperature.

Next, 100 mg of NHS-FA ester was dissolved in 10 mL of DMSO. A total amount of 100 mg of zein was added into the mixture, then 0.5 ml of triethylamine was added under stirring. The reaction was carried out for 24 hours at 35°C. The covalently linked FA-ZN was purified by dialysis (molecular weight cut off 20 kDa Spectra/POR RC membrane (Spectrum Rancho, CA, USA)) against 70% ethanol aqueous for 2 days to remove unreacted products. The solution was then dried under vacuum overnight, at room temperature.

4.2.2.2. Synthesis of Folic Acid-Covalently Linked Zein Nanoparticles (ZN-FA NPs)

The liquid-liquid dispersion technique was used to synthesize ZN-FA NPs. Briefly, 100 mg of ZN-FA was dissolved in 10 mL of 70% ethanol-aqueous solution and added to 40 mL of a combined lecithin and pluronic F127 solution (1:2 (w/w)). The suspension was microfluidized (Microfluidizer M110P, Microfluidics, MA) 3 times at 30,000 psi in an ice bath. Next, the ethanol was evaporated under vacuum (40 mm Hg) for 45 min (R-124 rotary evaporator Buchi Inc., New Castle, DE). The solvent-free solution was dialyzed for 2 days using 300 kDa Spectra/POR CE membrane (Spectrum Rancho, CA, USA) against deionized water to remove free surfactant. The freshly-made suspension with added trehalose (1:1, w/w) was freeze-dried with Labconco (2.5 plus freezone, Labconco corporation, MO, USA). Then, the lyophilized particles were stored at -20°C for further analysis. All preparations were performed in triplicate.

4.2.3. Preparation of Zein Nanoparticles with Entrapped Folic Acid (ZN(FA) NPs)

Zein nanoparticles with entrapped folic acid were synthesized following the method described below. Briefly, 100 mg of zein was dissolved in 7 mL of 70% ethanol aqueous solution and 3 mL of 50 mg/mL folic acid solution with sodium hydrogen carbonate solution to increase the solubility of folic acid under continuous stirring for 30 min. Then, the mixture was added to 40 mL of a combined lecithin and pluronic F127 solution (1:2 (w/w)). The suspension was microfluidized (Microfluidizer M110P, Microfluidics, MA) 3 times at 30,000 psi in an ice bath. Afterwards, the ethanol was evaporated under vacuum (40 mm Hg) for 45 min (R-124 rotary evaporator Buchi Inc., New Castle, DE). The solvent-free solution was purified for 2 days by dialysis method using 300 kDa Spectra/POR CE membrane (Spectrum Rancho, CA, USA) against deionized water to remove free surfactant. Trehalose (1:1, w/w) was added to the freshly-made suspension and then the suspension was freeze-dried with Labconco (2.5 plus freezone, Labconco corporation, MO, USA). Then, the lyophilized particles were stored at -20°C for further analysis. Empty zein nanoparticles were prepared by the same protocol without the addition of folic acid. All preparations were performed in triplicate.

4.2.4. Characterization of Folic Acid-Covalently Linked Zein Nanoparticles (ZN-FA NPs) and Zein Nanoparticles with Entrapped Folic Acid (ZN(FA) NPs)

4.2.4.1. Evaluation by FTIR, ^{1}H NMR, and UV Spectrophotometry

The covalent linking of folic acid to zein (ZN-FA) was confirmed by FTIR and ^{1}H-NMR spectroscopy. The degree of substitution (DS) of folic acid to amino acid chain of zein was calculated based on ^{1}H-NMR spectrum of FA-ZN and the amount was confirmed using a UV spectrophotometry technique as follows. The presence of amide linkages in covalently linked ZN-FA was evaluated by FTIR, which is an established

quantitative and qualitative analysis technique, based on the light absorption in the infrared region used to identify the presence of certain functional groups in a molecule and for characterizing intermolecular interaction. The spectra was acquired at 400–4000 cm^{-1} wavenumbers with 4 cm^{-1} resolution utilizing a Bruker Tensor 27 FT-IR spectrophotometer (Bruker Optics Inc., MA, USA) equipped with a Pt-diamond ATR cell.

^{1}H NMR spectroscopy is a powerful and non-destructive analytical chemistry technique used to determine for structural characterization of a chemical, and to quantitatively analyze mixtures containing known compounds. The ^{1}H NMR spectra were obtained on a Mercury 400 spectrometer (400 MHz for ^{1}H) in DMSO-d_6 as a solvent at 25°C to confirm the folic acid covalently linked in the ZN-FA construct. The degree of substitution (DS) of folic acid to amino acid residue of zein was calculated based on the ^{1}H-NMR spectrum of ZN-FA.

The amount of NHS-FA covalently linked with zein was also determined using UV spectrophotometry. Briefly, ZN-FA was dissolved in DMSO at a concentration of 1 mg/mL. Then, the solution was scanned in the range of 250 to 400 nm by a UV/Vis spectrophotometer (GENESYS 6, Thermo Electron Scienctific Instruments LLC, WI, USA), using the DMSO as a control. The amount of NHS-FA linked to zein was reported as the mean of triplicate experiments.

4.2.4.2. Particle Size, Polydispersity Index (PDI), and Zeta Potential Characterization

Suspension samples after dialysis were characterized by measuring average diameter size, PDI, and zeta potential by dynamic light scattering (DLS), using a Malvern Zetasizer Nano ZS (Malvern Instruments Ltd., Worcestershire, U.K.). Before the

measurements were taken, samples were diluted to a final concentration range of 0.2-0.3 mg/mL.

4.2.4.3. Morphology Analysis

The morphology of ZN-FA and ZN(FA) NPs was observed by transmission electron microscopy (TEM). One droplet of each sample was placed on a copper grid of 400 mesh with a carbon film, and the excess sample was removed with a filter paper prior to imaging. Uranyl acetate was used as a negative stain to improve the contrast of the image.

4.2.4.4. Loading Capacity Measurement (%)

The standard curve was prepared with a known concentration of folic acid, and it was used to calculate the loading capacity of covalently linked and entrapped folic acid. Briefly, 1 mg/mL of each freeze-dried nanoparticle sample (ZN-FA and ZN(FA) NPs) was re-suspended in DMSO and absorbance measured by a UV/Vis spectrophotometer (GENESYS 6, Thermo Electron Scienctific Instruments LLC, WI, USA) at 358 nm, to determine the amount of folic acid. The loading capacity (%) was calculated by $LC\ (\%) = \left(\frac{Folic\ acid\ in\ nanoparticles\ (mg)}{Total\ amount\ of\ nanoparticles\ (mg)}\right) x\ 100$. All measurements were performed in triplicate.

4.2.5. *In vitro* Release of Covalently Linked and Entrapped Folic Acid from Zein Nanoparticles in Phosphate-Buffered Saline (PBS)

The release mechanism of the linked and entrapped folic acid from zein nanoparticles was studied in phosphate-buffered saline (PBS) solution (0.15 M, pH 7.4) at 37°C. Briefly, 1 mg/mL of sample thoroughly dissolved in PBS was prepared. The mixture was divided and placed into 1.5 ml centrifuge tubes, placed into a shaking incubator (C25KC incubator shaker, New Brunswick Scientific, NJ, USA) at 37°C and 100 rpm for 7 days. At pre-defined time intervals, a centrifuge tube was randomly

sampled and centrifuged at 7,000 g (Allegra 64R centrifuge, Beckman coulter, Inc., CA, USA) for 1 hour. The supernatant was collected and the released folic acid content was determined using a UV/Vis spectrophotometer at 358 nm as described under loading capacity section. All measurements were performed in triplicate.

4.2.6. *In vitro* Cellular Studies

The covalently linked folic acid was hypothesized to enable the binding of the nanoparticles to the folate-receptors on the surface of cancer cells effectively. The cytotoxicity of the nanoparticle samples, including free folic acid was investigated against two types of cell lines (HeLa and A549), which have different amounts of folate receptor on their surface using a standard methyl thiazolyl tetrazolium (MTT) assay to reveal cell inhibition as previously described by Zhang et al., 2010 and 2012 (Zhang et al., 2010; Zhang et al., 2012). Free folic acid was used as a control.

4.2.6.1. Cell and Cell Culture Conditions

The human cervical carcinoma cell line (HeLa) and human lung adenocarcinoma cell line (A549) were cultured at 37°C with 5% CO_2 under humidified atmosphere. The culture medium was Dulbecco's Medium (DMEM) supplemented with 10% heat-inactivated fetal bovine serum and 100 units/mL penicillin/streptomycin.

4.2.6.2. Cytotoxicity Assay

The cytotoxicity of ZN-FA and ZN(FA) NPs in comparison with empty ZN NPs and free folic acid were evaluated using MTT assay. HeLa and A549 cells were seeded in a 96-well plate at a density of ~$1x10^4$ cells/mL, and then incubated for 24 hours at 37°C under 5% CO_2. The plates were incubated with 100 μL of samples (1 mg/mL) for 24 hours. The medium was replaced with fresh DMEM (100 μL). Then, 10 μl of MTT (5

mg/mL) was added to each well, followed by incubation for 24 hours at 37°C. The supernatant was carefully removed, and 200 μL of DMSO was added to each well. The absorbance of the solution was measured using a microplate reader at 570 nm. Cell viability was calculated by $Cell\ viability = \frac{OD_{treated}}{OD_{control}}\ x\ 100\%$. Where $OD_{treated}$ was obtained from the cells treated with the samples, $OD_{control}$ was obtained from the cells untreated with the samples. All measurements were performed in triplicate and the data were given as mean ± standard deviation (STD).

4.2.6.3. Cellular Uptake (Quantification)

The amount of the nanoparticles uptaken into HeLa and A549 cells was quantified using a spectroscopic method described by Zhang et al., 2010 with slightly modification (Zhang et al., 2010). Briefly, 100 μL of each sample (1 mg/mL) were added to 900 μL of DMEM culture medium (no phenol red) with ~1x10^3 cells/mL in a 1.5 mL microcentrifuge tube (Beckman), then incubated for 1 hour at 4°C and centrifuged at 1000 rpm (Allegra 64R centrifuge, Beckman coulter, Inc., CA, USA) for 5 min. The supernatant containing the free particles was stored and absorbance measured at 297 nm (maximum wavelength of the nanoparticles dissolved in DMEM). Fresh DMEM culture medium containing the same amount of nanoparticles was taken as a control. The absorbance values were converted to the amount of the nanoparticles (μg/10^3 cells) using the calibration curve. All measurements were performed in triplicate.

4.2.7. Data Statistical Analysis

All experiments were performed in triplicate and the results were reported as the mean ± standard error. Statistical analysis was performed in SAS (version 9.4, SAS

Institute Inc., NC, USA). The analysis of variance (ANOVA) was used to determine significant differences between the systems. The significance level (*P*) was set at 0.05.

4.3. Results and Discussion

4.3.1. Confirmation of Successful Covalent Link Between Folic Acid and Zein

Synthesis of the folic acid-zein was carried out with a three-step procedure. First, folic acid was activated using NHS, DCC, and TEA. Next, the NHS-folic acid ester was reacted to zein via a primary amide linkage through the γ-carboxylic group of folic acid due to its higher reactivity (Zhao et al., 2008; Kim et al., 2007). Successful linking of folic acid to zein was confirmed FTIR and ^{1}H NMR, and the amount linked was quantified by UV/Vis analysis, as follows.

4.3.1.1. FTIR Spectrum of Covalently Linked Folic Acid with Zein (ZN-FA)

The reaction of NHS and folic acid was confirmed by the presence of two increased absorption peaks at 1660 cm^{-1} due to the N-O bond, and at 1700 cm^{-1} due to the C=O bond formation, which proved the connecting link between folic acid and NHS as seen in Figure 4.1.

This phenomenon confirmed that folic acid was successfully attached to NHS. The conjugation of folic acid to zein was accomplished was carried out for 24 hours at 35°C. The activated γ-carboxylic group of folic acid was possibly linked with the primary amino acid side chain (-NH_2) of zein, which is more active than the amide II (-NH-) in the backbone (Appendix B.1). The FTIR bands of zein and folic acid assigned to their structures were used as references (Appendix B.2 and B.3).

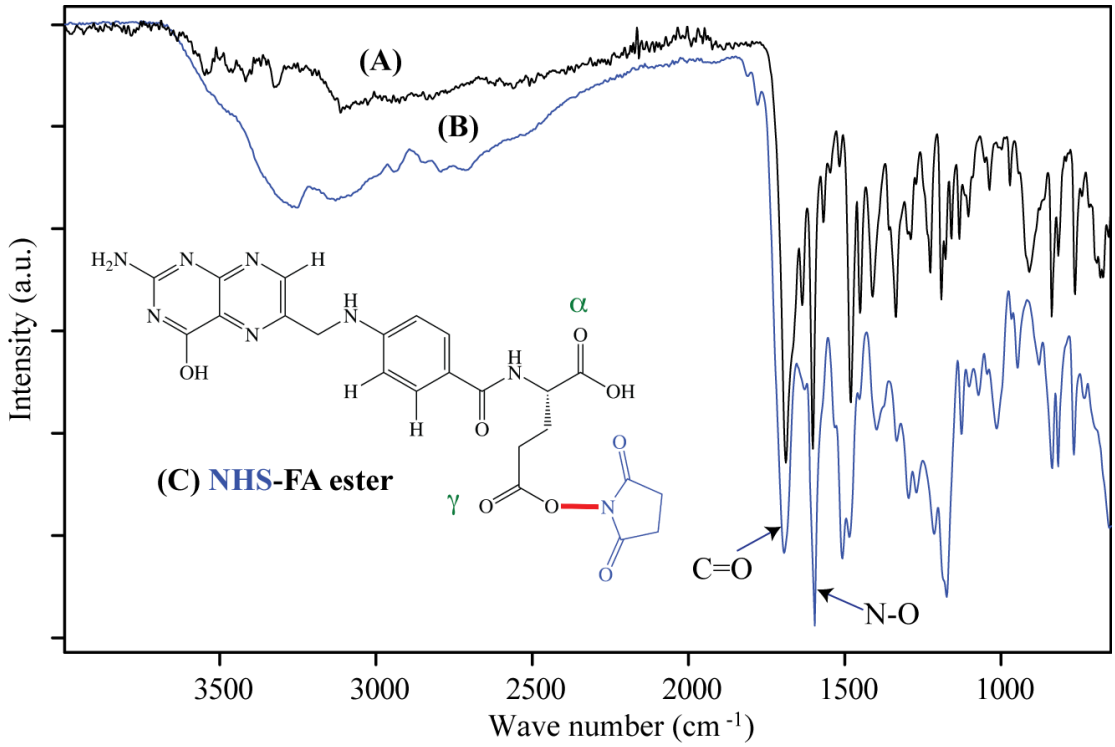

Figure 4.1. FTIR spectra of folic acid (A) and NHS-FA (B) and the schematic structure of NHS-FA ester (C)

The appearance of a weak and broad band in the range between ~3100 and ~3500 cm^{-1} of folic acid linked with zein is attributed to the stretching of either O-H groups and N-H primary amide on the structure of zein or the O-H carboxylic of glutamic acid and the N-H group of pterin ring of folic acid, which was broaden when linked together (Figure 4.2). The peak at ~2958 cm^{-1} is attributed to the C-H functional groups of zein. The small peak at ~1690 cm^{-1} in the ZN-FA product (C), slightly shifted, is assigned to the C=O carboxylic stretching vibration of folic acid. The stretching at ~1650 cm^{-1} belongs to the amide I carbonyl C=O ($-CONH_2$) of folic acid and zein, which is attributed to the backbone conformation, were slightly shifted and increased peak shown in the ZN-FA new product (C). The angular deformation vibration at ~1535 cm^{-1} represents the N-H amide II of zein, which also appeared in the ZN-FA (C). The

appearance of a band at 1108 cm^{-1} corresponds to C-N bond stretching assigned to the amide-functionalized ZN-FA sample. The peaks specific to the phenyl and pterin ring ranging from 1485-1520 cm^{-1} of folic acid were interfered with the same positions of Amide I and Amide II of zein. These results further confirmed the presence of folic acid covalently linked to zein via the amide functional group.

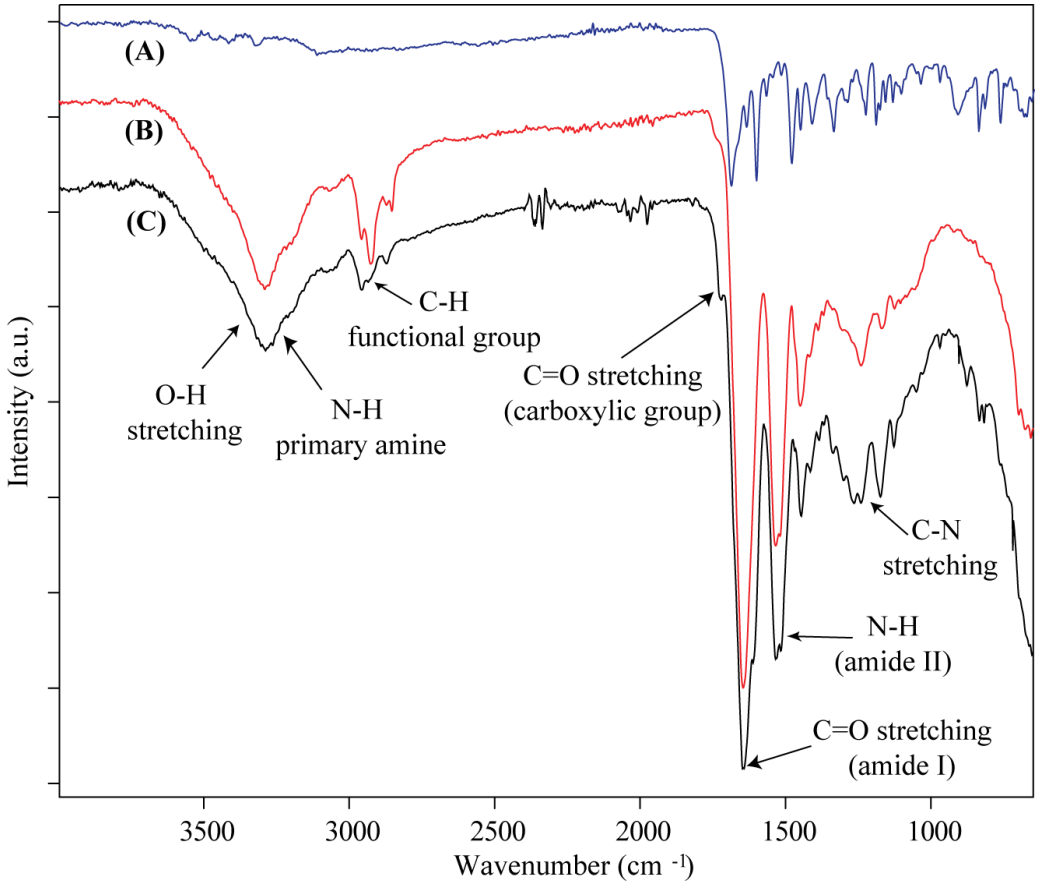

Figure 4.2. FTIR spectra of folic acid (A), zein (B), and folic acid-covalently linked with zein (ZN-FA) (C)

4.3.1.2. ^{1}H NMR Spectrum of Folic Acid Covalently Linked with Zein (ZN-FA)

In addition, the presence of the folic acid covalently linked to zein product was confirmed by ^{1}H NMR spectra (Figure 4.3). The activated γ-carboxylic group of folic acid attached mainly at the primary amino group on zein. The appearance of the

characteristic resonance peak signals at δ=8.67 ppm represents a 6-methylpteridin ring of folic acid, and at δ=7.65 and 6.63 ppm represents a phenyl ring, which corresponded to the aromatic protons of folic acid (B).

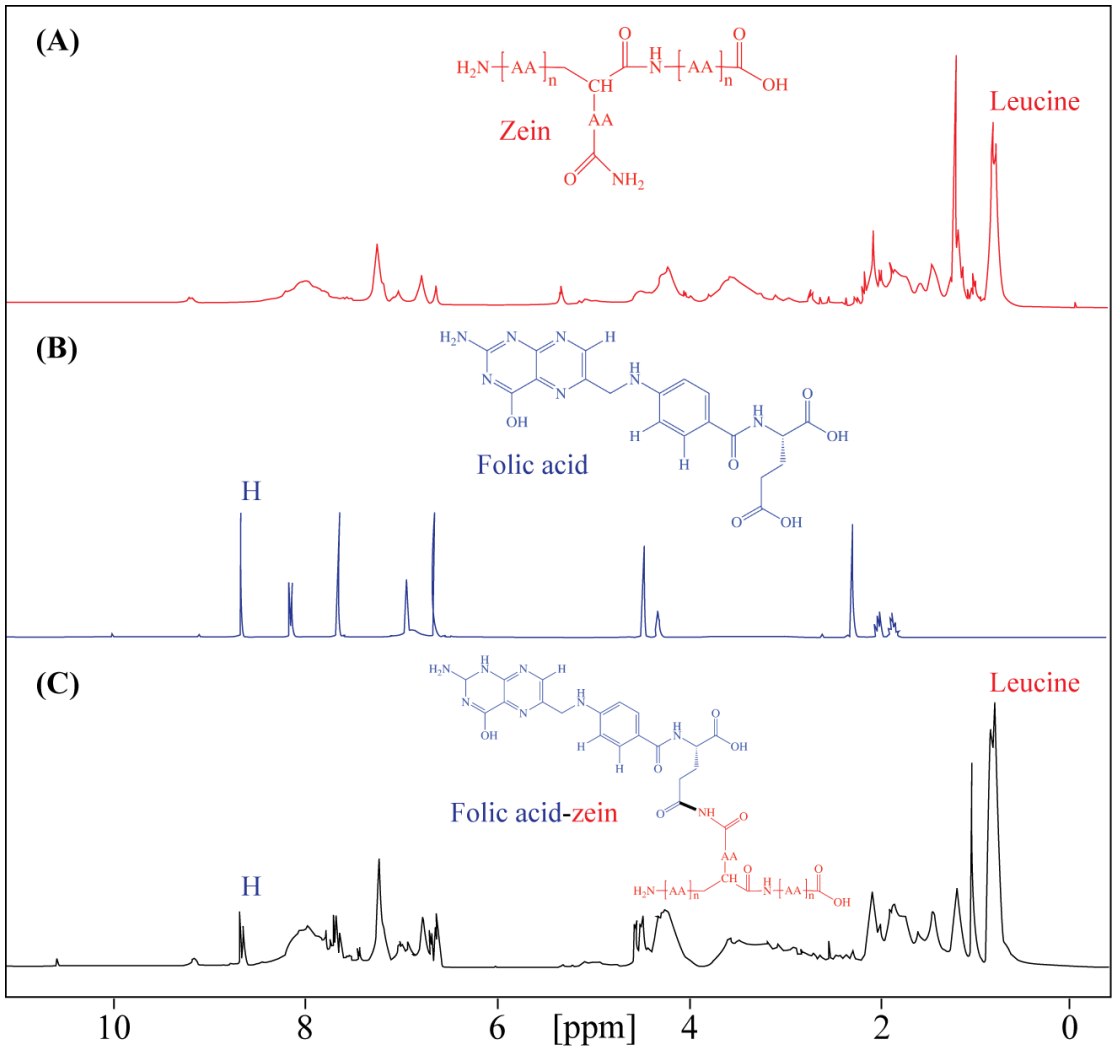

Figure 4.3. ^{1}H NMR spectra and chemical structures of zein (A), folic acid (B), and folic acid covalently linked with zein (ZN-FA) (C)

It was obvious that the resonance peak signal at δ=8.67 ppm was found in the structure of ZN-FA (C). The peak signal at δ=4.56 ppm also assigns to the C-H functional group of folic acid; however, it was interfered with the peak of zein at the same area. Additionally, the peak signal at δ=2.32 ppm, which corresponds to the CH

functional group close to the γ-carboxylic group of folic acid, was shifted to δ=2.10 ppm when folic acid was linked with zein. These finding indicated that folic acid could be effectively linked to the amino acid group of zein. The degree of substitution of folic acid to zein, calculated based on the area peaks between δ=8.67 ppm (1.00 = 1 H of folic acid) and the peak at δ=0.84 ppm (25.77 = 20% leucine of zein) was calculated to be 156.9 μg/mg, which would indicate that FA:ZN molar ratio was 8:1, which means that about eight folic acid molecules were estimated to bind to one zein molecule.

4.3.1.3. UV Spectrophotometry of Folic Acid Covalently Linked with Zein (ZN-FA) and the Amount of Folic Acid Linked with Zein (Quantification)

Zein has an extremely strong single peak at 285 nm under UV/Vis, whereas folic acid showed two absorption peaks at 295 and 358 nm, the latter being the maximum wavelength. The two absorption peaks of ZN-FA product were at 290 nm and 358 nm, which were not found in zein (Figure 4.4). The slight shift of the first position (295 nm) indicated that folic acid had successfully linked with zein, and the peak at 358 nm was chosen for the evaluation of folic acid linked to zein in this research.

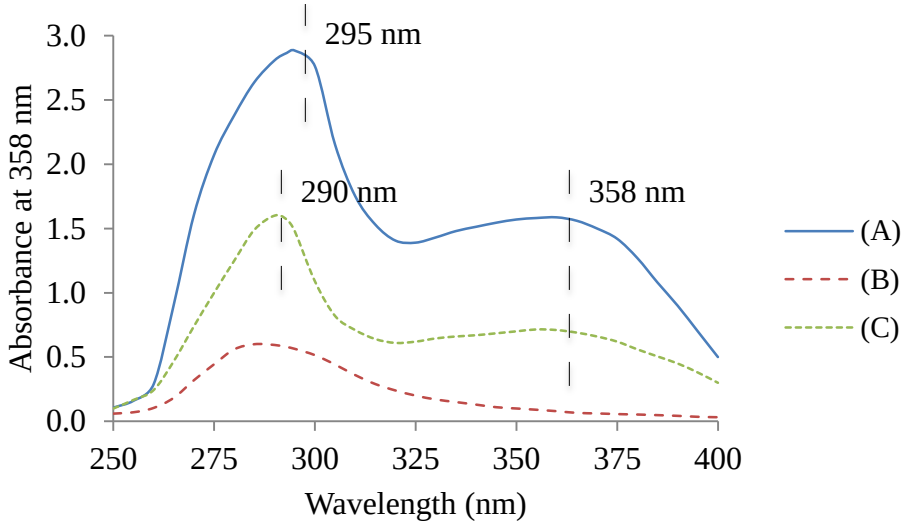

Figure 4.4. UV/Vis spectra of folic acid (A), zein (B), and folic acid-zein (ZN-FA) (C)

The amount of folic acid covalently linked to zein was checked by measuring the absorbance of the ZN-FA at 358 nm (FA, ε = 15,760 $M^{-1}cm^{-1}$) and the value was converted to concentration by using a calibration curve of the folic acid dissolved in DMSO. It was found that the amount of covalently linked folic acid was approximately 119.03 μg/mg of zein, similar to the value determined by ^{1}H NMR of 156.91 μg/mg.

4.3.2. Characterization of Folic Acid-Covalently Linked Zein Nanoparticles (ZN-FA NPs) and Zein Nanoparticles with Entrapped Folic Acid (ZN(FA) NPs)

A liquid-liquid dispersion method was successfully used to synthesize zein nanoparticles with covalently linked and physically entrapped folic acid. A combination of lecithin and pluronic F127 was used to stabilize the nanoparticles. Theoretically, the hydrophilic head of lecithin attaches with hydrophilic polyethylene glycol of pluronic F127 and the hydrophobic polypropylene possibly interwinds with the zein matrix resulting in a hydrophilic zein nanoparticle. In the physical entrapment system, folic acid was incorporated inside the matrix, particularly in the hydrophilic region, of zein by electrostatic interaction (Figure 4.5).

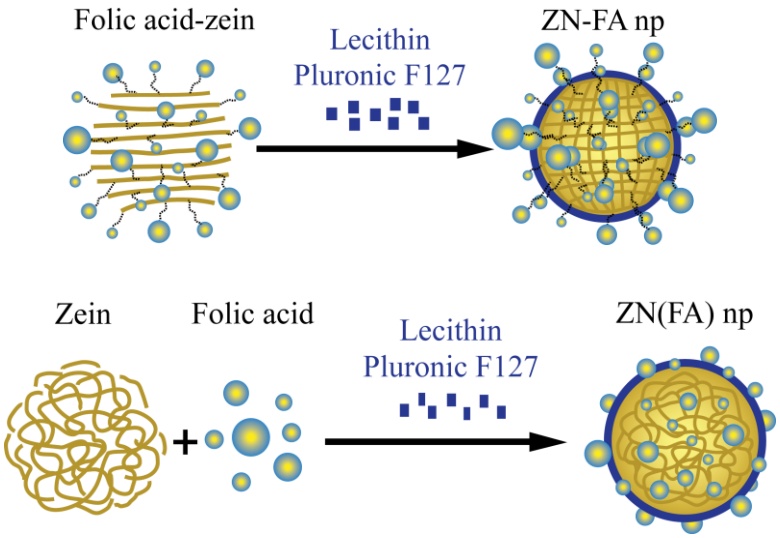

Figure 4.5. Proposed structures of folic acid-covalently linked zein nanoparticles (ZN-FA NPs) and zein nanoparticles with entrapped folic acid (ZN(FA) NPs)

ZN-FA and ZN(FA) NPs were characterized in freshly synthesized form in terms of size, size distribution (PDI), zeta potential, morphology, and loading capacity, as follows.

4.3.2.1. Size, PDI, Zeta potential, and Loading Capacity (%)

Dynamic Light Scattering (DLS) enabled measurement of ZN-FA and ZN(FA) NPs revealed that mean diameter of ZN-FA NPs was 67.2±6.6 nm, which was statistically smaller than 96.8±5.9 nm of the ZN(FA) NPs. ZN-FA NPs was made from purified zein after being chemically reacted and dialyzed with 20kDa, from which small sub-fractions (~10 kDa) were possibly removed. Mainly α-zein (~21-24 kDa) remained, resulting in a good rearrangement in the zein matrix and a smaller nanoparticle size. The polydispersities of the two systems (less than 0.3 in both cases) were statistically different between nanoparticle types. Zeta potential of the zein nanoparticles with entrapped folic acid was negative (-20.2±3.6 mV), while particles made from ZN-FA were even more negatively charged (-27.5±4.4 mV) (Table 4.1).

Table 4.1. Characteristics of folic acid-covalently linked zein nanoparticles (ZN-FA NPs) and zein nanoparticles with entrapped folic acid (ZN(FA) NPs)

Sample [a]	Size (nm)	PDI (a.u)	Zeta Potential (mV)	LC (%)
ZN-FA NPs	67.2±6.6*	0.22±0.02*	-27.5±4.4	7.10±0.3*
ZN(FA) NPs	96.8±5.9	0.16±0.01	-20.2±3.6	2.11±0.5

[a] ZN-FA and ZN(FA) NPs represent formulations of folic acid-covalently linked zein nanoparticles and zein nanoparticles with entrapped folic acid, respectively
* indicates statistically significant difference

The results were consistent with the literature; several studies pointed out that the non-charged or partly negatively charged residue of folic acid replaced the positively charged primary amino group when linked to zein. The loading capacity of ZN(FA) NPs

was 2.11±0.5%, smaller than that of ZN-FA NPs (7.10±0.3%) (Table 4.1). Due to the hydrophobicity of zein, the results are not surprising. Covalent linking of zein to folic acid improved the hydrophilic loading ability of zein nanoparticles.

4.3.2.2. Morphology

TEM images of ZN-FA and ZN(FA) NPs indicated that particle size varied from 50 to 100 nm and that NPs were uniformly dispersed (Figure 4.6), confirming the DLS data (Table 4.1). The covalent link did not result in a modification of the NP shape; both ZN-FA and ZN(FA) NPs were spherical in shape. However, surface properties of the ZN-FA NPs were different than those of ZN(FA) NPs, as indicated by the lighter color of the ZN-FA NPs versus ZN(FA) NPs. The darker shade of the ZN(FA) was most likely, due to the presence of the carboxyl group of zein, which could interact strongly with the negative stain resulting in more electron absorption around and in the crevices on the surfaces of the particles.

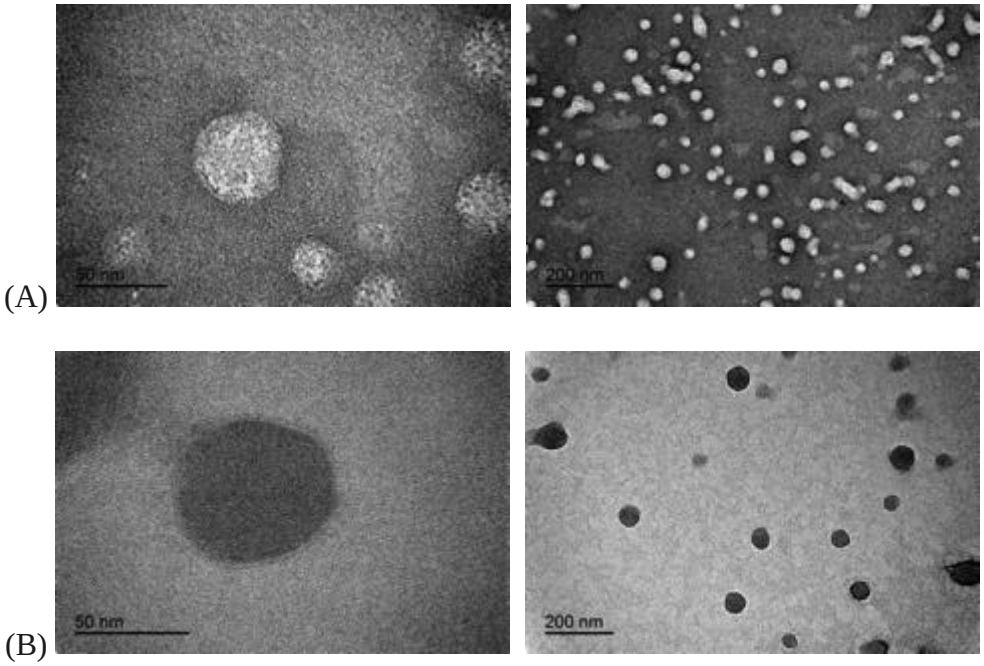

Figure 4.6. TEM images of folic acid-covalently linked zein nanoparticles (ZN-FA NPs) (A) and zein nanoparticles with entrapped folic acid (ZN(FA) NPs) (B)

4.3.3. *In vitro* Release Study

The release study of folic acid from ZN-FA and ZN(FA) NPs in PBS (pH 7.4) at 37°C over 168 hours (Figure 4.7) indicated that the release profile of folic acid from ZN(FA) NPs followed zero-order kinetic with an initial-burst release in the first 12 hours and complete release after 6 days, while the release pattern of folic acid from ZN-FA NPs followed a bi-phasic release with an initial fast release (55%) in the first 24 hours and gradually released (73%) until 7 days.

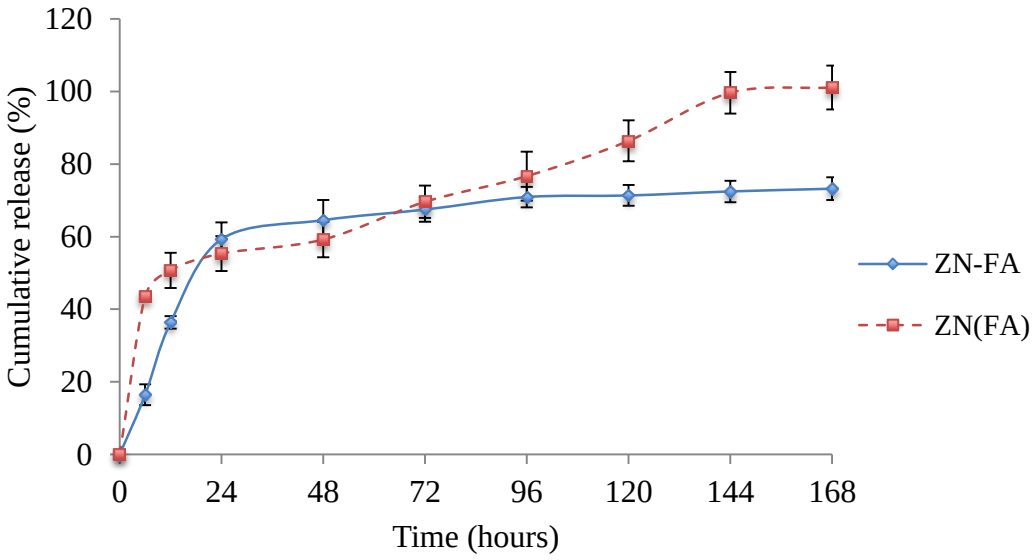

Figure 4.7. Release profiles of covalently-linked folic acid (ZN-FA) and physically entrapped folic acid (ZN(FA)) for 7 days under PBS (pH 7.4) at 37°C, 100 rpm. Error bars represent the standard error

The release kinetics of loaded folic acid from ZN-FA and ZN(FA) NPs differ in several aspects (Figure 4.8). For the first 12 hours, covalently linked folic acid released at a slower rate than nanoentrapped folic acid. The degradation of zein by hydrolysis in PBS at pH 7.4 over the next 6 days (Hurtado-Lopez and Murdan 2006) allowed loaded folic acid to be released in a sustained manner over this time frame (from 55.35% at 24 hours to 99.65% at 144 hours) whereas only a smaller amount of folic acid was released during

this time from the ZN-FA NPs (from 59.29% at 24 hours to 72.48% at 144 hours). The differences can be attributed not only to the folic acid cleavage from zein, but also to the different structures of zein nanoparticles impacting the diffusion and release of folic acid (Figure 4.8).

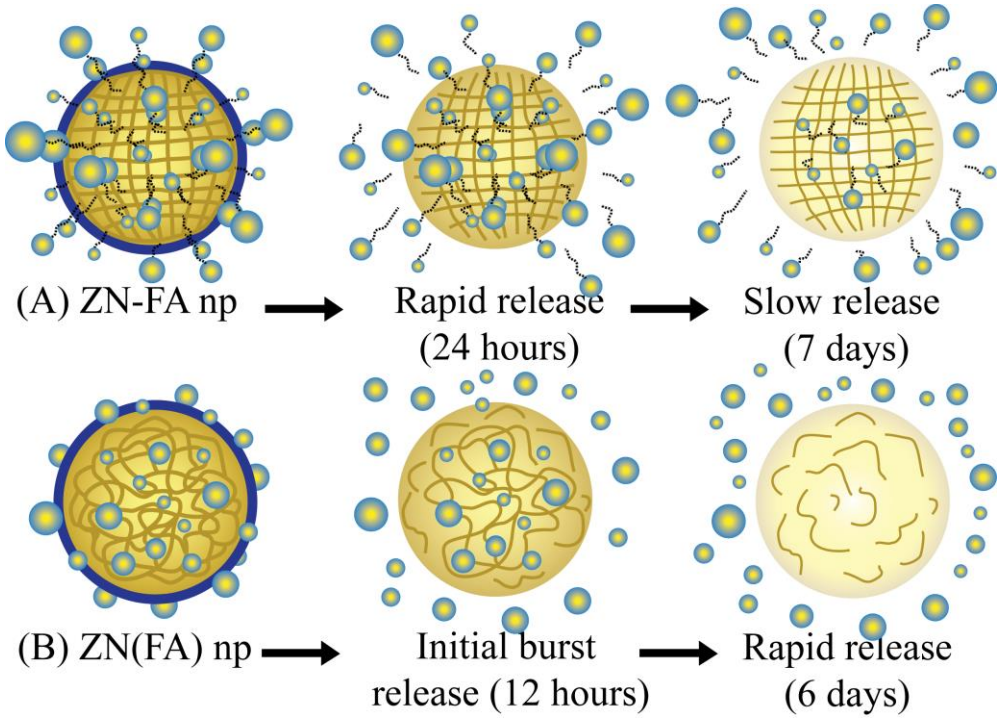

Figure 4.8. Illustrated release mechanisms of folic acid from ZN-FA NPs (A) and ZN(FA) NPs (B)

It is postulated that zein in the ZN-FA NPs was a much better organized matrix relative to zein in the ZN(FA) NPs due to the removal of the small fractions of zein in the raw material by dialysis following the ZN-FA synthesis step, forming a better barrier against release of covalently linked folic acid. The folic acid release was compared to the release of entrapped folic acid from a different type of polymeric nanoparticles made from poly(DL-lactide-co-glycolide) (Stevanović et al., 2008). The release of folic acid from PLGA NPs followed a tri-phasic pattern with an initial burst effect at the first day,

followed by a slow release from the matrix due to the diffusion of the drug (~20% release from day 1 to day 12), and then a sustained release due to the degradation of the polymer (82% at 24 days). The degradation of the polymer is directly responsible for the release kinetics of the bioactives and explain the different kinetics between folic acid released from PLGA nanoparticles reported in the literature and the release from zein nanoparticles reported herein. Overall, it was apparent that the sustained release of the covalently linked folic acid from 72 hours on was achieved, making this delivery system superior for use as an ideal targeting nanocarrier.

4.3.4. *In vitro* Cytotoxicity

The cytotoxicity of FA, ZN NPs, ZN-FA NPs, and ZN(FA) NPs to HeLa and A549 cells was determined by MTT assay (Figure 4.9). The cells were incubated with the samples in the medium at 37°C for 24 hours. All experiments were done at a constant folic acid concentration of 70 μg/mL. Cells treated with empty ZN NPs had the highest proliferation (%) compared to other treatments for both types of cells indicating that the delivery system in of itself was not toxic to the cells. This was in agreement with several studies which stated that zein had a positive effect and good compatibility to cells (Wang et al., 2005; Aswathy et al., 2012) and zein nanoparticles can be used as a folic acid nanocarrier for targeting purposes. When treated with folic acid loaded particles either covalently-linked or physically-loaded, the survival rates of both cell lines decreased. Survival rates of HeLa were statistically different than those of A549 for both nanoparticle systems, most likely due to an increase uptake of folic acid through a folate receptor-mediated process. HeLa cells are known to express folate receptors which can be targeted by folic acid when compared to negative folate receptor A549. These findings

strongly supported that zein nanoparticles had less toxicity to cells and also diminished the toxicity of folic acid reflected in the relative survival rates of cells.

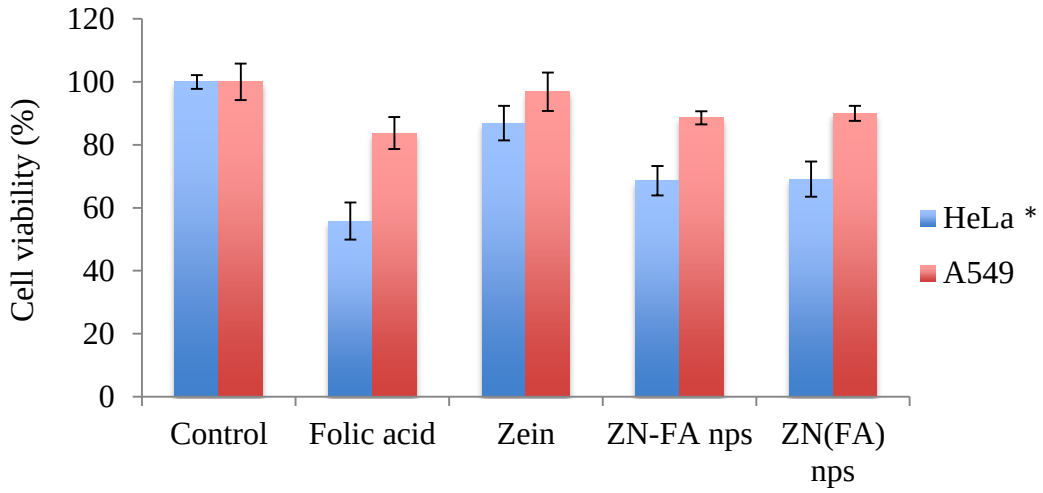

Figure 4.9. Effect of FA, ZN NPs, ZN-FA NPs and ZN(FA) NPs on the viability of HeLa and A549 cells, expressed in terms of the percentage of viable cells relative to control cells. All experiments were carried at 70 μg/mL folic acid, corresponding to 1 mg/ml ZN-FA and ZN NPs, and 3.36 mg/ml ZN(FA); * indicates statistically significant difference between HeLa and A549 cells

4.3.5. Nanoparticle uptake (Quantification)

Based on the cytotoxicity results, it was obvious that both types of nanoparticles had an effect on HeLa cells, causing a lower survival rate, while A549 cells lacking the folate-receptors had a better survival under the same conditions. When nanoparticle uptake was compared across the different cell lines, HeLa showed a higher percent uptake for all samples, compared with that of A549 (Figure 4.10), further supporting the cytotoxicity data (Figure 4.9). The highest NP uptake was found for ZN-FA NPs 4.25% in HeLa and 1.67% in A549, compare to ZN(FA) NPs (3.22% in HeLa and 1.19% in A549). These findings confirmed that the ZN-FA NPs have the potential ability to be endocytosed by cancer cells to a higher extent than ZN(FA) NPs, particularly cells containing folate receptors.

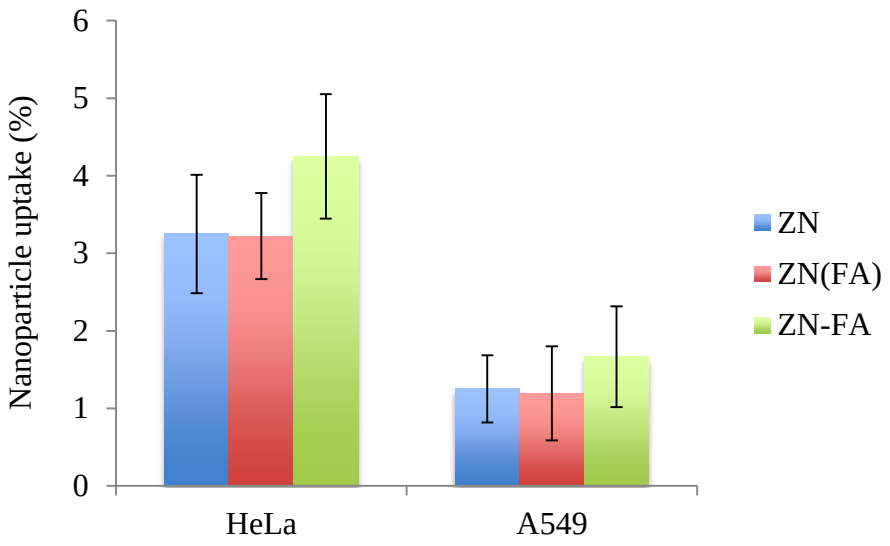

Figure 4.10. Percent uptake of ZN-FA NPs, ZN(FA) NPs, and ZN NPs by HeLa and A549 as target cells

4.4. Conclusion

Zein nanoparticles as a novel targeting nanocarrier was developed using folic acid as a targeting ligand. Zein was covalently linked with folic acid through the reaction between the carboxyl group of folic acid and the primary amino group of zein and the link was confirmed by FTIR and ^{1}H NMR, and the amount of linked folic acid to zein was quantified using ^{1}H NMR spectrum and UV spectrophotometry. ZN-FA NPs were smaller in size and have more negatively charged with slightly higher value of polydispersity index, compared to ZN(FA) NPs. Covalent linking of zein to folic acid improved the hydrophilic loading ability of zein nanoparticles. The release of the covalently linked was delayed when compared to release of physically entrapped folic acid, both systems being able to sustain the release of folic acid from zein nanoparticles over 7 days. Cytotoxicity results proved that zein nanoparticles were biocompatible to HeLa and A549 cells and both systems were able to diminish the adverse toxic effect of folic acid to cells. The increased uptake and toxicity of ZN-FA relative to ZN(FA)

supported the use of ZN-FA as targeting agents over-expressing folate receptor cells such as HeLa. Based on these findings, the modified zein nanoparticles with covalently linked folic acid were found superior for sustained release and targeting properties, and may be a promising targeted nanocarrier for delivery of drugs.

4.5. References

Ai, J., Y. Xu, D. Li, Z. Liu, and E. Wang (2012). "Folic acid as delivery vehicles: targeting folate conjugated fluorescent nanoparticles to tumors imaging". *Talanta,* 101 32-37.

Aswathy, R. G., B. Sivakumar, D. Brahatheeswaran, T. Fukuda, Y. Yoshida, T. Maekawa, and D. S. Kumar (2012). "Biocompatible fluorescent zein nanoparticles for simultaneous bioimaging and drug delivery application". *Advances in Natural Sciences: Nanoscience and Nanotechnology,* 3 (2), 025006.

Boddu, S. H., R. Vaishya, J. Jwala, A. Vadlapudi, D. Pal, and A. Mitra (2012). "Preparation and characterization of folate conjugated nanoparticles of doxorubicin using PLGA-PEG-FOL polymer". *Med chem,* 2 (Suppl 4), 68-75.

Castillo, J. J., T. Rindzevicius, L. V. Novoa, W. E. Svendsen, N. Rozlosnik, A. Boisen, P. Escobar, F. Martínez, and J. Castillo-León (2013). "Non-covalent conjugates of single-walled carbon nanotubes and folic acid for interaction with cells over-expressing folate receptors". *Journal of Materials Chemistry B,* 1 (10), 1475-1481.

Hurtado-Lopez, P. and S. Murdan (2006). "Zein microspheres as drug/antigen carriers: a study of their degradation and erosion, in the presence and absence of enzymes". *J Microencapsul,* 23 (3), 303-14.

Jagerstad, M. (2012). "Folic acid fortification prevents neural tube defects and may also reduce cancer risks". *Acta Paediatr,* 101 (10), 1007-12.

Kim, S.-L., H.-J. Jeong, E.-M. Kim, C.-M. Lee, T.-H. Kwon, and M.-H. Sohn (2007). "Folate receptor targeted imaging using poly (ethylene glycol)-folate: in vitro and in vivo studies". *Journal of Korean medical science,* 22 (3), 405-411.

Singh, P., U. Gupta, A. Asthana, and N. K. Jain (2008). "Folate and folate− PEG− PAMAM Dendrimers: synthesis, characterization, and targeted anticancer drug delivery potential in tumor bearing mice". *Bioconjugate chemistry,* 19 (11), 2239-2252.

Stevanović, M., A. Radulović, B. Jordović, and D. Uskoković (2008). "Poly (DL-lactide-co-glycolide) nanospheres for the sustained release of folic acid". *Journal of Biomedical Nanotechnology,* 4 (3), 349-358.

Taylor, C. M., C. Atkinson, C. Penfold, S. Bhattacharya, D. Campbell, G. Davey Smith, S. Leary, and A. Ness (2015). "Folic acid in pregnancy and mortality from cancer and cardiovascular disease: further follow-up of the Aberdeen folic acid supplementation trial". *J Epidemiol Community Health,* 69 (8), 789-94.

Teng, Z., Y. Luo, T. Wang, B. Zhang, and Q. Wang (2013). "Development and application of nanoparticles synthesized with folic acid conjugated soy protein". *Journal of agricultural and food chemistry,* 61 (10), 2556-2564.

Wang, H.-J., L. Di, Q.-S. Ren, and J.-Y. Wang (2009). "Applications and degradation of proteins used as tissue engineering materials". *Materials,* 2 (2), 613-635.

Wang, H. J., Z. X. Lin, X. M. Liu, S. Y. Sheng, and J. Y. Wang (2005). "Heparin-loaded zein microsphere film and hemocompatibility". *J Control Release,* 105 (1-2), 120-31.

Zhang, H., Z. Cai, Y. Sun, F. Yu, Y. Chen, and B. Sun (2012). "Folate-conjugated beta-cyclodextrin from click chemistry strategy and for tumor-targeted drug delivery". *J Biomed Mater Res A,* 100 (9), 2441-9.

Zhang, H., Z. Cai, Y. Sun, F. Yu, Y. Chen, and B. Sun (2012). "Folate- conjugated β-cyclodextrin from click chemistry strategy and for tumor- targeted drug delivery". *Journal of Biomedical Materials Research Part A,* 100 (9), 2441-2449.

Zhang, Z., J. Jia, Y. Lai, Y. Ma, J. Weng, and L. Sun (2010). "Conjugating folic acid to gold nanoparticles through glutathione for targeting and detecting cancer cells". *Bioorganic & medicinal chemistry,* 18 (15), 5528-5534.

Zhao, X., H. Li, and R. J. Lee (2008). "Targeted drug delivery via folate receptors". *Expert Opin Drug Deliv,* 5 (3), 309-19.

Zhou, J., G. Romero, E. Rojas, S. Moya, L. Ma, and C. Gao (2010). "Folic Acid Modified Poly (lactide- co- glycolide) Nanoparticles, Layer- by- Layer Surface Engineered for Targeted Delivery". *Macromolecular Chemistry and Physics,* 211 (4), 404-411.

Zu, Y., Q. Zhao, X. Zhao, S. Zu, and L. Meng (2011). "Process optimization for the preparation of oligomycin-loaded folate-conjugated chitosan nanoparticles as a tumor-targeted drug delivery system using a two-level factorial design method". *International journal of nanomedicine,* 6 3429.

CHAPTER 5
CONCLUSIONS AND FUTURE WORK

5.1. Conclusions

Engineered zein nanoparticles were designed to optimize the potential of nanodelivered antioxidants, lutein, β-carotene, and folic acid by providing enhanced chemical stability, controlled release kinetics, and improved functionality such as antioxidant and targeting ability (Table 5.1). The ability of zein nanoparticles, made with and without surfactants, to protect lutein from oxidation and to control the release kinetics of lutein under on-shelf and storage conditions was shown in Chapter 2. A combination of lecithin and pluronic F127 as surfactants improves physicochemical stability of the nanoparticles and chemical stability of entrapped lutein. Surfactant use resulted in an increased size, improved polydispersity index, decreased zeta potential, and improved entrapment efficiency. A two-phase lutein release profile was observed in PBS in the presence of surfactants that consisted of an initial-burst release at 24 hours, followed by a gradual zero-order release profile. Lutein degradation followed second-order kinetics with no significant difference between nanoentrapped lutein and emulsified control. Nanoparticles stabilized with surfactants did improve chemical stability of lutein under different temperatures over time and in the presence of UV. *Based on this data, zein nanoparticles stabilized with surfactants proved to be able to protect lutein against chemical degradation and to slow down lutein release under PBS conditions.*

The ability of zein nanoparticles to enhance chemical stability and the functionality (antioxidant activity) of the bioactive (β-carotene) in the absence and presence of milk as a food matrix, under simulated gastrointestinal (GI) conditions was

proven (Chapter 3). Zein nanoparticles showed good physical stability after 2 hours of exposure in simulated gastric fluid (SGF), and degraded when exposed to simulated intestinal fluid (SIF) for 24 hours, which was consistent with results by TEM pictures. The nanoentrapment proved to be beneficial to β-carotene stability, but this advantage was decreased in the presence of milk. Antioxidant activity level of β-carotene in the particle system measured by ABTS was higher than that of the emulsion system in SGF and SIF, respectively. With the addition of milk, the improvement in antioxidant activity of nanodelivered β-carotene was similar for β-carotene delivered by particles and emulsion. The TBARS results confirmed the advantage of entrapping β-carotene to improve its antioxidant activity by reducing MDA formation, effect enhanced in the presence of milk system. *In this chapter, it was concluded that zein nanoparticles improved chemical stability and antioxidant activity of entrapped β-carotene versus emulsions in the presence of milk under simulated gastrointestinal environments.*

Lastly, zein nanoparticles were surface functionalized by covalently linking folic acid as a ligand to create a novel nanocarrier for targeting purposes. Release kinetics, uptake, and cytotoxicity of the ZN-FA NPs were compared against ZN NPs with entrapped folic acid, ZN(FA) NPs (Chapter 4). The release profiles of folic acid from ZN-FA and ZN(FA) NPs were reported as bi-phasic patterns. The covalent link slowed the release of folic acid from zein nanoparticles over 7 days. The cytotoxicity results proved that zein nanoparticles had a good biocompatibility and diminished the adverse effect of folic acid to cells. Nanoparticles with covalently linked folic acid had a higher uptake, particularly in the over-expressing folate receptor cells. *Based on these results, the modified zein nanoparticles with covalently linked folic acid were biocompatible and*

able to achieve a sustained release of the folic acid. Folic acid-covalently linked zein nanoparticles could be developed into promising targeted drug nanocarriers for various applications.

5.2. Future Work

Nanodelivery systems have the potential to provide solutions for development of nano-enabled foods with a positive impact on human health. The scarcity of the methodologies able to track and measure stability of nanodelivery system in a complex food matrix is partly responsible for the lack of adoption of nanotechnology in foods. Incorporation of zein nanoparticles in food matrix can cause sensorial changes which have not been addressed in this study. The fate of the nanodelivery system from ingestion to excretion and safety concerns, have only tangentially been touched in this project, More studies are needed to fulfill this gap, and directions for new projects are provided in more detail below. Methodology development: New methods must be developed to be able to track organic nanoparticle fate in the food matrix and in the body. Nanoparticle-food interaction: Interaction between nanoparticles and complex food matrices (proteins, fats, carbohydrates) should be followed during processing, sterilization, and distribution to identify physical, chemical, and sensorial changes in the foods. Nanoparticles biotransformation: The characteristics of nanoparticles (e.g., size, surface charge, functionalities) and their change during GI transit should be identified and these changes correlated with the absorption, distribution, metabolism, and excretion (ADME) of nanoparticles. ADME should be studied in vivo to identify the fate of nanoparticles in the body. Nanoparticle toxicity: *In vivo* animal studies should be pursued in an attempt to address safety concerns of food-grade nanodelivery system for use in foods.

Table 5.1. Summary table of zein nanoparticle as the nanodelivery system for hydrophobic/hydrophilic antioxidants

System	ZN(LT) NP 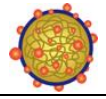	ZN(BC) NP 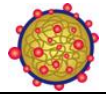	ZN(FA) NP 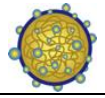	ZN-FA NP 
Antioxidant	Lutein	β-Carotene	Folic acid	Folic acid
Hydrophobicity	Hydrophobic	Hydrophobic	Hydrophilic	Hydrophilic
Loading mechanism	Physical entrapment	Physical entrapment	Physical entrapment	Covalent link
Characteristics	Size, PDI, zeta potential, and EE	Size, PDI, zeta potential, and EE	Size, PDI, zeta potential, and LC	
Morphology (TEM)	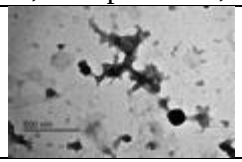	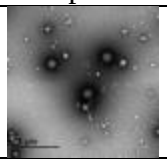	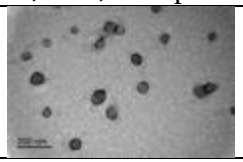	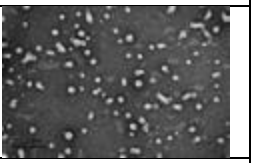
Release mechanism	Initial-burst (24 hours) and slow release profiles (7 days)	-	Initial-burst (12 hours) and rapid release profiles (6 days)	Rapid (24 hours) and slow release profiles (7 days)
Condition	On-shelf (temperature, time, and UV)	Food matrix interaction Simulated GI tract	Cell lines: HeLa and A549	
Stability	Degradation of entrapped lutein Physical stability of zein nanoparticles Chemical stability of entrapped lutein	Physical stability of zein nanoparticles Chemical stability of entrapped β-carotene	-	
Functionality	Protected lutein against chemical degradation and sustained release of entrapped lutein under PBS conditions	Improved chemical stability and antioxidant activity of entrapped β-carotene in the presence of milk under simulated GI tract	Sustained release and can be used as a targeting nanocarrier Biocompatible with the cells, diminished the toxic effect of folic acid to cells	

Note: ZN(LT), ZN(BC), and ZN(FA) NPs represent the formula of zein nanoparticles with entrapped lutein, β-carotene, and folic acid respectively. ZN-FA NP represents the formula of zein nanoparticles with covalently linked folic acid.

APPENDIX A. ADDITIONAL INFORMATION OF ZEIN

A.1. Amino acid composition of zein

Class	Amino acid	(g amino acid/100 g zein)
Non-polar	Glycine	0.7
	Alanine	8.3
	Valine	3.1
	Leucine	19.3
	Isoleucine	6.2
	Phenylalanine	6.8
	Tryptophane	NR*
	Proline	9
-OH	Serine	5.7
	Threonine	2.7
	Tyrosine	5.1
-S	Methionine	2
	Cysteine	0.8
Basic	Lysine	NR*
	Arginine	1.8
	Histidine	1.1
Acidic	Aspartic acid	4.5
	Glutamic acid	22.9

*****NR represents not reported

APPENDIX B. ADDITIONAL INFORMATION FOR THE PREPARATION OF FOLIC ACID-COVALENTLY LINKED ZEIN NANOPARTICLES

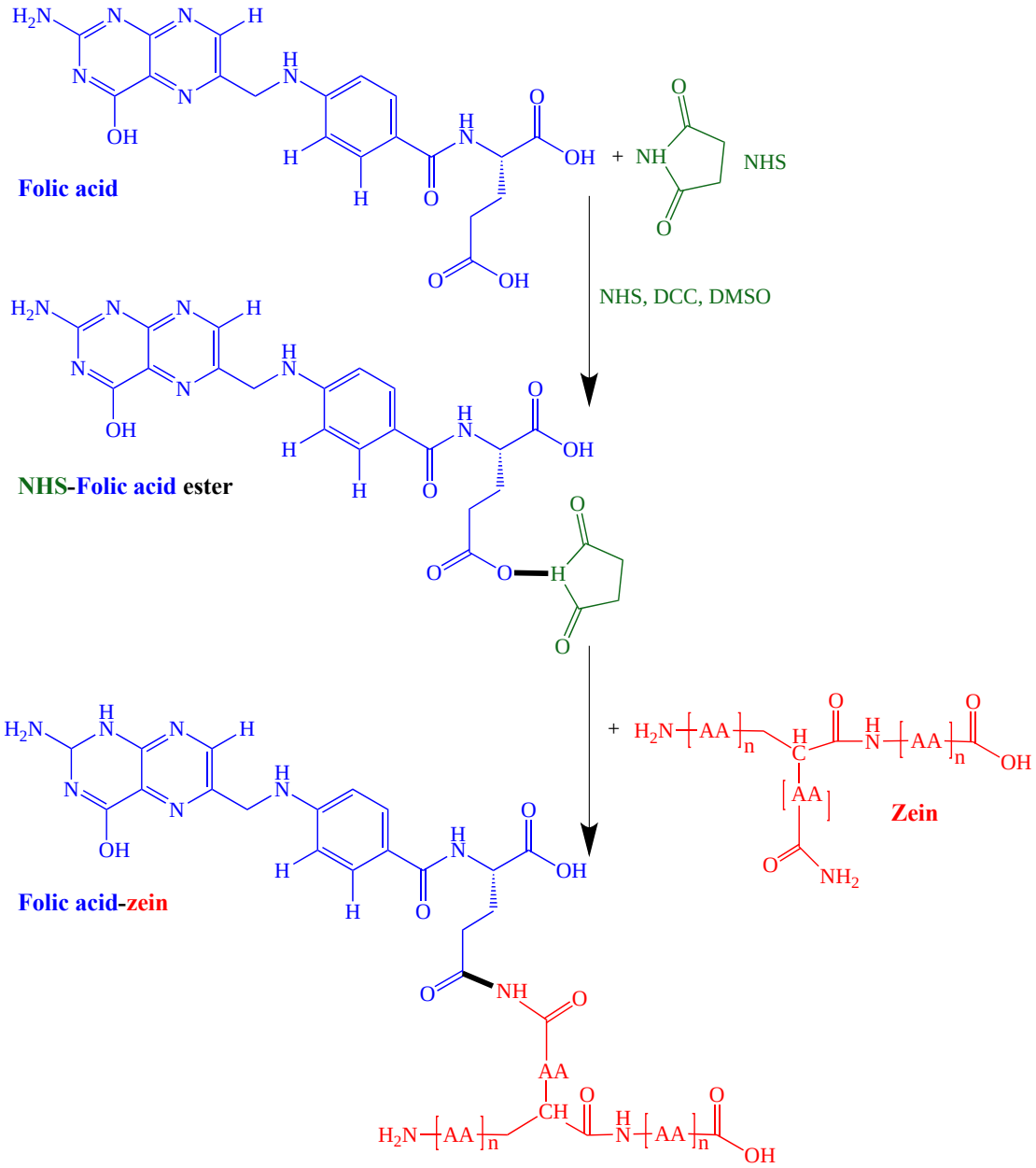

B.1. Schematic chemical structure of the formation of folic acid-covalently linked zein polymer

B.2. FTIR data of standard folic acid

Wave number (cm^{-1})	FTIR assignment
1485-1519	The Phenyl and pterin ring
1604	The bending of the N-H
1619	C=C aromatic
1639	C=N
1650	The stretching of the C=O (amide)
1693	The stretching of the C=O (carboxylic group)
3100-3500	The stretching of the O-H carboxylic of glutamic acid moiety and N-H group of pterin ring

B.3. FTIR data of standard zein

Wavenumber (cm^{-1})	FTIR assignment
1230	The axial deformation vibrations of the C-N bond
1540	The angular deformation vibrations of the N-H bond (amide II)
1650	The stretching of the C=O (amide I)
2800 - 3500	The stretching of the N-H and O-H bonds (primary amide)

VITA

Thanida Chuacharoen was born in Thailand in December 1979. She received her Bachelor of Science in Food Technology in June 2003 from Chulalongkorn University, Bangkok, Thailand and her Master of Science in Packaging Technology in July 2007 from Kasetsart University, Bangkok, Thailand. In August 2011, she obtained the Royal Thai Government Scholarship for pursuing a PhD degree in the US and began her doctoral program in Engineering Science at Louisiana State University. She expects to obtain her doctoral degree in December 2015.